

Enclosure 6 to E-58329

**Proposed Amendment 3, Revision 0 Changes to the
NUHOMS[®] EOS System Updated Final Safety Analysis
Report
(Public Version)**

Amendment 2 of this UFSAR incorporates the 61BTH Type 2 dry storage canister (DSC) for storage in the new NUHOMS® MATRIX (HSM-MX) design submitted under Amendment 1 to CoC 1042. The 61BTH Type 2 DSC is from CoC No. 1004 Amendment No. 15. The design will allow for intact, damaged, and failed fuel within the 61BTH Type 2 DSC, the definitions of which come from CoC No. 1042 Amendment No. 1. The EOS-89BTH DSC is limited to intact BWR fuel only. The design changes to the HSM-MX include front and rear DSC support spacer blocks, and a rear spacer block to maintain the centerline of the DSC.

Comprehensive analyses of components to the NUH61BTH Type 2 DSC and the OS197 TC as used in the HSM-MX are provided in Appendix B.

Additionally, Amendment 2 adds two new heat load zone configurations (HLZCs) for the EOS-37PTH for higher heat load assemblies, up to 3.5 kW/assembly, to allow for damaged and failed fuel storage. Amendment 2 also adds HLZCs (Type 1, Type 4L, and Type 5) that were introduced in CoC No. 1042 Amendment No. 1 to the EOS-37PTH Type 4H basket. For the EOS-TC108, Amendment 2 adds HLZCs 4 through 9 for the 4H basket and reduces the minimum cooling time to 2 years (HLZCs 2 through 9).

Amendment 3 updates the EOS-89BTH with five changes. The first change increases the heat load capacity of the EOS-89BTH to 48.2 kW and increases the per assembly heat load to 1.7 kW and reduces the cooling time to one year. A second change adds a maximum heat load configuration that is added to the Technical Specification as Figure 11 [1-7], which allows additional heat load zone configurations (HLZCs) to be qualified for use in the UFSAR when transferred in the EOS-TC125. Three new HLZCs are developed and evaluated for the thermal and structural design functions. A third change to the EOS-89BTH incorporates a modified version of the EOS-TC125 that varies the thickness of the lead gamma shielding. The fourth change to the EOS-89BTH adds ATRIUM 11 fuel as an allowable content. Lastly, the fifth change for the EOS-89BTH increases the U-235 maximum lattice average initial enrichment for BWR fuel to 5.0 wt% with Metal Matrix Composite (MMC).

Additionally, for both EOS-37PTH and EOS-89BTH, Amendment 3 permits ultrasonic testing a form of NDE and the use of a single pass HA-GTAW weld on the structural weld that connects the outer top cover plate to the DSC Shell. Amendment 3 also removes the fabrication pressure test requirement for EOS-DSCs fabricated using the single piece bottom forging option.

- Three EOS-89BTH DSC basket designs. Basket Types 1 through 3 correlate with the respective HLZC 1 through 3 (*Figure 2-2a through Figure 2-2c of Chapter 2*). Each of these basket types also allows for three levels of boron loading in the poison plates (Low, Moderate, and High). *Basket Type 1 also considers HLZCs 4, 5, and 6. Figure 2-2d through Figure 2-2f of Chapter 2 present HLZCs 4-6. In addition, Basket Type 1 can also be used to qualify additional HLZCs as noted per Figure 11 of the Technical Specification [1-7].*

EOS 89BTH Basket Types

Neutron Poison Loading Option	Type 1 (HLZC 1,4,5,6 max. 48.2 kW)	Type 2 (HLZC 2 max. 41.6 kW)	Type 3 (HLZC 3 max. 34.44 kW)
M1-A (Low B-10)	A1	A2	A3
M1-B (Moderate B-10)	B1	B2	B3
M2-A (High B-10)	C1	C2	C3

The criticality evaluations in Chapter 7 refer to the basket types based on the boron content in the poison plates. In Chapter 7, the references to the basket types differ from the above table. The correlations between the basket types used in Chapter 7 and basket types identified in the above table are clarified below:

- EOS-37PTH basket types A1, A2, A3, A4H, A4L, and/or A5 are identified as EOS-37PTH basket type A in Chapter 7
- EOS-37PTH basket types B1, B2, B3, B4H, B4L, and/or B5 are identified as EOS-37PTH basket type B in Chapter 7
- EOS-89BTH basket types A1, A2, and/or A3 are identified as EOS-89BTH basket type M1-A in Chapter 7
- EOS-89BTH basket types B1, B2, and/or B3 are identified as EOS-89BTH basket type M1-B in Chapter 7
- EOS-89BTH basket types C1, C2, and/or C3 are identified as EOS-89BTH basket type M2-A in Chapter 7

The thermal evaluation in Chapter 4 refers directly to the HLZC instead of using the basket types.

Provisions have been made for storage of up to eight damaged fuel assemblies in lieu of an equal number of intact assemblies placed in cells located in the EOS-37PTH basket. Damaged fuel assemblies are defined in Section 1.1 of the Technical Specifications [1-7].

The EOS-37PTH DSC is also designed to accommodate up to a maximum of four FFCs, placed in cells located at the outer edge of the DSC. Failed fuel is defined in Section 1.1 of the Technical Specifications [1-7].

- An EOS-TC system is provided with a top cover plate that allows air circulation through the TC/DSC annulus during transfer operations at certain heat loads when time limits for transfer operations cannot be satisfied. The EOS-TC system consists of a 135-ton cask (EOS-TC135), a 125-ton cask (EOS-TC125), and *the EOS-TC108 Cask*.

The EOS-37PTH DSC is designed for a maximum heat load of 50 kW when transferred in the EOS-TC125/135 or EOS-TC108. The EOS-89BTH DSC is designed for a maximum heat load of 48.2 kW when transferred in the EOS-TC125, and a maximum heat load of 41.6 kW when transferred in the EOS-TC108. The EOS-37PTH DSC can be transferred in any EOS-TC with a maximum heat load of 36.35 kW without air circulation available and, similarly, the EOS-89BTH with a maximum heat load of 34.4 kW.

The NUHOMS® EOS System is designed to be compatible with removal of the stored DSC for transportation and ultimate disposal by the Department of Energy, in accordance with 10 CFR 236(m). However, this application only addresses the storage of the spent fuel in the NUHOMS® EOS System.

The cavity length of the DSCs is adjustable to match the length of the fuel to be stored. This eliminates or reduces the need for fuel spacers to address secondary impact of the fuel on the lids during transportation accident scenarios.

The NUHOMS® EOS System provides structural integrity, confinement, shielding, criticality control, and passive heat removal independent of any other facility structures or components.

The EOS-HSMs and DSCs are intended for outdoor or sheltered storage on a reinforced concrete pad at a nuclear power plant. In addition to these components, the system requires use of an onsite TC, transfer trailer, and other auxiliary equipment that are described in this UFSAR. Similar equipment was previously licensed under NUHOMS® HD System UFSAR, Revision 4. Sufficient information for the transfer system and auxiliary equipment is included in this UFSAR to demonstrate that means for safe operation of the system are provided.

1.2 General Description and Operational Features of the NUHOMS® EOS System

The NUHOMS® EOS System provides for the horizontal, dry storage of canisterized SFAs in a concrete EOS-HSM. The storage system components consist of a reinforced concrete EOS-HSM and a stainless or duplex steel DSC confinement vessel that houses the SFAs. The general arrangement of the NUHOMS® EOS System components is shown in Figure 1-8. The confinement boundary is defined in Section 5.1 and shown in Figure 5-1. This UFSAR addresses the design and analysis of the storage system components, including the EOS-37PTH DSC, the EOS-89BTH DSC, the TC135, the TC125, the TC108, the EOS-HSM, and the EOS-HSMS, which are important to safety in accordance with 10 CFR 72.

In addition to these storage system components, the NUHOMS® EOS System also utilizes transfer equipment to move the DSCs from the plant's fuel or reactor building, where they are loaded with SFAs and prepared for storage in the EOS-HSM where they are stored. This transfer system consists of a TC, a lifting yoke, a ram system, a prime mover, a transfer trailer, a cask support skid, and a skid positioning system. This transfer system interfaces with the existing plant fuel pool, the cask handling crane, the site infrastructure (i.e., roadways and topography) and other site-specific conditions and procedural requirements. Auxiliary equipment, such as a TC/DSC annulus seal, a vacuum drying system, and a welding system, are also used to facilitate DSC loading, draining, drying, inerting, and sealing operations. Similar transfer system and auxiliary equipment has been previously licensed under the NUHOMS® HD System.

During dry storage of the spent fuel, no active systems are required for the removal and dissipation of the decay heat from the fuel. The NUHOMS® EOS System is designed to transfer the decay heat from the fuel to the DSC and from the DSC to the surrounding air by conduction, radiation and natural convection. The NUHOMS® EOS System ISFSI can also be housed in enclosed buildings provided the ISFSI with the building design is bounded by the design criteria described in Chapter 2 and the Technical Specifications [1-7]. No credit is taken for the building in the Safety Analysis of the NUHOMS® EOS System.

Each PWR DSC is identified by a Model Number, XXX-EOS-37PTH-YYY-~~ZZZ~~, where XXX typically identifies the site for which the EOS-37PTH DSC was fabricated, ~~ZZZ~~ designates the basket type, and YYY is a sequential number corresponding to a specific DSC. The basket types are defined by both the HLZC and neutron poison loading and are described in UFSAR drawing no. EOS01-1010-SAR for the intact and damaged/failed fuel basket. Similarly, each BWR DSC is identified by a Model Number, XXX-EOS-89BTH-YYY-~~ZZ~~. The basket types are described in UFSAR drawing no. EOS01-1020-SAR.

The NUHOMS® EOS System components do not include receptacles, valves, sampling ports, impact limiters, protrusions, or pressure relief systems, except for the neutron shield tanks on the EOS-TCs, which include pressure relief valves.

1.2.1.2 EOS-89BTH DSC

The key design parameters of the EOS-89BTH DSC are listed in Table 1-1. The primary confinement boundary for the EOS-89BTH DSC consists of the cylindrical shell, the top and bottom inner cover plates *or the optional Alternate 1-Bottom Forging*, the drain port cover plate, vent *port* plug, and the associated welds. The top and bottom cover plates, test port plug and associated welds form the redundant *sealing required by 10 CFR 72.236(e)*. The top and bottom shield plugs *or the optional Alternate 1-Bottom Forging* provide shielding for the EOS-89BTH DSC to minimize occupational doses at the ends during drying, sealing, handling, and transfer operations. *To provide additional operational flexibility, the top shield plug may be integrated with the inner top cover plate. When used without distinction, the terms inner top cover plate or shield plug will also include the shield plug integrated inner top cover plate.*

72.48

72.48

The cylindrical shell and inner bottom cover plate *or the optional Alternate 1-Bottom Forging* confinement boundary welds are fully compliant with Subsection NB of the ASME Code *with the exception of NB-6000 when the optional Alternate 1-Bottom Forging is used. These welds* are made during fabrication. The confinement boundary weld between the shell and the inner top cover (including drain port cover plate and vent *port* plug welds), and structural attachment weld between the shell and the outer top cover plate (including the test plug weld) are in accordance with Alternatives to the ASME code as described in Section 4.4.4 of the Technical Specifications [1-7].

72.48

72.48

Both drain port cover plate and vent *port* plug welds are made after drying operations are complete. There are no credible accidents that could breach the confinement boundary of the EOS-89BTH DSC as documented in Chapters 3 and 12.

72.48

The EOS-89BTH DSC basket structure, shown schematically in Figure 1-4, consists of interlocking slotted plates to form an egg-crate-type structure. The egg-crate structure forms a grid of 89 fuel compartments that house the BWR SFAs. The egg-crate grid structure is composed of one or more of the following: a steel plate, an aluminum plate, and a neutron absorber plate. The steel plates are fabricated from HSLA steels such as ASTM A829 Gr 4130 (AISI 4130) steel, hot rolled, heat-treated and tempered to provide structural support for the FAs. The poison plates are made of borated MMCs or BORAL® and provide the necessary criticality control. The aluminum plates, together with the poison plates, provide a heat conduction path from the FAs to the DSC rails and shell.

Basket “transition rails” provide the transition between the rectangular basket structure and the cylindrical DSC shell. The transition rails are made of extruded aluminum open or solid sections, which are reinforced with internal steel as necessary. These transition rails provide the transition to a cylindrical exterior surface to match the inside surface of the DSC shell. The transition rails support the fuel basket egg-crate structure and transfer mechanical loads to the DSC shell. They also provide the thermal conduction path from the basket assembly to the DSC shell wall, making the basket assembly efficient in rejecting heat from its payload. The nominal dimension of each fuel compartment opening is sized to accommodate the limiting assembly with sufficient clearance around the FA.

The EOS-89BTH DSC is designed for a maximum heat load of 48.2 kW. The internal basket assembly contains a storage position for each FA. The criticality analysis credits the fixed borated neutron absorbing material placed between the FAs. Sub-criticality during wet loading/unloading, drying, sealing, transfer, and storage operations is maintained through the geometric separation of the FAs by the basket assembly, and the neutron absorbing capability of the EOS-89BTH DSC materials, as applicable. Based on poison material and boron loading, and the HLZC, nine basket types are provided, as shown on drawing EOS01-1020-SAR. Poison material and boron loading requirements are discussed in Chapter 10.

In general, the dimensions of the EOS-89BTH DSC components described in the text and provided in figures and tables of this UFSAR are nominal dimensions for general system description purposes. Actual design dimensions are contained in the drawings in Section 1.3.2 of this UFSAR. See Sections 1.4.2 and 2.2.2 for a discussion of the contents authorized to be stored in this DSC.

1.2.1.3 Horizontal Storage Module

Each EOS-HSM or EOS-HSMS provides a self-contained modular structure for storage of spent fuel canisterized in an EOS-37PTH or EOS-89BTH DSC. The EOS-HSMS is essentially identical to the EOS-HSM except that the base is split into two sections (upper and lower), which are tied together via shear keys and six grouted tie rods. Henceforth in this UFSAR, EOS-HSM is used interchangeably for both the EOS-HSM and EOS-HSMS. The EOS-HSM is constructed from reinforced concrete and structural steel. The thick concrete roof and walls provide substantial neutron and gamma shielding. Contact doses for the EOS-HSM are designed to be ALARA. The key design parameters of the EOS-HSM are listed in Table 1-1.

The nominal thickness of the EOS-HSM roof is four feet for biological shielding. Separate shield walls at the end of a module row in conjunction with the module base wall, provide a minimum total thickness of four feet for shielding. Similarly, an additional shield wall is used at the rear of the module if the ISFSI is configured as single module arrays to provide a minimum total thickness of four feet of shielding with the module base rear wall. Sufficient shielding is provided by thick concrete side walls between EOS-HSMs in an array to minimize doses in adjacent EOS-HSMs during loading and retrieval operations.

1.2.1.4 Transfer Casks

The EOS-TCs are designed to provide shielding and protection from potential hazards during DSC loading and closure operations and transfer to the EOS-HSM. The key design parameters of the TC are listed in Table 1-1. The EOS-TCs included in this UFSAR are limited to onsite use under 10 CFR 72. The EOS-TCs are non-pressure-retaining, except the neutron shield tanks, atmospheric cylindrical vessels with welded bottom assemblies, and bolted top cover plates, and they are designed to ASME Division III Subsection NF Class 1 criteria. The neutron shield tanks retain pressure and are designed to ASME III Subsection ND criteria. The primary function of the EOS-TC is to provide onsite transport of loaded DSCs between the plant's spent fuel pool and the plant's onsite ISFSI. The TC provides the principal biological shielding and heat rejection mechanism for the EOS-DSC and SFAs during handling in the fuel or reactor building, EOS-DSC closure operations, transfer to the ISFSI, and placement in the EOS-HSM.

The TC is designed to provide sufficient shielding to provide reasonable assurance that dose rates are ALARA. *The EOS-TC125 lead gamma shielding thickness may vary between 3.12 and 3.56 inches when transferring the EOS-89BTH for a weight reduction of up to 11,210 pounds. This change is made to allow for use of the EOS-TC125 at sites with lower crane capacities to minimize/eliminate the need for limiting the allowable contents or use weight management techniques such as draining water or switching out a lighter aluminum lid.* Two top-lifting trunnions are provided for handling the TC using a lifting yoke and overhead crane. Lower pocket trunnions are provided for rotating the cask from/to the vertical and horizontal positions on the support skid/transport trailer.

The EOS-TC108 is designed with *the capability to remove the* neutron shield for use at nuclear plant sites with space limitations and/or crane capacity limits and, therefore, cannot use one of the other EOS-TCs. *Provided that the EOS-TC108 is designed to be used in situations of limited space or crane capacity, the EOS-TC108 can be modified to allow alternative configurations necessary to fit the loading environment restrictions.* A schematic sketch of the EOS-TC125/135 is shown in Figure 1-6, and of the EOS-TC108 with removable neutron shield is shown in Figure 1-7.

A cask spacer is required in the bottom of the EOS-TC to provide the correct interface at the top of the EOS-TC during loading, drying, and sealing operations for DSCs that are shorter than the cavity length. All EOS-TCs utilize a bottom cover incorporating wedges and top cover assembly that allows for air circulation. This mechanism enables cooling air to travel through the annular space between the EOS-DSC and the TC inner diameter through the entire cask length and to exit through the vent passages in the modified top cover assembly of the cask.

Dimensions of the EOS-TC components described in the text and provided in figures and tables of this UFSAR are in general nominal dimensions for general system description purposes. Actual design dimensions are contained in the drawings in Section 1.3.4.

1.2.1.5 System Configurations

As discussed in Sections 1.2.1.1 through 1.2.1.4, the various system configurations are determined based on basket type, heat load, fuel type, storage module, transfer cask, etc. *Eight* alternate system configurations for the EOS-37PTH DSC, and *four* system configurations for the EOS-89BTH, are summarized in Table 1-2.

1.2.2 Transfer Equipment for Loading EOS-HSMs

Transfer Trailer:

The typical transfer trailer for the NUHOMS® EOS System consists of a heavy industrial trailer used to transfer the empty cask, support skid and the loaded transfer cask between the plant's fuel or reactor building and the ISFSI. The trailer is designed to ride as low to the ground as possible to minimize the overall EOS-HSM height and the transfer cask height during DSC transfer operations. The trailer is equipped with leveling jacks to provide vertical alignment of the cask with the EOS-HSM. The trailer is self-powered or towed by a conventional heavy-haul truck tractor or other suitable prime mover. A typical transfer trailer is depicted in Figure 1-9.

Cask Support Skid:

A typical cask support skid for the NUHOMS® EOS System is shown in Figure 1-10, and is similar to the cask support skids described in the NUHOMS® HD System UFSAR. Key design features are:

- The skid is mounted on a surface with sliding support bearings and positioners to provide alignment of the cask with the EOS-HSM. A mechanism is provided to prevent movement during trailer towing.
- A hydraulic or mechanical ram is mounted on the skid to insert or retrieve the DSC from the EOS-HSM.
- The cask support skid is mounted on a low profile heavy-haul or self-powered industrial trailer.

The plant's fuel or reactor building crane or other suitable lifting device is used to lower the cask onto the support skid, which is secured to the transfer trailer. Specific details of this operation and the plant-specific building arrangement are covered by the provisions of the 10 CFR 50 operating license for the plant.

Ram:

A hydraulic or mechanical ram system consists of a hydraulic cylinder or mechanical frame with a capacity and a reach sufficient for DSC insertion into and retrieval from the EOS-HSM. The design of the ram support system provides a direct load path for the ram reaction forces during DSC insertion and retrieval. The system uses a rear ram support for alignment of the ram to the DSC. The design provides positive alignment of the major components during DSC insertion and retrieval.

**Proprietary and Security Related Information
for Drawing EOS01-1000-SAR, Rev. 5A
Withheld Pursuant to 10 CFR 2.390**

**Proprietary and Security Related Information
for Drawing EOS01-1001-SAR, Rev. 3A
Withheld Pursuant to 10 CFR 2.390**

**Proprietary and Security Related Information
for Drawing EOS01-1005-SAR, Rev. 4A
Withheld Pursuant to 10 CFR 2.390**

**Proprietary and Security Related Information
for Drawing EOS01-1006-SAR, Rev. 2A
Withheld Pursuant to 10 CFR 2.390**

**Proprietary and Security Related Information
for Drawing EOS01-2010-SAR, Rev. 4A
Withheld Pursuant to 10 CFR 2.390**

**Proprietary and Security Related Information
for Drawing EOS01-2011-SAR, Rev. 4A
Withheld Pursuant to 10 CFR 2.390**

**Proprietary and Security Related Information
for Drawing EOS01-2012-SAR, Rev. 3A
Withheld Pursuant to 10 CFR 2.390**

1.4 NUHOMS® EOS System Contents

1.4.1 EOS-37PTH DSC Contents

The EOS-37PTH DSC is designed to store up to 37 intact PWR FAs *(with or without CCs), up to eight damaged FAs, or up to four failed FAs, as described in the Technical Specifications [1-7].*

The EOS-37PTH DSC is qualified for storage of Babcock and Wilcox (B&W) 15 x 15 class, Combustion Engineering (CE) 14 x 14 class, CE 15 x 15 class, CE 16 x 16 class, Westinghouse (WE) 14 x 14 class, WE 15 x 15 class, and WE 17x17 class PWR FA designs, as described in Chapter 2.

The EOS-37PTH DSC payload may include CCs that are contained within the FA, such as described in Chapter 2.

Reconstituted assemblies containing up to five replacement irradiated stainless steel rods per assembly or an unlimited number of low enriched or natural uranium fuel rods or unirradiated non-fuel rods are acceptable for storage in an EOS-37PTH DSC as intact FAs.

The EOS-37PTH DSC is also authorized to store FAs containing blended low enriched uranium (BLEU) fuel material.

The contents of the DSC are stored in an inert atmosphere of helium.

The maximum allowable planar average initial enrichment of the fuel to be stored is 5.00 wt. % U-235, and the maximum assembly average burnup is 62,000 MWd/MTU. The FAs (with or without CCs) must be cooled to meet the decay heat limits specified in the Technical Specifications [1-7] prior to storage.

The criticality control features of the EOS-37PTH DSC are designed to maintain the neutron multiplication factor k-effective (including uncertainties and calculational bias) at less than 0.95 under normal, off-normal, and accident conditions.

The gamma and neutron source terms in the SFAs are described and tabulated in Chapter 6. Chapter 7 covers the criticality safety of the EOS-37PTH DSC and its parameters. These parameters include rod pitch, rod outside diameter, material densities, moderator ratios, soluble boron content and geometric configurations. The maximum pressure buildup in the EOS-37PTH DSC cavity is addressed in Chapter 4.

1.4.2 EOS-89BTH DSC Contents

The EOS-89BTH DSC is designed to store up to 89 intact BWR FAs with or without channels.

The EOS-89BTH DSC is qualified for storage of 7x7, 8x8, 9x9, 10x10, and 11x11 class BWR FAs of initial design or equivalent reload FAs as described in Chapter 2.

Reconstituted assemblies containing *a limited number of* replacement irradiated stainless steel rods per assembly or an unlimited number of low enriched or natural uranium fuel rods or unirradiated non-fuel rods are acceptable for storage in an EOS-89BTH DSC as intact FAs. *Restrictions on the maximum number of irradiated stainless steel rods per fuel assembly differ between transfer in the EOS-TC125 and EOS-TC108. These restrictions are provided in the Technical Specifications, Table 22 and Table 23 [1-7].*

The EOS-89BTH DSC is also authorized to store FAs containing BLEU fuel material.

The contents of the DSC are stored in an inert atmosphere of helium.

The maximum allowable lattice average initial enrichment of the fuel to be stored is 5.00 wt. % U-235 and the maximum assembly average burnup is 62,000 MWd/MTU. The FAs (with or without channels) must be cooled to meet the decay heat limits as specified in the Technical Specifications [1-7] and Chapter 2 prior to storage.

The criticality control features of the EOS-89BTH DSC are designed to maintain the neutron multiplication factor k-effective (including uncertainties and calculational bias) at less than 0.95 under normal, off-normal, and accident conditions.

The gamma and neutron source terms in the SFAs are described and tabulated in Chapter 6. Chapter 7 covers the criticality safety of the EOS-89BTH DSC and its parameters. These parameters include rod pitch, rod outside diameter, material densities, moderator ratios, and geometric configurations. The maximum pressure buildup in the EOS-89BTH DSC cavity is addressed in Chapter 4.

1.7 References

- 1-1 Title 10, Code of Federal Regulations, Part 72, “Licensing Requirements for the Independent Storage of Spent Nuclear Fuel, High-Level Radioactive Waste, and Reactor-Related Greater Than Class C Waste.”
- 1-2 NUREG-1536, “Standard Review Plan for Spent Fuel Dry Storage Systems at a General License Facility,” Revision 1, U.S. Nuclear Regulatory Commission, Office of Nuclear Material Safety and Safeguards, July 2010.
- 1-3 U.S. Nuclear Regulatory Commission, “Certificate of Compliance 72-1030, NUHOMS® HD Horizontal Modular Storage System for Irradiated Nuclear Fuel,” Amendment No. 2, October 14, 2014.
- 1-4 *TN Americas LLC*, Updated Final Safety Analysis Report, “NUHOMS® HD Horizontal Modular Storage System for Irradiated Nuclear Fuel,” Revision 6, U.S. Nuclear Regulatory Commission Docket No. 72-1030, September 2017.
- 1-5 Title 10, Code of Federal Regulations, Part 50, “Domestic Licensing of Production and Utilization Facilities.”
- 1-6 TN Americas LLC, “TN Americas LLC Quality Assurance Program Description Manual for 10 CFR Part 71, Subpart H and 10 CFR Part 72, Subpart G,” current revision.
- 1-7 CoC 1042 Appendix A, NUHOMS® EOS System Generic Technical Specifications, Amendment 3.

Table 1-1
Key Design Parameters of the NUHOMS® EOS System
Components
(2 Pages)

Horizontal Storage Module (EOS-HSM/EOS-HSMS):	
Overall length (without back shield wall)	19' EOS-Short
	20' 8" EOS-Medium
	22' 4" EOS-Long
Overall width (without end shield walls)	9'-8"
Overall height (without vent covers)	18' 6"
Total Weight not including DSC (lbs.)	311,000 EOS-Short
	334,000 EOS-Medium
	351,000 EOS-Long
Materials of Construction	Reinforced concrete and structural steel
Heat Removal	Conduction, convection, and radiation
OnSite Transfer Cask (EOS-TC)	
Overall Length (in)	206.76 EOS-TC108
	208.21 EOS-TC125
	228.71 EOS-TC135
Outside Diameter (in)	90.61 EOS-TC108 w/ NS tank
	88.50 EOS-TC108 w/o NS tank
	95.38 <i>maximum</i> EOS-TC125
	95.38 EOS-TC135
Cavity Length (in)	199.17 EOS-TC108
	199.25 EOS-TC125
	219.75 EOS-TC135
Lead Thickness (in)	2.50 EOS-TC108
	3.12-3.56 EOS-TC125
	3.56 EOS-TC135
Gross Weight (with neutron shield and steel lid and no payload) (tons)	46.5 EOS-TC108
	62.1 <i>maximum</i> EOS-TC125
	67.9 EOS-TC135
Materials of Construction	Carbon steel shell assemblies and closures with lead shielding, aluminum and carbon steel lids and aluminum neutron shield tank for the TC108
Internal Atmosphere	Air

Table 1-2
System Configurations for the NUHOMS® EOS System and NUHOMS® MATRIX System
(2 Pages)

DSC	System Configuration	Basket Design	Basket Type	Emissivity/ Poison	Storage Module	Wind Deflector	HLZC	Intact	Damaged/ Failed	Transfer Cask
EOS-37PTH	S1	Non-Staggered	1	High	EOS-HSM	Yes	1	Yes	No	EOS-TC125/135
	S2	Non-Staggered	2	High	EOS-HSM	No	2	Yes	No	EOS-TC108/125/135
		Non-Staggered	3	High	EOS-HSM	No	3	Yes	No	EOS-TC108/125/135
	S3	Staggered	4L	Low	EOS-HSM	Yes	4	Yes	No	EOS-TC125/135
		Staggered	4L	Low	EOS-HSM	Yes	5	Yes	No	EOS-TC125/135
		Staggered	4L	Low	EOS-HSM	Yes	6	Yes	Yes	EOS-TC125/135
	S3a	<i>Staggered</i>	<i>4H</i>	<i>High</i>	<i>EOS-HSM</i>	<i>Yes⁽¹⁾</i>	<i>1</i>	<i>Yes</i>	<i>No</i>	<i>EOS-TC125/135</i>
		<i>Staggered</i>	<i>4H</i>	<i>High</i>	<i>EOS-HSM</i>	<i>Yes⁽¹⁾</i>	<i>4</i>	<i>Yes</i>	<i>No</i>	<i>EOS-TC108/125/135</i>
		<i>Staggered</i>	<i>4H</i>	<i>High</i>	<i>EOS-HSM</i>	<i>Yes⁽¹⁾</i>	<i>5</i>	<i>Yes</i>	<i>No</i>	<i>EOS-TC108/125/135</i>
		<i>Staggered</i>	<i>4H</i>	<i>High</i>	<i>EOS-HSM</i>	<i>Yes⁽¹⁾</i>	<i>6</i>	<i>Yes</i>	<i>Yes</i>	<i>EOS-TC108/125/135</i>
		<i>Staggered</i>	<i>4H</i>	<i>High</i>	<i>EOS-HSM</i>	<i>Yes⁽¹⁾</i>	<i>10</i>	<i>Yes</i>	<i>Yes</i>	<i>EOS-TC125/135</i>
		<i>Staggered</i>	<i>4H</i>	<i>High</i>	<i>EOS-HSM</i>	<i>Yes⁽¹⁾</i>	<i>11</i>	<i>Yes</i>	<i>Yes</i>	<i>EOS-TC125/135</i>
	S4	Non-staggered	5	Low	EOS-HSM	Yes	4	Yes	No	EOS-TC125/135
		Non-staggered	5	Low	EOS-HSM	Yes	5	Yes	No	EOS-TC125/135
	S5	Staggered	4H	High	HSM-MX	N/A	7	Yes	No	EOS-TC108/125/135
		<i>Staggered</i>	<i>4H</i>	<i>High</i>	<i>HSM-MX</i>	<i>N/A</i>	<i>8</i>	<i>Yes</i>	<i>Yes</i>	<i>EOS-TC108/125/135</i>
		<i>Staggered</i>	<i>4H</i>	<i>High</i>	<i>HSM-MX</i>	<i>N/A</i>	<i>9</i>	<i>Yes</i>	<i>No</i>	<i>EOS-TC108/125/135</i>
		<i>Staggered</i>	<i>4H</i>	<i>High</i>	<i>HSM-MX</i>	<i>N/A</i>	<i>11</i>	<i>Yes</i>	<i>Yes</i>	<i>EOS-TC125/135</i>
	S6	Staggered	4L	Low	HSM-MX	N/A	8	Yes	Yes	EOS-TC125/135
		Staggered	4L.	Low	HSM-MX	N/A	9	Yes	No	EOS-TC125/135
	S7	Non-staggered	5	Low	HSM-MX	N/A	8	Yes	No	EOS-TC125/135
		Non-staggered	5	Low	HSM-MX	N/A	9	Yes	No	EOS-TC125/135

Table 1-2
System Configurations for the NUHOMS® EOS System and NUHOMS® MATRIX System
(2 Pages)

DSC	System Configuration	Basket Design	Basket Type	Emissivity/ Poison	Storage Module	Wind Deflector	HLZC	Intact	Damaged/ Failed	Transfer Cask
EOS-89BTH	S8	Non-Staggered	1	High	EOS-HSM	Yes	1	Yes	No	EOS-TC125
		<i>Non-Staggered</i>	<i>1</i>	<i>High</i>	<i>EOS-HSM</i>	<i>Yes</i>	<i>4</i>	<i>Yes</i>	<i>No</i>	<i>EOS-TC125</i>
		<i>Non-Staggered</i>	<i>1</i>	<i>High</i>	<i>EOS-HSM</i>	<i>Yes</i>	<i>5</i>	<i>Yes</i>	<i>No</i>	<i>EOS-TC125</i>
		<i>Non-Staggered</i>	<i>1</i>	<i>High</i>	<i>EOS-HSM</i>	<i>Yes</i>	<i>6</i>	<i>Yes</i>	<i>No</i>	<i>EOS-TC125</i>
	S9	Non-Staggered	2	High	EOS-HSM	No	2	Yes	No	EOS-TC108/125
		Non-Staggered	3	High	EOS-HSM	No	3	Yes	No	EOS-TC108/125
	S10	Non-Staggered	3	High	HSM-MX	N/A	3	Yes	No	EOS-TC108/125
	<i>S11</i>	<i>Non-Staggered</i>	<i>1</i>	<i>High</i>	<i>HSM-MX</i>	<i>N/A</i>	<i>4</i>	<i>Yes</i>	<i>No</i>	<i>EOS-TC125</i>
		<i>Non-Staggered</i>	<i>1</i>	<i>High</i>	<i>HSM-MX</i>	<i>N/A</i>	<i>5</i>	<i>Yes</i>	<i>No</i>	<i>EOS-TC125</i>
		<i>Non-Staggered</i>	<i>1</i>	<i>High</i>	<i>HSM-MX</i>	<i>N/A</i>	<i>6</i>	<i>Yes</i>	<i>No</i>	<i>EOS-TC125</i>

Notes:

1. Wind deflectors are needed only if the heat load is greater than 41.8 kW.
2. For HLZC 5, wind deflectors are needed only if the heat load of a single fuel assembly is greater than 1.625 kW.

2.2 Spent Fuel to Be Stored

The NUHOMS® EOS System is designed to accommodate pressurized water reactor (PWR) (14x14, 15x15, 16x16 and 17x17 array designs) and boiling water reactor (BWR) (7x7, 8x8, 9x9, 10x10, and 11x11 array designs) fuel types that are available for storage. As described in Chapter 1, there are two DSC designs for the NUHOMS® EOS System: the EOS-37PTH DSC for PWR fuel and EOS-89BTH DSC for BWR fuel. The EOS-37PTH DSC is designed to accommodate up to 37 intact PWR FAs with uranium dioxide (UO₂) fuel, zirconium-alloy cladding, and with or without control components. The EOS-37PTH DSC is also designed to accommodate up to eight damaged FAs or up to four failed fuel canisters (FFCs), with the balance being intact FAs. The EOS-89BTH DSC is designed to accommodate up to 89 intact BWR FAs with UO₂ fuel, zirconium-alloy cladding, and with or without fuel channels. Specifications for the fuel to be stored in the NUHOMS® EOS System are provided in Technical Specifications (TS) Sections 2.1 and 2.2.

The cavity length of the DSC is determined for a specific site to match the FA length used at that site, including control components (CCs), as applicable. Both DSCs store intact, including reconstituted and blended low enriched uranium (BLEU), FAs as specified in Table 2-2, Table 2-3 and Table 2-4. Any FA that has fuel characteristics within the range of Table 2-2, Table 2-3 and Table 2-4 and meets the other limits specified for initial enrichment, burnup and heat loads is acceptable for storage in the NUHOMS® EOS System. Equivalent fuels manufactured by other vendors are also acceptable.

Damaged and failed fuel from the FA classes detailed in Table 2-2 and PWR fuels in Table 2-4 are also acceptable for storage in the EOS-37PTH DSC in the appropriate compartments. The potential for fuel reconfiguration for intact, damaged, and failed fuel under normal, off-normal, and accident conditions is summarized in Table 2-4a.

All fuel categorized as failed shall be placed in a failed fuel canister (FFC). Failed fuel may include FAs, fuel rods, segments of fuel rods, fuel pellets, and debris. FFCs are not required for damaged FAs, because damaged FAs maintain their geometry under normal and off-normal conditions.

The failed fuel content of each FFC is limited to the maximum metric tons of uranium (MTU) of an intact fuel assembly for each class. These limits are summarized in Table 2-4b. Failed CCs may also be stored inside an FFC. *Failed CCs are defined as CCs that may not maintain configuration for normal or off-normal conditions and thus could impact the safety function of the basket, degrade the fuel cladding, or result in an unanalyzed condition. Disassembled CCs are considered failed. A CC with missing rods or components that is otherwise structurally sound is considered intact.* The maximum Co-60 content for failed CCs is the same as intact CCs and is defined in Table 3 of the Technical Specifications [2-18].

The maximum allowable assembly average burnup is limited to 62 GWd/MTU and the minimum cooling time is two years *for the EOS-37PTH DSC and 1 year for the EOS-89BTH DSC*. Dummy FAs and reconstituted FAs are also included in the EOS-37PTH DSC and EOS-89BTH DSC payloads. Low enriched or natural uranium fuel rods or unirradiated non-fuel rods are acceptable for storage in an EOS-37PTH DSC and EOS-89BTH DSC as intact FAs.

Fuel assemblies that contain fixed integral non-fuel rods are also considered as intact FAs. These FAs are different than reconstituted assemblies because fuel rods are not “replaced” by non-fuel rods, rather the non-fuel rods are part of the initial fuel design. The non-fuel rods displace the same amount of moderator, with zirconium-alloy (or aluminum) cladding and typically contain burnable absorber (or other non-fuel) material. The radiation and thermal source terms for the non-fuel rods are significantly lower than those of the fuel rods since there is no significant radioactive decay source. The internal pressure of the non-fuel rods after irradiation is lower than those of the fuel rods since there is no fission gas generation. The reactivity of the fuel rods (from a criticality standpoint) is significantly higher than that of non-fuel rods. In summary, the mechanical, thermal, shielding, and criticality evaluations for these rods are bounded by those of the regular fuel rods. Therefore, no further evaluations are required for the qualification of these FAs.

Reconstituted fuel assemblies with irradiated stainless steel rods are allowed, with additional restrictions. These restrictions vary between the EOS-37PTH DSC and EOS-89BTH DSC and are defined in the Technical Specifications, Sections 2.1 and 2.2 [2-18].

The EOS-37PTH DSC may contain less than 37 FAs and the EOS-89BTH DSC may contain less than 89 FAs. In both DSCs, the basket slots not loaded with FAs may have empty slots or be loaded with dummy FAs. The dummy FAs approximate the weight and center of gravity of an FA.

The NUHOMS® EOS-37PTH DSC can also accommodate up to eight damaged FAs placed in the DSC. Damaged PWR FAs are defined in Section 1.1 of the Technical Specifications [2-18].

The NUHOMS® EOS-37PTH DSCs can also accommodate up to a maximum of four FFCs, placed in cells located on the outer edge of the DSC. Failed fuel is defined in Section 1.1 of the Technical Specifications [2-18].

Following loading, each DSC is evacuated and then backfilled with an inert gas, helium, to preclude detrimental chemical reaction between the fuel and the DSC interior atmosphere during storage. Multilayer, *confinement boundary* welds at each end of the DSC and multi-layer circumferential and longitudinal DSC shell welds ensure retention of the helium atmosphere for the full storage period.

The fuel compartment and the top and bottom end cap together form the “acceptable alternative,” per NUREG-1536 Revision 1 for confinement of damaged fuel. If fuel particles are released from the damaged assembly, the top and bottom end caps provide for the confinement of gross fuel particles to a known volume. Similarly, the FFC provides confinement of the FFC contents to a known volume, and has lifting features to allow the ability to unload the FFC. Additionally, consistent with ISG-2, Revision 2, ready retrieval of the damaged and failed fuel is based on the ability to remove a canister from the HSM.

The structural analysis for damaged fuel cladding described in Chapter 3 demonstrates that the cladding does not undergo additional degradation under normal and off-normal conditions of storage. The structural analyses performed for FFCs are provided in Section 3.9.2.1A. The criticality analysis described in Chapter 7 is based on damaged and failed fuel in the most limiting credible geometry and material reconfigurations under normal, off-normal, and accident conditions. The maximum enrichment values for damaged and/or failed fuel are reduced to account for fuel reconfiguration. The thermal analysis described in Chapter 4 limits the maximum allowable heat load per DSC storing damaged or failed fuel to be less than that for when storing only intact FAs. The shielding analysis described in Chapter 6 demonstrates that damaged or failed fuel reconfiguration has a negligible effect on dose rates compared to intact fuel.

Calculations were performed to determine the FA type that was most limiting for each of the analyses including shielding, criticality, thermal and confinement. These evaluations are performed in Chapter 6, 7, 4 and 5, respectively.

2.2.2 EOS-89BTH DSC

The EOS-89BTH DSC design accommodates up to 89 intact BWR FAs with characteristics as described in Table 2-3, and the BWR FAs listed in Table 2-4. One or more BWR FA designs are grouped under a “BWR Fuel ID”. The EOS-89BTH accommodates:

- Fuel assemblies with and without channels,
- Fuel assemblies with and without channel fasteners.

10 CFR 72.236 (a) requires the maximum heat designed to be dissipated and the maximum spent fuel loading limit to be specified in the Technical Specifications (TS). Figure 11 of the Technical Specifications provides this required information, wherein the maximum heat load of the DSC is limited to 48.2 kW in the EOS-HSM and Lower Compartment of the HSM-MX and 41.8 kW in the upper compartment of the HSM-MX. It also provides limits on the maximum allowable heat loads in each fuel compartment and zone.

The limits on the total decay heat load of the DSC and the maximum heat load in each fuel compartment and zone in Figure 11 of the Technical Specification are used to qualify the various HLZCs and to also verify the corresponding radiation source term is consistent with the shielding analysis presented in Chapter 6. The maximum weight of an FA plus channel, if applicable, is 705 lbs.

Furthermore, since TS Figure 11 presents only the maximum heat loads, there can be a multitude of ways that the heat loads in each fuel compartment and zone can be adjusted to meet the total heat load limit of the DSC. To ensure this adjustment meets all the design criteria, the various HLZCs that are developed based on Figure 11 must be evaluated and pre-qualified. It should be noted that the pre-qualification is limited to thermal and structural design functions, since the shielding evaluation in Chapter 6 considers a bounding evaluation that encompasses the maximum heat loads in Figure 11.

UFSAR Figure 2-2a through Figure 2-2f present six such examples for EOS-89BTH wherein HLZCs 1 through 6 are qualified based on the limitations and constraints of TS Figure 11. Chapter 4, Section 4.4 and 4.5 presents the evaluation of HLZC 1-3 and Section 4.9.8 provides the evaluation of HLZC 4-6 in the EOS-HSM and EOS-TC125. Appendix A.4 presents the methodology for qualifying HLZCs 4 through 6 in EOS-89BTH during storage in HSM-MX.

In addition, LCO 3.1.3 of the TS [2-18] notes that a minimum duration of 13 hours shall be allowed for transfer operations (8 hours for the transfer and 5 hours for recovery as allowed by the action statements). Table 2-10 presents the minimum transfer time limits for the various HLZCs. It should be noted that these time limits are the minimum required time limits for transfer operations based on the maximum allowable heat loads for each HLZC and a new time limit may be determined to allow for longer time limits if the DSC is loaded to less than the maximum allowable limit.

The evaluations presented for storage in EOS-HSM, HSM-MX and EOS-TC125 in Chapter 4 and A.4 present the methodology to evaluate and pre-qualify additional HLZCs.

Section 2.4.3.1 presents the detailed methodology to evaluate and pre-qualify additional HLZCs based on these evaluations.

The heat loads listed in *Figure 2-2a through Figure 2-2f for the various HLZCs based on Figure 11* of the Technical Specification [2-18] are the maximum allowable heat loads for each FA and the maximum allowable heat load per DSC. These heat loads can be reduced to ensure adequate heat removal capability is maintained to accommodate site-specific conditions. Some examples of the site-specific conditions are a higher ambient temperature, different blocked vent duration, a requirement to use a different neutron absorber plate or a requirement for a specific coating on the basket steel plates. Each of these changes could result in a change to the inputs of the thermal evaluation utilized in the UFSAR. To ensure that adequate heat removal is maintained with these modified inputs, the bounding evaluations for storage and transfer operations should be re-evaluated. The maximum fuel cladding temperature determined for these evaluation based on the modified inputs shall be lower than the maximum fuel cladding temperatures listed in the Chapter 4 and Chapter A.4 for the same bounding evaluations.

Calculations were performed to determine the FA type that was most limiting for each of the analyses including shielding, criticality, thermal and confinement. These evaluations are performed in Chapter 6, 7, 4 and 5, respectively.

The DSC itself has a series of barriers to ensure the confinement of radioactive materials. The cylindrical shell is fabricated from rolled ASME stainless steel plate or duplex steel, which is joined with full penetration welds that are 100% inspected by non-destructive examination. All top and bottom end *confinement boundary* welds are multiple-layer welds. This effectively eliminates any pinhole leaks that might occur in a single pass weld, since the chance of pinholes being in alignment on successive weld passes is not credible. Furthermore, the cover plates are sealed by separate, redundant closure welds. Pressure boundary welds and welders are qualified in accordance with Section IX of the ASME Boiler and Pressure Vessel Code and inspected according to the appropriate articles of Section III, Division 1, Subsection NB including alternatives to ASME Code as specified in Section 4.4.4 of the Technical Specifications [2-18]. These criteria ensure that the as-deposited weld filler metal is as sound as the parent metal of the pressure vessel.

Pressure monitoring instrumentation is not used since penetration of the pressure boundary would be required. The penetration itself would then become a potential leakage path and by its presence compromise the integrity of the DSC design. The shell and welded cover plates provide total confinement of radioactive materials. Once the DSC is sealed, there are no credible events, as discussed in Chapter 12, which could fail the cylindrical shell or the closure plates that form the confinement boundary.

The NUHOMS® EOS System provides safe and long-term dry storage of SFAs. The key elements of the NUHOMS® EOS System, and its operation requiring special design consideration, are:

- A. Minimizing contamination of the DSC exterior by fuel pool water.
- B. Double-closure seal welds on the DSC shell to form a pressure retaining containment boundary, and to maintain the DSC interior helium atmosphere.
- C. Minimizing personnel radiation exposure during DSC loading, closure, and transfer operations.
- D. Maintaining EOS-TC and DSC ITS features under postulated accident conditions.
- E. Passive ventilation of the HSM providing effective decay heat removal thereby maintaining fuel cladding temperature below the maximum limit.
- F. DSC basket assembly to ensure that the SFAs are maintained in a subcritical configuration.

Components of the NUHOMS® EOS System that are ITS and NITS are listed in Table 2-1.

2.4.2 Structural

2.4.2.1 EOS-DSC Design Criteria

The principal design criteria for the DSCs are presented in Table 2-5 and Table 2-6. The EOS-37PTH DSC is designed to store intact PWR FAs with or without CCs, damaged fuel and failed fuel canisters. The EOS-89BTH DSC is designed to store intact BWR FAs with or without fuel channels. The maximum total heat generation rate of the stored fuel is limited to 50 kW per DSC for the EOS-37PTH DSC and 48.2 kW per DSC for the EOS-89BTH DSC, in order to keep the maximum fuel cladding temperature below the limit necessary to ensure cladding integrity. The maximum heat load for any single assembly is 3.5 kW for the EOS-37PTH DSC and 1.7 kW for the EOS-89BTH DSC. The fuel cladding integrity is assured by limiting fuel cladding temperature and maintaining a nonoxidizing environment in the DSC cavity as described in Chapter 4.

2.4.2.2 EOS-HSM Design Criteria

The principal design criteria for the EOS-HSM/EOS-HSMS, both the module and DSC support structure, are presented in Table 2-7.

The EOS reinforced concrete EOS-HSM is designed to meet the requirements of ACI 349-06 [2-3]. The ultimate strength method of analysis is utilized with the appropriate strength reduction factors as described in Appendix 3.9.4. The load combinations specified in Section 6.17.3.1 of ANSI 57.9-1984 are used for combining normal operating, off-normal, and accident loads for the EOS-HSM. All seven load combinations specified are considered and the governing combinations are selected for detailed design and analysis. The resulting EOS-HSM load combinations and the appropriate load factors are presented in Appendix 3.9.4. The effects of duty cycle on the EOS-HSM are considered and found to have negligible effect on the design.

2.4.2.3 EOS-TC Design Criteria

The EOS-TCs are designed in accordance with the applicable portions of the ASME Code, Section III, Division 1, Subsection NF for Class 1 vessels, except for the neutron shield tank, which is designed to ASME Code, Section III, Division 1, Subsection ND, since it will see pressure greater than 15 psig. The load combinations considered for the TC normal, off-normal, and postulated accident loadings are shown in Table 2-8. Service Levels A and B allowables are used for all normal operating and off-normal loadings. Service Levels C and D allowables are used for load combinations that include postulated accident loadings. The maximum shear stress theory is used to calculate principal stresses in the cask structural shell. Allowable stress limits for the lifting trunnions conservatively meet the requirements of ANSI N14.6- 1993 [2-14] for critical loads.

2.4.3 Thermal

The NUHOMS® EOS System relies on natural convection through the air space in the EOS-HSM to cool the DSC. This passive convective ventilation system is driven by the pressure difference due to the stack effect (ΔP_s) provided by the height difference between the bottom of the DSC and the EOS-HSM air outlet. This pressure difference is greater than the flow pressure drop (ΔP_f) at the design air inlet and outlet temperatures. The details of the ventilation system design are provided in Chapter 4.

Thermal analysis is based on FAs with decay heat up to 50.0 kW per DSC for the EOS-37PTH and up to 48.2 kW per DSC for the EOS-89BTH. Zoning is used to accommodate high per assembly heat loads. The heat load zoning configurations (HLZCs) for the DSCs are shown in Figures 1A through 1K of the Technical Specifications [2-18] for the EOS-37PTH DSC. For the EOS-89BTH DSC based on the discussion in Section 2.2.2, Figure 1I presents the maximum allowable heat loads in the Technical Specifications while the individual HLZCs are presented in Section 2.4.3.2. As noted in Section 2.1 of Technical Specification [2-18], the maximum allowable heat loads may be reduced based on the methodology presented in Chapter 4 or Chapter A.4 for each FA type allowed in either the EOS-37PTH DSC or the EOS-89BTH DSC. The thermal properties for the various FA types should be determined based on the methodology presented in Chapter 4, Appendix 4.9.1.

The thermal analyses is performed for the environmental conditions listed in Table 2-9.

Peak clad temperature of the fuel at the beginning of the long-term storage does not exceed 400 °C for normal conditions of storage, and for short-term operations, including DSC drying and backfilling. Fuel cladding temperature shall be maintained below 570 °C (1058 °F) for accident conditions involving fire or off-normal storage conditions.

For onsite transfer in the EOS-TC, air circulation may be used, as a recovery action, to facilitate transfer operations when the heat loads in the EOS-37PTH DSC are above 36.35 kW and 34.4 kW in the EOS-89BTH DSC as described in the Technical Specifications [2-18].

Wind deflectors are installed on the EOS-HSM to eliminate the effect of sustained winds for DSCs with Type 1 or Type 2 baskets as described in Section 5.5 of the Technical Specifications [2-18].

2.4.3.1 Methodology for Evaluating Additional HLZCs in EOS-89BTH DSC

2.4.3.2 HLZCs for EOS-89BTH DSC

HLZCs 1 through 6 that are qualified for use with the EOS-89BTH DSC based on the methodology presented in Section 2.4.3.1 are presented in Figure 2-2a through Figure 2-2f. In addition to these HLZCs, additional HLZCs may be qualified based on the methodology presented in Section 2.4.3.1. Note that HLZCs 1-3 were previously approved by the NRC in Amendment 0.

2.4.4 Shielding/Confinement/Radiation Protection

As described earlier, the DSC shells are a welded stainless or duplex steel pressure vessel that includes thick shield plugs at both ends to maintain occupational exposures as low as reasonably achievable (ALARA). The top end of the DSC has nominally 10 inches of steel shielding and the bottom eight inches of steel shielding. The confinement boundary is designed, fabricated, and tested to ensure that it is leaktight in accordance with [2-15]. Section 2.4.2.1 provides a summary of the features of the DSCs that ensure confinement of the contents.

These two neutron poison loading options allow flexibility to accommodate the payload fuel types and initial enrichments, with and without CCs, and credit for soluble boron (2000 – 2600 ppm) in the fuel pool during loading and unloading operations. Table 4 of the Technical Specifications [2-18] and Chapter 7 documents the minimum soluble boron required as a function of basket type and FA design/initial enrichment to be stored. Pressurized water reactor FAs with maximum planar average enrichments up to 5.0 wt. % U-235 can be stored.

For the EOS-89BTH DSC, a combination of fixed poison in the basket and geometry are relied on to maintain criticality control. The structural analysis shows that there is no deformation of the basket under accident conditions that would increase reactivity. The EOS-89BTH basket is fabricated with one of three neutron poison loading options as shown in Table 8 of the Technical Specifications [2-18].

These three neutron poison loading options allow flexibility to accommodate the payload fuel types and initial enrichments, with and without channels during loading and unloading operations. Table 8 *and Figure 10* of the Technical Specifications [2-18] and Chapter 7 documents the allowed fuel assembly design/initial enrichment as a function of neutron poison loading allowed to be stored. Fuel assemblies with maximum lattice average enrichments up to 5.0 wt. % U-235 can be stored in the EOS-89BTH with neutron poison loading option C.

The criticality analysis in Chapter 7 takes 90% credit for the B-10 content of the metal matrix composite (MMC) material and 75% credit for the B-10 content of the BORAL® material. Chapter 10 provides the testing requirements to justify the B-10 credit used in the criticality analysis.

2.4.6 Material Selection

Materials are selected based on their corrosion resistance, susceptibility to stress corrosion cracking, embrittlement properties, and the environment in which they operate during normal off-normal and accident conditions. The confinement boundary for the DSC materials meet the requirements of ASME Boiler and Pressure Vessel Code, Section III, Article NB-2000 and the specification requirements of Section II, Part D, with code alternatives provided in Section 4.4.4 of the Technical Specifications [2-18]. The DSC and TC materials are resistant to corrosion and are not susceptible to other galvanic reactions. Studies under severe marine environments have demonstrated that the shell materials used in the DSC shells are expected to demonstrate minimal corrosion during a 80-year exposure. The DSC internals are enveloped in a dry, helium-inerted environment and are designed for all postulated environmental conditions. The HSM is a reinforced concrete component with an internal DSC support structure (EOS-HSM) or rear DSC support (HSM-MX) that is fabricated to ACI and AISC Code requirements with code alternatives provided in Section 4.4.4 of the Technical Specifications [2-18], respectively; both have durability well beyond their design life of 80 years. Chapter 8 and Chapter A.8 provide additional discussion related to the materials used for the NUHOMS® EOS System.

- 2-18 CoC 1042 Appendix A, NUHOMS® EOS System Generic Technical Specifications, Amendment 3.
- 2-19 Updated Final Safety Analysis Report For The Standardized Advanced NUHOMS® Horizontal Modular Storage System For Irradiated Nuclear Fuel, 72-1029, Revision 6
- 2-20 DOE/RW-0184 Volume 1 of 6, “Characteristics of Spent Fuel, High-Level Waste, and Other Radioactive Wastes Which May Require Long-Term Isolation,” December 1987, U.S. Department of Energy, Office of Civilian Radioactive Waste Management.

Table 2-3
BWR Fuel Assembly Design Characteristics
 4 Pages

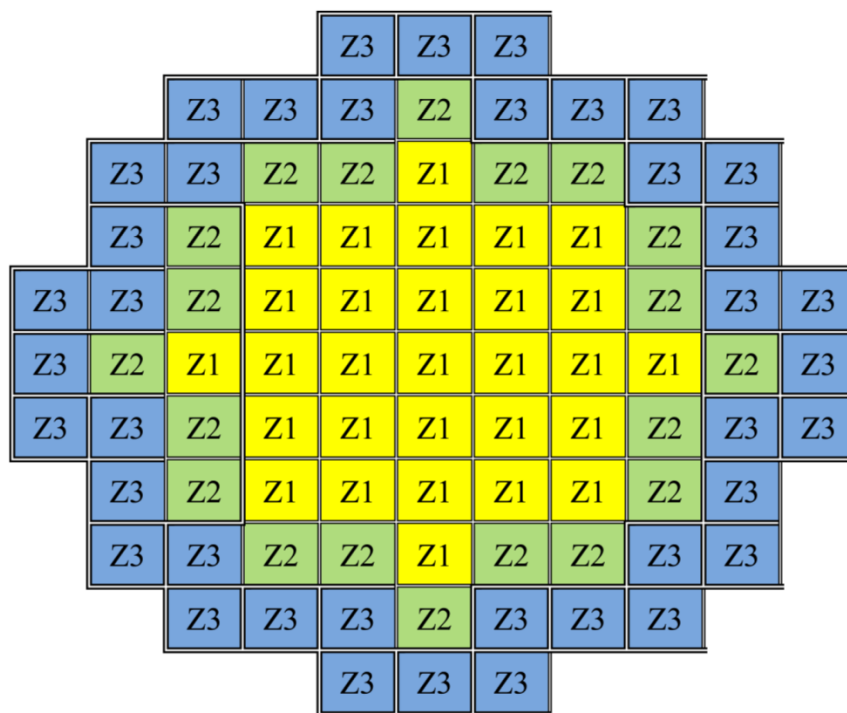
BWR Fuel ID /(Fuel Class)	ABB-10-A (10 x 10)	ABB-10-C (10 x 10)	
FA Design	4x(5x5-3) 4x(5x5-1) Optima 1	4x(5x5-4) 4x(5x5-2) 4x(5x5-1) Optima2	
Reload Fuel Designation ⁽¹⁾⁽²⁾	SVEA-96Opt ⁽⁴⁾⁽⁵⁾	SVEA-96Op2 ⁽⁴⁾⁽⁵⁾	
Rod Pitch (in.)	0.496 - 0.500	0.484 - 0.512	
No of Fueled Rods	88, 96	84, 92, 96	
Maximum Active Fuel Length (in.)	150.42	150.42	
Fuel Rod OD (in.)	0.379-0.406	0.387	
Clad Thickness (in.)	0.0248 -0.0268	0.0238	
Fuel Pellet OD (in.)	0.323-0.346	0.334	
No of Water Rods	0	0	
Water Rod OD (in.)	---	---	
Water Rod ID (in.)	---	---	

Notes:

1. All dimensions shown are nominal.
2. Reload FAs from other manufacturers with these parameters are also acceptable.
3. Solid Zircaloy rod(s).
4. Fuel bundles designated as ABB or SVEA are typically assembled from four sub-assemblies. There is a cruciform internal water channel between the sub-assemblies. The thickness of the water channel is 0.8 mm, the inner width of the channel is 4 mm for most ABB or SVEA bundles, except 2.4 mm for SVEA-Optima 1 and SVEA-Optima 2.
5. There is one rod that occupies the four central fuel rod locations and four water bars/channels that divide the FA into four quadrants.
6. Includes ENC III-E and ENC III-F
7. *Integral water channel which occupies the 3x3 center of the fuel rod array.*

Table 2-10
Time Limits for Transfer by HLZC

<i>DSC Model</i>	<i>Applicable HLZC</i>	<i>Time Limits (Hours)</i>
<i>EOS-89BTH</i>	<i>HLZC 1 or 2</i>	<i>10</i>
<i>EOS-89BTH</i>	<i>HLZC 3</i>	<i>No Limit</i>
<i>EOS-89BTH</i>	<i>HLZC 4-6</i>	<i>8</i>



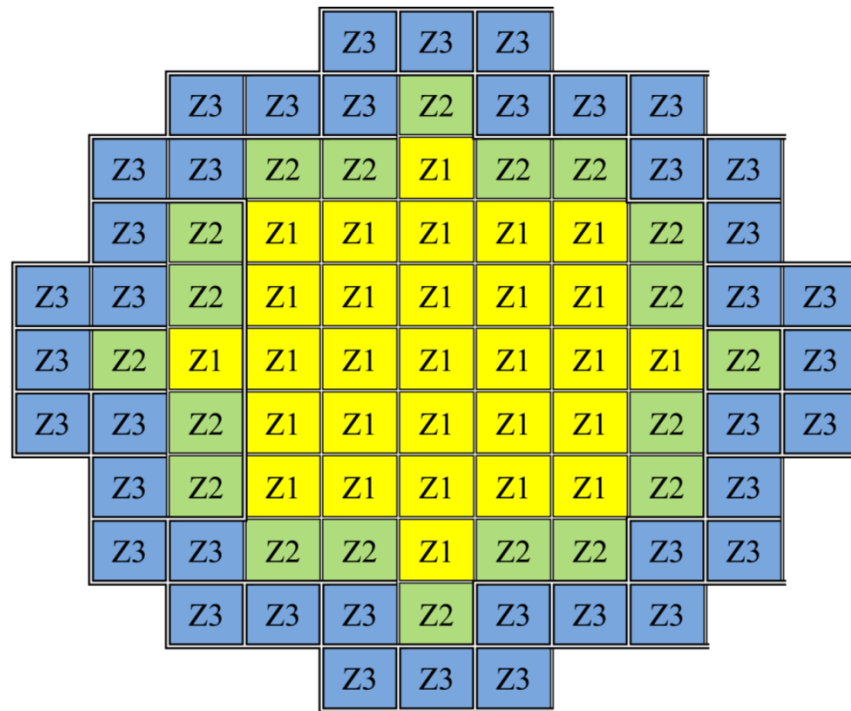
Heat Load Zone Configuration 1 for the EOS-89BTH DSC

Zone Number	1	2	3
Maximum Decay Heat ⁽¹⁾ (kW/FA plus channel, if included)	0.4	0.6	0.5
Maximum Number of Fuel Assemblies	29	20	40
Maximum Decay Heat per DSC (kW)	43.6		

Note:

1. See Systems Configuration Table 1-2 for allowable loading configurations.

Figure 2-2a
Heat Load Zone Configuration 1 for the EOS-89BTH DSC

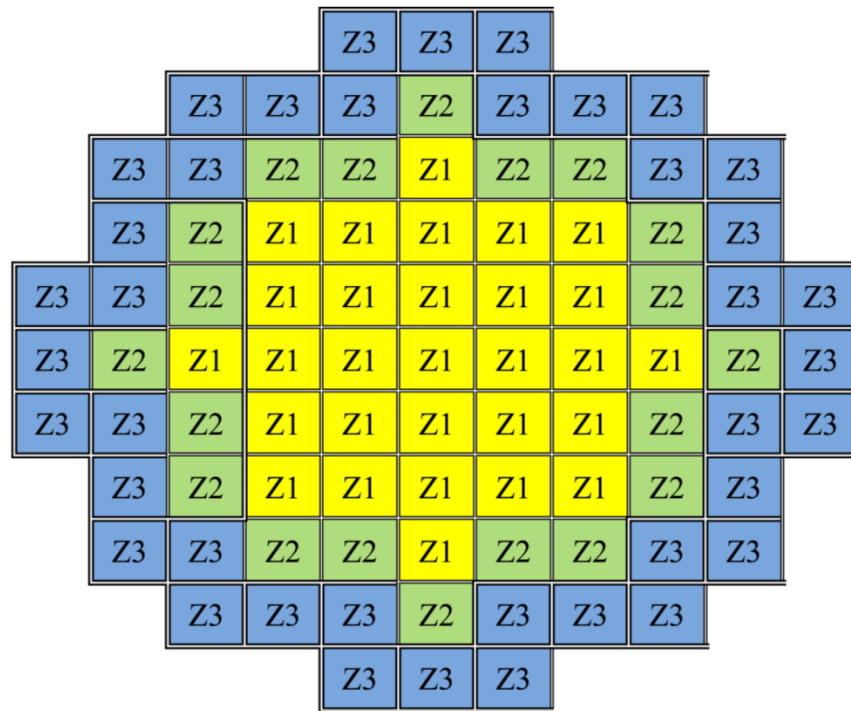


Zone Number	1 ⁽¹⁾	2 ⁽¹⁾	3 ⁽¹⁾
Maximum Decay Heat (kW/FA plus channel, if included)	0.4	0.5	0.5
Maximum Number of Fuel Assemblies	29	20	40
Maximum Decay Heat per DSC (kW)	41.6		

Notes:

1. For the EOS-TC108, the minimum cooling time is 3.0 years in Zones 1 and 2 and 9.7 years in Zone 3.
2. See Systems Configuration Table 1-2 for allowable loading configurations.

Figure 2-2b
Heat Load Zone Configuration 2 for the EOS-89BTH⁽²⁾

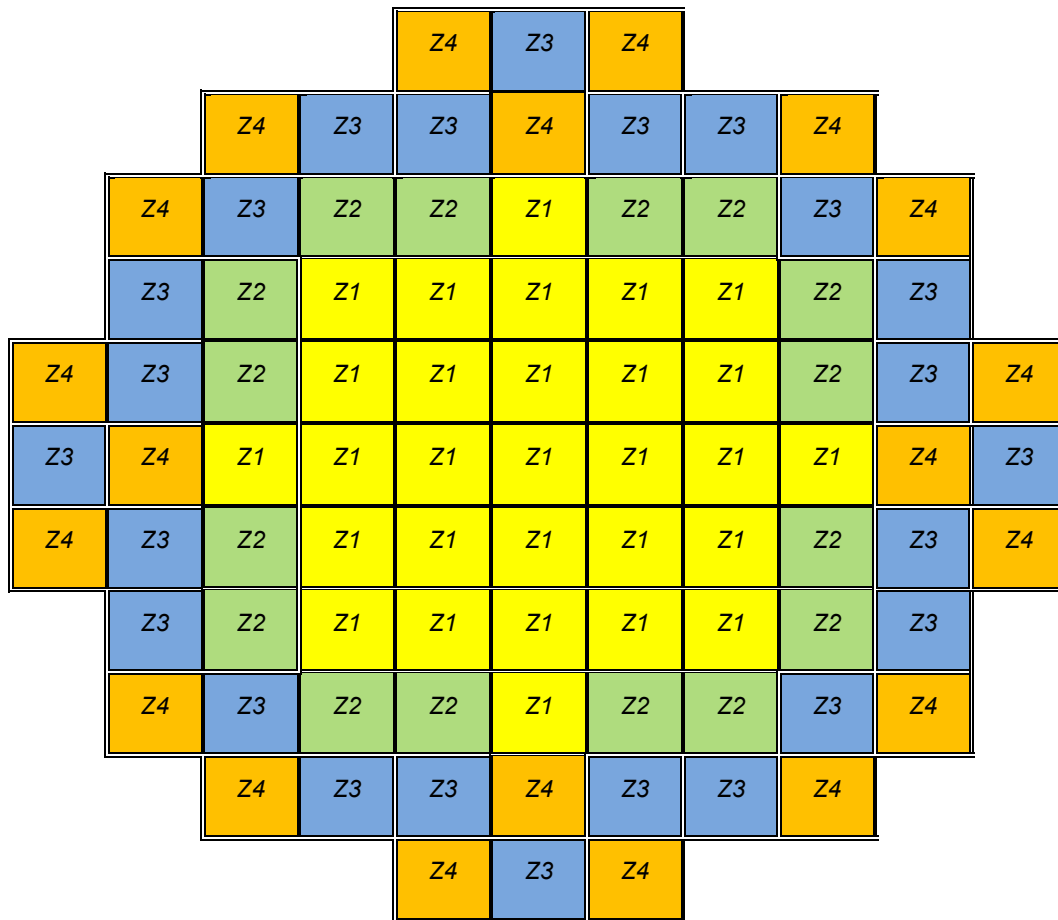


Zone Number	1 ⁽¹⁾	2 ⁽¹⁾	3 ⁽¹⁾
Maximum Decay Heat (kW/FA plus channel, if included)	0.36	0.4	0.4
Maximum Number of Fuel Assemblies	29	20	40
Maximum Decay Heat per DSC (kW)	34.44		

Notes:

1. For the EOS-TC108, the minimum cooling time is 3.0 years in Zones 1 and 2 and 9.0 years in Zone 3.
2. See Systems Configuration Table 1-2 for allowable loading configurations.

Figure 2-2c
Heat Load Zone Configuration 3 for the EOS-89BTH⁽²⁾

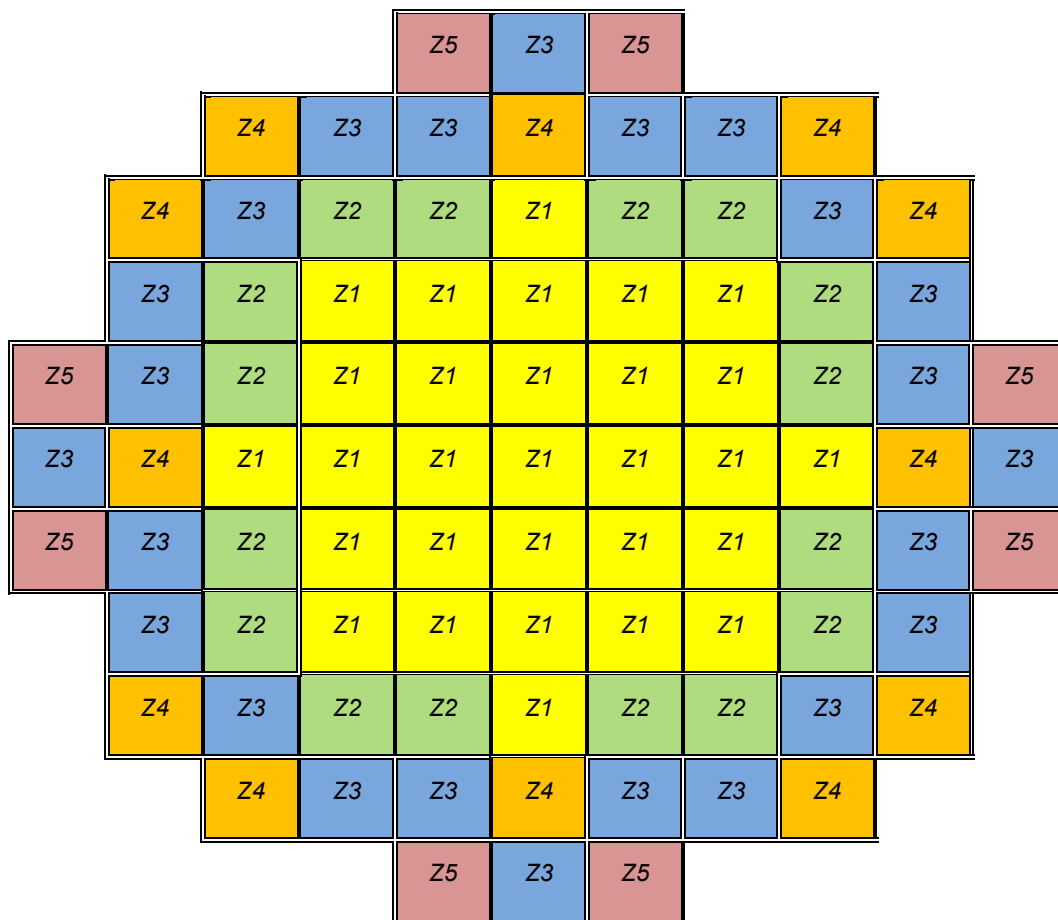


Zone No.	1	2	3	4
<i>EOS-HSM and HSM-MX Lower Compartment</i>				
<i>Max. Decay Heat per SFA (kW)</i>	0.400	0.600	0.500	0.75
<i>No. of Fuel Assemblies</i>	29	16	24	20
<i>Heat Load Per Zone</i>	11.6	9.6	12	15
<i>Max. Decay Heat per DSC (kW)</i>	EOS-HSM and HSM-MX Lower Compartment: 48.2 ⁽¹⁾ HSM-MX Upper Compartment: 41.8 ⁽¹⁾			

Notes:

1. Adjust payload to maintain total DSC heat load within the specified limit.
2. See Systems Configuration Table 1-2 for allowable loading configurations.

Figure 2-2d
Heat Load Zone Configuration 4 for the EOS-89BTH⁽²⁾

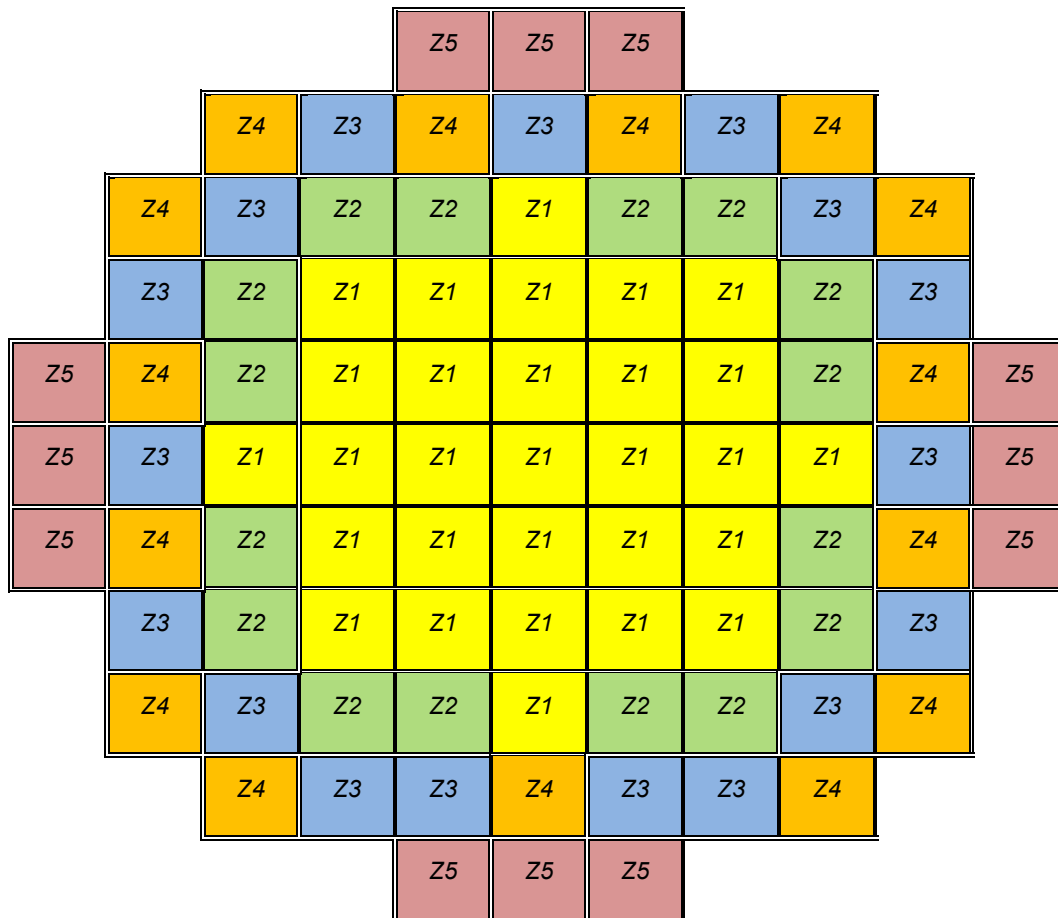


Zone No.	1	2	3	4	5
<i>EOS-HSM and HSM-MX</i>					
<i>Max. Decay Heat per SFA (kW)</i>	<i>0.300</i>	<i>0.400</i>	<i>0.500</i>	<i>1.200</i>	<i>1.700</i>
<i>No. of Fuel Assemblies</i>	<i>29</i>	<i>16</i>	<i>24</i>	<i>12</i>	<i>8</i>
<i>Heat Load Per Zone</i>	<i>8.7</i>	<i>6.4</i>	<i>12</i>	<i>14.4</i>	<i>13.6</i>
<i>Max. Decay Heat per DSC (kW)</i>	<i>EOS-HSM and HSM-MX Lower Compartment: 48.2⁽¹⁾</i> <i>HSM-MX Upper Compartment: 41.8⁽¹⁾</i>				

Notes:

1. Adjust payload to maintain total DSC heat load within the specified limit.
2. See Systems Configuration Table 1-2 for allowable loading configurations.

Figure 2-2e
Heat Load Zone Configuration 5 for the EOS-89BTH⁽²⁾



Zone No.	1	2	3	4	5
<i>EOS-HSM and HSM-MX Lower Compartment</i>					
<i>Max. Decay Heat per SFA (kW)</i>	0.300	0.400	0.500	1.300	1.000
<i>No. of Fuel Assemblies</i>	29	16	17	15	12
<i>Heat Load Per Zone</i>	8.7	6.4	8.5	19.5	12
<i>Max. Decay Heat per DSC (kW)</i>	<i>EOS-HSM and HSM-MX Lower Compartment: 48.2⁽¹⁾</i> <i>HSM-MX Upper Compartment: 41.8⁽¹⁾</i>				

Notes:

1. Adjust payload to maintain total DSC heat load within the specified limit.
2. See Systems Configuration Table 1-2 for allowable loading configurations.

Figure 2-2f
Heat Load Zone Configuration 6 for the EOS-89BTH⁽²⁾

load combinations, stress intensities under individual loads are added to obtain resultant stress intensities for the specified combined loads. This addition at the stress intensity level for the combined loads, instead of at component stress level, is also a conservative method for reducing the number of analysis runs.

The stresses of all components are assessed by means of elastic analysis methodology for all load combinations, except for accident loading conditions. Elastic-plastic analysis methodology is used to assess the stresses for Service Level D load combinations.

A detailed description of each load combination is provided in Section 3.9.1.2.8.

3.9.1.2.1 Material Properties

For elastic analysis, temperature dependent material properties used for each component of DSC shell assembly are obtained from the American Society of Mechanical Engineers (ASME) code [3.9.1-2], and are summarized in Chapter 8. Material properties used for stress evaluations are conservatively taken at 500 °F *under normal loading conditions*. For the partial penetration welds and grapple assembly, 350 °F allowable stresses are used for comparison to load induced stresses as these components remain below this lower temperature *under normal loading conditions*.

For plastic analysis, a bilinear stress-strain curve with a 5% tangent modulus is used for steel components. The non-linear material properties at 500 °F for side drop analysis are shown in Table 3.9.1-3. Steel material (except shield plugs) is modeled by bilinear kinematic hardening method (TB, BKIN – [3.9.1-9]).

3.9.1.2.2 DSC Shell Stress Criteria

The calculated stresses in the DSC shell assembly structural components are compared with the allowable stresses set forth by ASME Boiler and Pressure Vessel (B&PV) Code, Section III, Subsection NB [3.9.1-3] under normal (Level A), and off-normal (Level B) loading conditions. Appendix F of the ASME B&PV Code is used to evaluate the calculated stresses in the DSC shell assembly under accident (Level D) loading conditions. Allowable stress limits for Levels A, B and D service loading conditions, as appropriate, are summarized in Table 3-1, and the corresponding allowable stress values at different temperatures are summarized in Table 3.9.1-5 and Table 3.9.1-5a.

The OTCP-to-DSC shell weld and the ITCP-to-DSC shell weld, which are both partial penetration welds, are to be evaluated using a joint efficiency factor of 0.8. Per NUREG-1536 [3.9.1-7], the minimum inspection requirement for end closure welds is multi-pass dye penetrant testing (PT) using a stress (allowable) reduction factor of 0.8. *The OTCP-to-shell weld may instead be inspected by ultrasonic examination (UT), for which a stress reduction factor is not required.* The allowable weld stresses are summarized in Table 3.9.1-4 and Table 3.9.1-4a.

Amc 2 &
72.48

Horizontal Position in EOS-HSM

When stored in the EOS-HSM, the DSC shell is supported by two, 3-inch wide EOS-HSM slide rails at $\pm 30^\circ$ from the bottom centerline. The inertial loads for DSC internals are accounted for by applying equivalent pressure onto the inner surface of DSC shell representing the EOS-HSM support rail or EOS-HSM-FPS support rail only. The magnitude of the pressure is determined based on the payload of 105 kips and projected area that are in interface with the EOS-HSM support rail.

The interface between the DSC and the EOS-HSM support rail is modeled through node-to-node contact elements (CONTA178). Nodes that interface with the EOS-HSM support rail are selected and copied, creating new nodes. Each row of nodes represents the width of the EOS-HSM support rail (there are three nodes across the width of the rail). Each node of the row is coupled with its neighboring node in all DOF using CERIG command, creating a rigid platform. Figure 3.9.1-7 and Figure 3.9.1-7a show the pressure load and boundary conditions applied to the FEM.

Each middle node of this platform is connected in the axial direction of the DSC through BEAM188 element. Finally, these new nodes representing the EOS-HSM are connected to the original nodes belonging to the DSC shell through the CONTA178 contact elements. Gaps are set to zero, placing the DSC shell and the EOS-HSM support rail in initial contact. Nodes representing the EOS-HSM support rail are constrained in all DOF along a length of 16.5 inches from bottom end and 20.5 inches from the top end. The BEAM188 elements have the properties of the wide-flange steel beam that supports the DSC when inside the EOS-HSM or the plate that supports the DSC when inside the EOS-HSM-FPS.

3.9.1.2.7.2 Fabrication Pressure and Leak Testing

Pressurization and leak testing is performed on the DSC shell and IBCP during fabrication. *This pressure test is not required if the single piece of forged bottom is used. See Drawings EOS01-1001-SAR and EOS01-1006-SAR, sheet 2, detail 1, alternate 1.* No other DSC components are in place during this test. A seal plate is placed on the open top of the DSC shell and preloaded through the application of torque on eight bolts that are connected with a flange at the bottom of the DSC shell. The resulting preload to be considered in the evaluation is 155 kips. The DSC is then evacuated to a partial vacuum (simplified to full vacuum) and then re-pressurized with helium. Therefore, two load conditions are evaluated for the DSC shell and IBCP:

1. Leak Test: 155 kip axial compression + 14.7 psi external pressure (full vacuum) on the DSC shell between the top edge and the IBCP + 14.7 psi external pressure on the IBCP. Note that the vacuum will add axial load to the 155 kips preload.

For DSCs supported by the DSC support structure, the maximum ratio of induced load to allowable load for a confinement boundary area is 0.82, in the weld between the ITCP and the DSC shell during a side drop event. The maximum overall ratio of 0.92 occurs in the grapple ring support, seconded by a ratio of 0.85 in the non-confinement area of the DSC shell during a grapple pull/accident scenario.

For DSCs supported by the FPS DSC support structure, the maximum ratio of induced load to allowable load for a confinement boundary area is 0.74 and occurs in the confinement boundary area of the DSC shell while the DSC is in horizontal position as described in LC9. The maximum overall stress ratio is 0.92 and occurs in the grapple ring support, seconded by a ratio of 0.85 in the non-confinement area of the DSC shell during a grapple pull/accident scenario.

For the option with the Alternate 1-Bottom Forging, stress intensities in the Alternate 1-Bottom Forging are compared with ASME code allowables and the resulting stress ratios are summarized in Table 3.9.1-16. The maximum ratio of 0.45 occurs in the Alternate 1-Bottom Forging during a side drop. Stress intensities for the DSC without the Alternate 1-Bottom Forging are generally bounding for the other components.

The maximum OTCP-to-shell weld stress ratio is 0.68, which is based on the use of PT testing and the stress reduction factor of 0.8. When the weld is inspected by UT, the stress reduction factor is not required and the resulting minimum required weld size, for a stress ratio of 0.90, is 0.30 inch.

The above evaluations, specifically the closure welds, are supplemented with additional limit load and strain criteria analyses. These analyses are presented in Section 3.9.1.2.6. The results of the limit load analysis show that there is sufficient margin compared to the design loads. The results of the strain criteria analysis show a maximum equivalent plastic strain of 0.065 in/in during a side drop event, compared to the allowable uniform strain limit of 0.17 in/in, demonstrating a minimum factor of safety of 2.6 in the design. The factor of safety is calculated by dividing the maximum allowable strain by the maximum equivalent plastic strain, and must be greater than 1.

The structural integrity of the DSC shell, including closure welds, is maintained since the maximum stress ratio is less than 1 and the limit load and strain criteria analyses results were lower than their respective limits.

72.48

3.9.5 NUHOMS® EOS-TC BODY STRUCTURAL ANALYSIS

3.9.5.1 General Information

This appendix covers the structural evaluation of the transfer cask (TC) when carrying a loaded DSC. The TC structure is designed to American Society of Mechanical Engineers (ASME) NF-3200 [3.9.5-3] stress limits to the greatest degree practical. The trunnions and trunnion welds to the TC top ring are designed to American National Standards Institute (ANSI) N14.6 [3.9.5-2] stress limits for non-redundant lifting. Structural evaluation of the TC for the missile impact load cases is covered in Appendix 3.9.7, and not presented in this Appendix.

A geometric- and load-bounding representation, enveloping the three EOS-TCs (EOS-TC108, EOS-TC125 and EOS-TC135), is referred to as EOS-TCMAX in this evaluation. The geometric dimensions for this bounding model are selected to yield the most bounding stresses and deformations. *The bounding model lead thickness is 2.5", based on the EOS-TC108 lead dimension, and is therefore inclusive of the EOS-TC125 in all lead thickness variations.*

3.9.5.2 EOS Transfer Cask Accident (Side and End) Drop Evaluation for 65g Static Load

The purpose of this section is to summarize the structural evaluation of the EOS-TC for the postulated accident side and end drop conditions. The Service Level D drop evaluations are done by means of 3-D elastic-plastic model. Structural integrity of the design is evaluated by means of plastic analysis criteria of Reference [3.9.5-3].

3.9.5.2.1 Material Properties

Mechanical properties of cask components are evaluated at a temperature of 400 °F, except for the trunnions, which are evaluated at 367 °F. These temperatures exceed the maximum temperature of cask body for all cask designs. A bilinear stress-strain curve with a 5% tangent modulus is used for steel components. The lead material is modeled by bilinear kinematic hardening method. All the EOS-TC material properties are listed in Chapter 8.

3.9.5.2.2 Design Criteria

The EOS-TC is analyzed using ASME code, Section III, Appendix F requirements service level D allowable stresses for plastic analysis.

Proprietary Information on Pages 3.9.6-10 and 3.9.6-11
Withheld Pursuant to 10 CFR 2.390

Proprietary Information on Pages 3.9.6-13 through 3.9.6-15
Withheld Pursuant to 10 CFR 2.390

Proprietary Information on Pages 3.9.6-24 through 3.9.6-29
Withheld Pursuant to 10 CFR 2.390

Proprietary Information on Pages 3.9.6-58 through 3.9.6-60
Withheld Pursuant to 10 CFR 2.390

4. THERMAL EVALUATION

NOTE: For *EOS-37PTH DSC and the EOS-89BTH DSC with* HLZCs 1 through 3, the basket types directly correlate to the Heat Load Zone Configurations (HLZCs), throughout this chapter, basket types are directly referred to by the HLZC. For HLZCs 4 through 11 *for EOS-37PTH DSC and HLZCs 4 through 6 for EOS-89BTH DSC*, the basket types do not directly correlate to the HLZC. A description of the various basket assembly types is presented in Chapter 1, Section 1.1.

The thermal evaluation described in this chapter is applicable to the NUHOMS® EOS System that includes an EOS-37PTH or EOS-89BTH dry shielded canisters (DSCs) loaded inside the EOS-TC108, EOS-TC125 or EOS-TC135 transfer cask (TC) and the EOS horizontal storage module (HSM) or EOS-HSMS. With respect to thermal evaluations, the EOS-HSM and EOS-HSMS are identical; therefore, when the EOS-HSM is referred to in this chapter, the analysis is applicable to both the EOS-HSM and EOS-HSMS. A flat plate support structure (FPS) is an option for the medium length EOS-HSM/HSMS, which allows a DSC support structure to be built up from a flat plate. This option is referred to as the EOS-HSM-FPS or EOS-HSMS-FPS.

A summary of the EOS-37PTH and EOS-89BTH DSC configurations analyzed in this chapter and Chapter A.4 is shown in Chapter 1, Table 1-2.

Descriptions of the detailed analyses performed for normal, off-normal, and hypothetical accident conditions are provided in Section 4.4 for storage operations in the EOS-HSM, Section 4.5 for transfer operations in the EOS-TC125/EOS-TC135, and Section 4.6 for transfer operations in the EOS-TC108 up to a maximum heat load of 41.8 kW in EOS-37PTH DSC and 41.6 kW in EOS-89BTH DSC. The thermal analyses performed for the loading and unloading conditions are described in Section 4.5.11. DSC internal pressures are discussed in Section 4.7. The thermal performance of the FPS option of the EOS-HSM is discussed in Appendix 4.9.5.

Appendix 4.9.6 and Chapter A.4 present the thermal evaluation of the EOS-37PTH DSC with HLZCs 4 through 6 and HLZCs 7 through 9, respectively for storage operations. Thermal evaluation of the EOS-37PTH DSC with HLZCs 4 through 9 is presented in Appendix 4.9.6 for transfer operations. Appendix 4.9.6 also includes the thermal evaluation of transfer operations for EOS-TC108 with EOS-37PTH DSC and heat loads greater than 41.8 kW. Appendix 4.9.7 presents the thermal evaluation of the EOS-37PTH DSC with HLZCs 10 and 11 for storage operations in the EOS-HSM and transfer operations in the EOS-TC125/EOS-TC135. Section A.4.6 in Chapter A.4 presents the thermal storage evaluation of the EOS-37PTH DSC with HLZC 11 in the HSM-MX. Thermal evaluation of the EOS-89BTH DSC with HLZCs 3 through 6 during storage operations in the HSM-MX is presented in Chapter A.4.

Appendix 4.9.8 presents the thermal evaluation of the EOS-89BTH DSC with HLZCs 4 through 6 for storage operations in the EOS-HSM and transfer operations in the EOS-TC125.

4.1 Discussion of Decay Heat Removal System

The EOS-37PTH and EOS-89BTH DSCs are designed to passively reject decay heat during storage and transfer for normal, off-normal, and hypothetical accident conditions while maintaining temperatures and pressures within specified limits. Objectives of the thermal analyses performed for this evaluation include:

- Determination of maximum and minimum temperatures with respect to material limits to ensure components perform their intended safety functions,
- Determination of temperature distributions to support the calculation of thermal stresses,
- Determination of maximum DSC internal pressures for normal, off-normal, and hypothetical accident conditions, and
- Determination of the maximum fuel cladding temperature, and to confirm that this temperature will remain sufficiently low to prevent unacceptable degradation of the fuel during storage.

The EOS-37PTH DSC is analyzed based on a maximum heat load of 50.0 kW from 37 pressurized water reactor (PWR) fuel assemblies (FAs) with a maximum heat load of 3.5 kW per assembly. The EOS-89BTH DSC is analyzed based on a maximum heat load of 48.2 kW from 89 boiling water reactor (BWR) fuel assemblies (FAs) with a maximum heat load of 1.7 kW per assembly. The authorized HLZCs for the EOS-37PTH DSC are provided in Figure 1 of the Technical Specification [4-24]. Figure 1 of the Technical Specification [4-24] is split into eleven sub parts, one for each HLZC of the EOS-37PTH DSC. The authorized HLZCs for the EOS-89BTH DSC are provided in Figure 2-2a through Figure 2-2f in Chapter 2 for transfer in the EOS-TC125 and Figure 2 of the TS [4-24] for the EOS-89BTH when transferred in the EOS-TC108.

Fuel assemblies are considered as homogenized materials in the fuel compartments. The effective thermal conductivity of the FAs used in the thermal analysis is based on the conservative assumption that heat transfer within the fuel region occurs only by conduction and radiation where any convection heat transfer is neglected. The lowest effective properties among the applicable FAs are selected to perform the thermal analysis. Evaluations of heat transfer from the FAs to the basket assembly credits conduction through the basket assembly materials (steel/metal matrix composite/aluminum) and helium fill gas within the DSC. Convection and radiation heat transfer within the basket assembly are conservatively ignored.

8.a Bounding Effective Specific Heat and Density of Fuel Assemblies in EOS-89BTH DSC

<i>T</i>	<i>C_{p eff}</i>	<i>ρ_{eff}</i>
<i>(K)</i>	<i>(J/kg-K)</i>	<i>(kg/m³)</i>
300.15	243	2592
400.15	271	
640.15	301	
1090.15	327	

Proprietary Information on Pages 4-20 and 4-21
Withheld Pursuant to 10 CFR 2.390

Proprietary Information on Pages 4-24 and 4-25
Withheld Pursuant to 10 CFR 2.390

Airflow Calculations

Table 4-9 summarizes the air temperatures and mass flow rates at the inlet and outlet for Load Cases 3 and 4 for off-normal conditions of storage. The air temperatures are increased by 99 °F and 75 °F for off-normal hot and cold conditions, respectively. The mass flow rate imbalances between the inlet and outlet are five to six orders of magnitude lower than the mass flow rates through the inlet and outlet for off-normal conditions. Therefore, the airflow calculations are convergent.

4.4.5 EOS-37PTH DSC - Hypothetical Accident Conditions of Storage

Temperature Calculations

The maximum temperatures of fuel cladding and concrete of EOS-HSM loaded with EOS-37PTH DSC for hypothetical accident condition of storage (Load Case 5) are summarized in Table 4-5.

The maximum temperatures of various components of the EOS-HSM loaded with the EOS-37PTH DSC for hypothetical accident condition of storage (Load Case 5) are summarized in Table 4-6. The average temperatures of key components of the EOS-HSM loaded with the EOS-37PTH DSC for hypothetical accident condition of storage (Load Case 5) are summarized in Table 4-7. The values listed in Table 4-6 and Table 4-7 for Load Case 5 are based on transient simulation results at 40 hours.

Typical temperature plots for the key components in the EOS-HSM loaded with the EOS-37PTH DSC are shown in Figure 4-15 for hypothetical accident conditions.

For the accident blocked vent condition, the time histories of the maximum and average temperatures for the key components are shown in Figure 4-16. All the temperatures increase steadily during the 40 hours of blocked vent event.

4.4.6 EOS-89BTH DSC - Description of Loading Cases for Storage

To determine the thermal performance of the EOS-HSM loaded with the EOS-89BTH DSC, the load cases listed in Table 4-14 are evaluated for normal, off-normal and accident conditions using the CFD model described in Section 4.4.7.3.

The HLZCs 1, 2, and 3 are described in Figure 2-2a through Figure 2-2c in Chapter 2 for the EOS-89BTH DSC. As shown in Figure 2-2a through Figure 2-2c in Chapter 2, HLZCs 1, 2 and 3 have identical zoning with different allowable heat loads. Since HLZC 1 has the maximum total heat load and the maximum heat load per fuel assembly in each zone, it is the bounding HLZC among all HLZCs. Therefore, load cases for normal, off-normal, and accident conditions will be evaluated with HLZC 1. No thermal evaluation is performed for HLZCs 2 and 3 for all storage conditions.

Proprietary Information on This Page
Withheld Pursuant to 10 CFR 2.390

As discussed in Appendix 4.9.6.1.1, EOS-37PTH Type 4H basket has the same emissivity of steel plates and conductivity of poison material as those of the EOS-37PTH Type 1 basket. Therefore, the thermal evaluations for EOS-37PTH Type 1 basket for transfer conditions in this section are also applicable to EOS-37PTH Type 4H basket. However, the time limit for transfer operations for HLZC 1 when loaded in an EOS-37PTH Type 4H basket is reduced from 10 hours to 8 hours. Based on the thermal evaluation for Load Case 1 for HLZC 1, the maximum fuel cladding temperature at 8 hours is 697 °F. If the transfer operations cannot be completed within this time limit, LCO 3.1.3 of Technical Specification [4-24] allows 5 hours to complete recovery actions A.1 or A.2 or A.3. Including this 5 hours, the maximum fuel cladding temperature at the end of 13 hours (8 hours for initial transfer + 5 hours for recovery actions) is 730 °F.

Table 4-31 presents an overview of time limits of the transfer operations based on the discussions presented in Section 4.5.3.

The time limits for transfer operations presented in Table 4-31 are based on the maximum heat load of 50.0 kW and the bounding ambient conditions noted in Section 4.3. However, if the maximum heat load for a loaded DSC is between 36.35 kW and 50 kW, the time limits for transfer operations can be recalculated based on the maximum heat load and ambient conditions for that DSC using the methodology/models presented in Sections 4.5.1 and 4.5.2 to provide more accurate time limits for transfer operations.

4.5.5 EOS-37PTH DSC - Hypothetical Accident Conditions of Transfer

Temperature Calculations

As noted in Section 4.5.1, the accident condition with loss of neutron shield and loss of air circulation (Load Case 5) is bounding for the fire accident case. The maximum temperatures for the bounding Load Case 5 are presented in Table 4-28. As shown in Table 4-28, maximum component temperatures are below the allowable limits. Figure 4-39 presents the temperature profiles for the loss of neutron shield and loss of air circulation accident condition for the EOS- TC125 TC loaded with the EOS-37PTH DSC and 50.0 kW heat load.

4.5.6 EOS-89BTH DSC - Description of Load Cases for Transfer

The loading cases considered for transfer of the EOS-89BTH DSC are identical to those described for the EOS-37PTH DSC in Section 4.5.1 and listed in Table 4-23. However, the maximum heat loads and HLZCs for the EOS-89BTH DSC are different from those considered for the EOS-37PTH DSC. The load cases listed in Table 4-23 are applicable to the EOS-89BTH DSC based on the maximum heat loads and the HLZCs 1, 2, and 3 shown in Figure 2-2a through Figure 2-2c in Chapter 2. As shown in Figure 2-2a through Figure 2-2c in Chapter 2, HLZCs 1, 2 and 3 are subject to maximum heat loads of 43.6, 41.60 and 34.44 kW, respectively.

4.5.11 Thermal Evaluation for Loading/Unloading Conditions

All fuel loading operations occur when the EOS-37PTH/EOS-89BTH DSCs and EOS-TC125/TC135/TC108 are in the spent fuel pool. The fuel is always submerged in free-flowing pool water permitting heat dissipation. After completion of the fuel loading, the TC and DSC are removed from the pool and the DSC is drained, dried, sealed, and backfilled with helium. These operations occur when the annulus between the TC and DSC remains filled with water.

The water in the annulus is monitored and replenished with fresh water to maintain the water level if excessive evaporation occurs, as noted for the fuel loading operation procedures in Section 9.1. Presence of water within the annulus maintains the maximum DSC shell temperature below the boiling temperature of water in the annulus between the DSC and TC (223 °F).

Water in the DSC cavity is forced out of the cavity (blowdown operation) before the start of vacuum drying. Helium is used as the medium to remove water and subsequent vacuum drying occurs with a helium environment in the DSC cavity. Since the DSC is filled with helium after drainage of water and water is maintained in the annulus between the DSC and TC, there is no time limit for completion of the vacuum drying process.

The vacuum drying of the DSC does not reduce the pressure sufficiently to reduce the thermal conductivity of the helium in the DSC cavity. Section 10-5 of [4-29] reviews the impact of low pressures on thermal conductivity of gases and concludes that when pressure is above 10^{-3} bar (0.75 Torr), there is a negligible change in the thermal conductivity with pressure.

72.48

With helium being present during vacuum drying operations and the TC/DSC annulus water temperature equal to water boiling temperature of 223 °F, the EOS-37PTH and EOS-89BTH DSC models described in Sections 4.5.2 and 4.5.7, respectively, are used in a steady-state analysis to determine the maximum fuel cladding temperatures for vacuum drying operations in the EOS-37PTH and EOS-89BTH DSCs. The maximum fuel cladding temperatures for vacuum drying operations in the EOS-37PTH and EOS-89BTH DSCs are, respectively, 648 °F at 50 kW decay heat load and 637 °F at 43.6 kW decay heat load, as noted in Table 4-32.

For EOS-89BTH DSC with HLZC 4, 5 and 6 with a maximum heat load of 48.2 kW, the maximum fuel cladding temperature for vacuum drying operations is 653 °F based on the initial conditions for LC 1 as shown in Table 4.9.8-9.

The presence of helium during blowdown and vacuum drying operations and the cooling provided by water in the annulus between the DSC and TC eliminate the thermal cycling of fuel cladding during helium backfilling of the DSCs subsequent to vacuum drying. Therefore, the thermal cycling limit of 65 °C (117 °F) for short-term operations set by NUREG-1536 [4-1] is satisfied for vacuum drying operation.

4.6 Thermal Evaluation for Transfer in EOS-TC108

This section presents a summary of the thermal evaluation of the EOS-TC108 with the EOS-37PTH DSC or the EOS-89BTH DSC. As shown in Table 1-1, the EOS-TC108 has a lower weight compared to the EOS-TC125/EOS-TC135, which in turn, contributes to a lower thermal mass. Due to this lower thermal mass, the maximum heat loads allowed are limited to 41.8 kW for EOS-37PTH DSC and 41.6 kW for EOS-89BTH DSC.

Similar to the EOS-TC125, the EOS-TC108 contains design provisions for the use of air circulation system to improve its thermal performance for heat loads greater than 36.35 kW and 34.44 kW for EOS-37PTH and EOS-89BTH DSCs, respectively. The air circulation system consists of redundant, industrial grade pressure blowers and power systems, ducting, etc. When operating, the fan system is expected to generate a flow rate of 850 cfm or greater, which will be ducted to the location of the ram access cover at the bottom of the TC. The air circulation system is not needed for heat loads ≤ 36.35 kW in EOS-37PTH DSC and ≤ 34.44 kW in EOS-89BTH DSC.

4.6.1 Description of Load Cases for Transfer

The various load cases considered for evaluating the thermal performance of the EOS-TC108 are listed in Table 4-36. The load cases shown in Table 4-36 for EOS-TC108 are similar to the load cases shown in Table 4-23 for EOS-TC125, except for the maximum allowable heat load for Load Cases 1 through 7. For Load Cases 1 through 7, the transfer operations in EOS-TC108 are limited to heat loads based on HLZC 2, shown in Figure 1 of the Technical Specifications [4-24], for EOS-37PTH DSC, and in *Figure 2 of the TS [4-24]* for the EOS-89BTH DSC, unlike the EOS-TC125, where both HLZCs 1 and 2 are allowed. For Load Cases 8 through 10, based on HLZC 3, the maximum heat load of the EOS-37PTH DSC and the EOS-89BTH DSC, during transfer in EOS-TC108, remains identical to that considered in EOS-TC125.

Similar to the approach presented in in Section 4.5.6 for the thermal evaluation of EOS-89BTH DSC in EOS-TC125, the thermal evaluation for EOS-37PTH and EOS-89BTH DSCs during transfer in EOS-TC108 does not analyze all the load cases shown in Table 4-36. Instead, the thermal evaluations are only performed to verify that the maximum temperatures and time limits computed for the EOS-37PTH DSC in EOS-TC125 remain bounding for the EOS-TC108 with either the EOS-37PTH DSC or the EOS-89BTH DSC.

[

]

The methodology to determine the axial conductivity is described in Section P.4.8.1.3 of the Standardized NUHOMS® System UFSAR [4.9.1-2] and is used in this evaluation based on the bounding FA and the properties described above. Similarly, the effective density and specific heat are determined based on the methodology presented in Section P.4.8.2 of the Standardized NUHOMS® System UFSAR, using the bounding FA and the properties described above.

Using the methodology presented in Appendix P, Section P.4.8.1.4 of the Standardized NUHOMS® System [4.9.1-2], a two-dimensional (2D) finite element model (FEM) of WE14x14 OFA FA is developed in ANSYS [4.9.1-3] to determine the transverse effective conductivity. The outer surfaces, representing the fuel compartment walls, are held at a constant temperature, and heat generating boundary condition is applied to the fuel pellets within the model. The models were run with a series of isothermal boundary conditions applied to the nodes representing the fuel compartment walls. The FEMs of WE14x14 OFA FA is shown in Figure 4.9.1-1. Figure 4.9.1-2 shows the heat generation rate and temperature boundary conditions.

The computed FA transverse and axial effective conductivities as functions of temperature for irradiated WE14x14 FA are listed in Table 4.9.1-3 and also summarized in Section 4.2.1. The effective specific heat and density for irradiated WE14x14 FA is shown is listed in Table 4.9.1-4 and also summarized in Section 4.2.1. The effective thermal conductivities for the FAs are also applicable for vacuum drying conditions since helium is used for water blowdown from the DSC.

4.9.1.2 Effective Thermal Properties for BWR Spent Fuel Assemblies in EOS-89BTH DSC

The FAs considered for storage in the EOS-89BTH DSC including the design data for each FA, are listed in Table 2-3 and Table 2-4. The FAs listed in Table 2-3 are previously studied in Section T.4.8 and Section Y.4.9 of the Standardized NUHOMS® System UFSAR[4.9.1-2], except for the GNF2 FA. However, the dimensions of GNF2 FA listed in Table 2-3 are very similar to the previously evaluated GE12/GE14 FAs from Section T.4.8 and Section Y.4.9 of the Standardized NUHOMS® System UFSAR. Therefore, the thermal properties for the GE12/GE14 FAs are also applicable to the GNF2 FA.

Section T.4.8.1.6 and Section T.4.8.2 of Standardized NUHOMS® System UFSAR [4.9.1-2], evaluated the effective thermal properties of ATRIUM-11 for storage in the NUHOMS® 61BTH DSC and concluded that ATRIUM-11 remains bounded by other FAs. Since the same methodology is used in evaluating the bounding properties for the fuel assemblies stored in EOS-89BTH, a similar behavior will be observed and no further evaluation is needed.

In addition to the FAs analyzed in Section T.4.8 and Section Y.4.9 of the Standardized NUHOMS® System UFSAR, the EOS-89BTH DSC allows for the storage of certain European and Japanese FAs as shown in Table 2-4.

A comparison of the FA characteristics of the European and Japanese FAs from Table 2-4 to those previously analyzed in Table 2-3 shows that they are either identical or very similar as described below.

- Geometries of Japanese boiling water reactor (BWR) FA (assembly type 8x8 Step II) and Switzerland– KKL BWR 1/4 fuel assembly (assembly type 8x8) from Table 2-4 are similar to GE8 Type II FA (TN ID: 8x8-60/4) from Table 2-3.
- Geometry of Switzerland– KKL BWR 2/5/8 FA (assembly type 9x9) from Table 2-4 is similar to GE 11/13 FA (TN ID: 9x9-74/2) from Table 2-3.
- Geometry of Switzerland– KKL BWR 3/9/12/13 FA (assembly type 10x10) from Table 2-4 is similar to GE 12/14 FA (TN ID: 10x10-92/2) from Table 2-3.
- Geometry of Switzerland– KKL BWR 6 FA (assembly type 4x4x4) from Table 2-4 is identical or similar to SVEA-64 FA from Table 2-3.
- Geometries of Switzerland– KKL BWR 7/14 FA (assembly type 4x(5x5-1)), BWR 10/15 FA (assembly type 4x(5x5-3)/4x(5x5-1)) and BWR 11/16 FA (assembly type 4x(5x5-4)/4x(5x5-2)/4x(5x5-1)) from Table 2-4 are similar to SVEA-96 FA from Table 2-3.

Since the European or Japanese FAs are identical or very similar to the assemblies presented in Table 2-3, the thermal properties for these FAs will be bounded by the properties of the corresponding assemblies from Table 2-3. Among the various FAs listed in Table 2-3, based on the study in Section T.4.8 and Section Y.4.9 of the Standardized NUHOMS® System UFSAR, the FANP 9x9-81 FA has the bounding transverse effective conductivity. Therefore, the transverse effective conductivities are recomputed using the methodologies presented in Section T.4.8 of the Standardized NUHOMS® System UFSAR using irradiated UO₂ properties and the EOS-89BTH DSC basket configuration shown in the drawings in Section 1.3.2.

Using the methodology presented in Section T.4.8.1.4 of the Standardized NUHOMS® System UFSAR, a 2D FEM of FANP 9x9-81 FA is developed in ANSYS [4.9.1-3] to determine the transverse effective conductivity. The outer surfaces, representing the fuel compartment walls, are held at a constant temperature, and heat generating boundary condition is applied to the fuel pellets within the model. The models were run with a series of isothermal boundary conditions applied to the nodes representing the fuel compartment walls. The FEMs FANP 9x9-81 FA is shown in Figure 4.9.1-3. Figure 4.9.1-4 shows the heat generation rate and temperature boundary conditions.

The methodology to determine the axial conductivity is described in Section T.4.8.1.3 of the Standardized NUHOMS® System [4.9.1-2] and is used in this evaluation for the various FAs listed in Table 2-3 and Table 2-4.

The computed bounding fuel assembly transverse and axial effective conductivities as functions of temperature for the various FAs allowed for storage in EOS-89BTH DSC are listed in Table 4.9.1-5 and also summarized in Section 4.2.1. The effective thermal conductivities determined for the bounding FAs are also applicable for vacuum drying conditions since helium is used for water blowdown from the DSC.

The bounding effective specific heat based on GE1/2/3 FA and bounding effective density based on Switzerland- KKL BWR 10/15 FA are listed in Table 4.9.1-7 and also summarized in Section 4.2.1.

4.9.1.3

Scaling Factors for Short and Long Fuel Assemblies

The various heat load zone configuration (HLZCs) presented in Figure 1 of the Technical Specifications [4.9.1-6] for the EOS-37PTH DSC and *Figure 2-2a through Figure 2-2f in Chapter 2* for the EOS-89BTH DSC are evaluated in Sections 4.4, 4.5, 4.6, and *Appendix 4.9.8* at the maximum allowable heat loads for each HLZC, assuming that the FA has an active fuel length of 144 inches.

For FAs with active fuel length shorter than 144 inches, there is a possibility that the concentration of the heat generation in a smaller volume might result in a non-conservative temperature distribution. To ensure that the temperature distributions evaluated in Sections 4.4, 4.5, and 4.6 remain bounding, the maximum allowable heat load for FAs with active fuel length shorter than 144 inches should be determined as discussed below.

Since conduction with effective conductivities is the only heat transfer path considered in the EOS-37PTH and EOS-89BTH DSCs, the temperatures are directly proportional to the FA heat load and inversely proportional to the active fuel length and effective fuel conductivity. Therefore, the following equations are used to determine the heat load for FAs with active fuel length shorter than 144 inches in order to maintain the temperatures at the same level as those determined from the bounding FAs.

$$\left(\frac{q}{L_a k_{eff}} \right)_{Short\ FA} = \left(\frac{q}{L_a k_{eff}} \right)_{Bounding\ FA}$$

$$q_{Short\ FA} = q_{Bounding\ FA} \cdot SF,$$

$$SF = \frac{L_{a,Short\ FA}}{L_{a,Bounding\ FA}} \cdot \frac{k_{eff,Short\ FA}}{k_{eff,Bounding\ FA}}.$$

Where,

k_{eff} = Effective conductivity for FA,

q = Decay heat load per assembly defined for each loading zone,

L_a = Active fuel length,

SF = Scaling factor (SF) for short FAs.

The SF determined from the equation should be used to reduce the maximum heat load per FA in each loading zone of the HLZCs presented Figure 1 of the Technical Specifications [4.9.1-6] for the EOS-37PTH DSC and *Figure 2-2a through Figure 2-2f in Chapter 2* for the EOS-89BTH DSC.

In the above equation, the effective conductivities for the bounding FA are presented in Table 4.9.1-3 and Table 4.9.1-5 for the EOS-37PTH DSC and EOS-89BTH DSC, respectively. The effective conductivity for the shorter FA should be determined using the same approach presented in Section 4.9.1.1 for the PWR FAs and Section 4.9.1.2 for the BWR FAs.

An alternate option with a low emissivity coating is used for the basket steel plates in the EOS-37PTH DSC. The effective thermal properties for the bounding FA with the low emissivity coating is presented in Section 4.9.1.4.

However, for FAs with active fuel length greater than 144 inches, no scaling is necessary and the maximum heat loads listed for each HLZC in Figure 1 of the Technical Specifications [4.9.1-6] for the EOS-37PTH DSC and *Figure 2-2a through Figure 2-2f in Chapter 2* for the EOS-89BTH DSC are applicable.

4.9.1.5 References

- 4.9.1-1 NUREG-1536, “Standard Review Plan for Spent Fuel Dry Cask Storage Systems at a General License Facility,” Revision 1, U.S. Nuclear Regulatory Commission, July 2010.
- 4.9.1-2 Areva TN Americas, “Updated Final Safety Analysis Report, Standardized NUHOMS® Horizontal Modular Storage System for Irradiated Nuclear Fuel, NUH-003,” Revision 14, September 2014.
- 4.9.1-3 ANSYS Mechanical APDL, Version 10.0.
- 4.9.1-4 NUREG/CR-7024 (PNNL-19417), “Material Property Correlations: Comparisons between FRAPCON-3.4, FRAPTRAN 1.4, and MATPRO,” U.S. Nuclear Regulatory Commission, March 2011.
- 4.9.1-5 Oak Ridge National Laboratory, RSIC Computer Code Collection, “SCALE, A Modular Code System for Performing Standardized Computer Analysis for Licensing Evaluation,” NUREG/CR-0200, Rev. 6, Volume 3, Section M8 (ORNL/NUREG/CSD-2/V3/R6), Oak Ridge National Laboratory, Oak Ridge, Tennessee, May 2000.
- 4.9.1-6 CoC 1042 Appendix A, NUHOMS® EOS System Generic Technical Specifications, Amendment 3.

Table 4.9.1-7
Bounding Effective Specific Heat and Density in EOS-89BTH DSC

<i>Bounding SFA</i>	<i>GE1/2/3 FA</i>	<i>Switzerland – KKL BWR 10/15 FA</i>
<i>T</i>	<i>C_{p eff}</i>	<i>ρ_{eff}</i>
<i>(°F)</i>	<i>(Btu/lb_m-°F)</i>	<i>(lb_m/in³)</i>
80	0.0581	0.0936
260	0.0648	
692	0.0719	
1502	0.0780	
<i>SI Units</i>		
<i>T</i>	<i>C_{p eff}</i>	<i>ρ_{eff}</i>
<i>(°C)</i>	<i>(kJ/kg-K)</i>	<i>(kg/m³)</i>
27	0.243	2592
127	0.271	
367	0.301	
817	0.327	

APPENDIX 4.9.8

THERMAL EVALUATION OF EOS-89BTH DSC FOR HLZCS 4 THROUGH 6

Table of Contents

4.9.8 THERMAL EVALUATION OF EOS-89BTH DSC FOR HLZCS 4 THROUGH 6.....	4.9.8-1
4.9.8.1 Description of HLZCs 4, 5 and 6	4.9.8-1
4.9.8.2 Storage Evaluation in HLZCs 4, 5 and 6	4.9.8-3
4.9.8.3 Transfer Evaluation in HLZCs 4, 5 and 6	4.9.8-8
4.9.8.4 References	4.9.8-14

List of Tables

Table 4.9.8-1	Design Load Cases for EOS-HSM Loaded with EOS-89BTH DSC Basket.....	4.9.8-15
Table 4.9.8-2	Summary of Convergences	4.9.8-16
Table 4.9.8-3	Maximum Fuel Cladding and Concrete Temperatures of EOS-HSM loaded with EOS-89BTH DSC	4.9.8-17
Table 4.9.8-4	Maximum Temperatures of Key Components of EOS-HSM Loaded with EOS-89BTH DSC.....	4.9.8-18
Table 4.9.8-5	Average Temperatures of Key Components of EOS-HSM Loaded with EOS-89BTH DSC	4.9.8-19
Table 4.9.8-6	Summary of Air Temperatures and Mass Flow Rates at Inlet and Outlet of EOS-HSM Loaded with EOS-89BTH DSC.....	4.9.8-20
Table 4.9.8-7	Average Temperatures of Helium Gas in EOS-89BTH DSC Cavity	4.9.8-21
Table 4.9.8-8	Design Load Cases for EOS-TC125 Loaded with EOS-89BTH DSC.....	4.9.8-22
Table 4.9.8-9	Maximum Temperatures of EOS-TC125 with EOS-89BTH DSC at 48.2 kW, without Air Circulation	4.9.8-23
Table 4.9.8-10	Maximum Temperatures of EOS-TC125 with EOS-89BTH DSC at 48.2 kW, With Air Circulation	4.9.8-24
Table 4.9.8-11	Maximum Temperatures of EOS-TC125 with EOS-89BTH DSC at 48.2 kW, Accident Loss of Neutron Shield with Loss of Air Circulation Accident Conditions.....	4.9.8-25
Table 4.9.8-12	Maximum Temperatures of EOS-TC125 with EOS-89BTH DSC at 48.2 kW, Air Circulation Turned Off / Air Circulation Failure during Transfer Operations.	4.9.8-26
Table 4.9.8-13	Time Limit Operations.....	4.9.8-27
Table 4.9.8-14	Maximum Temperatures of Key Components in EOS-TC125 loaded with EOS-89BTH DSC	4.9.8-28
Table 4.9.8-15	Average Temperatures of Key Components in EOS-TC125 Loaded with EOS-89BTH DSC	4.9.8-29

List of Figures

Figure 4.9.8-1	Temperature Profiles (in °F) for EOS-HSM Loaded with EOS-89BTH DSC for Normal Hot Storage Condition (LC 1).....	4.9.8-30
Figure 4.9.8-2	Temperature Profiles (in °F) for EOS-HSM Loaded with EOS-89BTH DSC for Normal Hot Storage Condition (LC 1b).....	4.9.8-32
Figure 4.9.8-3	Temperature Profiles (in °F) for EOS-HSM Loaded with EOS-89BTH DSC for Off-Normal Hot Storage Condition (LC 2).....	4.9.8-34
Figure 4.9.8-4	Temperature Profiles (in °F) for EOS-HSM Loaded with EOS-89BTH DSC for Accident Storage Condition (LC 3).....	4.9.8-36
Figure 4.9.8-5	Streamlines (in m/s) of Airflow inside the EOS-HSM Cavity with EOS-89BTH DSC for Normal Hot Storage Condition (LC 1).....	4.9.8-38
Figure 4.9.8-6	Temperature Distribution of EOS-TC125 Loaded with EOS-89BTH DSC at 48.2 kW, Normal Hot, Vertical Transfer Operations at 13 Hours (LC 1).....	4.9.8-39
Figure 4.9.8-7	Temperature Distribution of EOS-TC125 Loaded with EOS-89BTH DSC at 48.2 kW, Normal Hot, and Horizontal Transfer Operations at 13 Hours (LC 3).....	4.9.8-41
Figure 4.9.8-8	Temperature Distribution of EOS-TC125 loaded with EOS-89BTH DSC at 48.2 kW, Accident condition, Loss of Water in Neutron Shield. (LC 5).....	4.9.8-43
Figure 4.9.8-9	Temperature Distribution of EOS-TC125 Loaded with EOS-89BTH DSC at 48.2 kW, Air Circulation Turned on, Transient at 8 hours. (LC 6a).....	4.9.8-45
Figure 4.9.8-10	Temperature Distribution of EOS-TC125 Loaded with EOS-89BTH DSC at 48.2 kW, Air Circulation Turned on, Steady State. (LC 6b).....	4.9.8-47
Figure 4.9.8-11	Temperature Distribution of EOS-TC125 loaded with EOS-89BTH DSC at 48.2 kW, Air Circulation Turned off, Transient at 4 hours (LC 7).....	4.9.8-49
Figure 4.9.8-12	Maximum Fuel Cladding Temperature versus Time in Transient Cases, LCs 1 and 3 for 13 Hours Duration	4.9.8-51
Figure 4.9.8-13	Maximum Fuel Cladding Temperature versus Time in Transient Cases, LCs 3, 6a, and 7	4.9.8-52
Figure 4.9.8-14	Streamlines of Airflow Inside the TC/DSC Annulus of the EOS-TC125 Loaded with EOS-89BTH DSC for LC 6a	4.9.8-53

4.9.8 THERMAL EVALUATION OF EOS-89BTH DSC FOR HLZCS 4 THROUGH 6

This appendix evaluates the thermal performance of the EOS-89BTH Dry Shielded Canister (DSC) for normal, off-normal, and accident conditions with Heat Load Zone Configurations (HLZCs) 4, 5, and 6 for both storage and transfer operations.

The various basket assembly types within the EOS-89BTH DSC are described in Chapter 1, Section 1.1, and the various system configurations allowed for these basket assembly types are listed in Table 1-2. HLZCs 4, 5, and 6 evaluated in this appendix can be loaded in an EOS-89BTH DSC.

A summary of the EOS-89BTH DSC configurations analyzed in this appendix is shown below.

DSC Type	Heat Load Zone Configuration (HLZC)	Max. Heat Load (kW)	Transfer Cask	Storage Module ⁽¹⁾
EOS-89BTH	4	48.2	EOS-TC125	EOS-HSM/EOS-HSMS EOS-HSM-FPS/ EOS-HSMS-FPS/ HSM-MX ⁽²⁾
	5	48.2		
	6	48.2		

Note:

1. EOS-HSM and EOS-HSMS are identical in thermal performance, and EOS-HSM-FPS and EOS-HSMS-FPS are identical in thermal performance, as discussed in Section 4.
2. Thermal evaluations of HLZCs 4 through 6 for storage operations in HSM-MX are presented in Section A.4.5.6.

Section 4.9.8.1 presents descriptions of HLZCs 4, 5, and 6. Section 4.9.8.2 presents the storage evaluation of the EOS-89BTH DSC with HLZCs 4 through 6 in EOS-HSM. Section 4.9.8.3 presents the transfer evaluation of the EOS-89BTH DSC with HLZCs 4 through 6 in EOS-TC125.

4.9.8.1 Description of HLZCs 4, 5 and 6

HLZCs 4, 5, and 6 considered in this appendix are described in Figure 2-2d, Figure 2-2e, and Figure 2-2f in Chapter 2, respectively. As discussed in Section 2.4.3, the total heat load per DSC is limited to 48.2 kW when loaded in the EOS-HSM per HLZCs 4 through 6; therefore, all the zones cannot be fully loaded with the maximum defined heat load per assembly for HLZCs 5 and 6. Therefore, HLZC 5 and 6 are adjusted to meet the allowable decay heat load limits.

For HLZC 6, the outer zone heat loads (Zone 4 and Zone 6) are adjusted to maintain the total decay heat load below allowable limits.

The heat loads considered in this evaluation for HLZCs 4 through 6 are summarized below:

HLZC #	Zone	No. of FAs	Heat Load / FA (kW)	Heat Load / Zone (kW)
4	1	29	0.4	11.6
	2	16	0.6	9.6
	3	24	0.5	12
	4	20	0.75	15
	Total Heat Load / DSC (kW)			48.2
5	1	29	0.3	8.7
	2	16	0.4	6.4
	3	12 ⁽¹⁾	0.5	6
	4	12	1.2	14.4
	5	8	1.7	13.6
	Total Heat Load / DSC (kW)			49.1 ⁽²⁾
6	1	29	0.3	8.7
	2	16	0.4	6.4
	3	17	0.5	8.5
	4	15	1.3	19.5
	5	12	0.5 ⁽³⁾	6
Total Heat Load / DSC (kW)			49.1 ⁽²⁾	

Notes:

- (1) As marked in Figure A.4-30, 12 of the FAs in the outermost compartments of Zone 3 are left empty.
- (2) The total heat load used in the thermal model is conservatively higher than the maximum heat load (48.2 kW) specified in Figure 2-2e and Figure 2-2f in Chapter 2.

- (3) The heat load of the outermost Zone 5 of Figure 2-2f in Chapter 2 is reduced to 0.5 kW to maintain the total heat load.

4.9.8.2 Storage Evaluation in HLZCs 4, 5 and 6

The EOS-HSM has an alternative design option with the flat plate support structure (FPS). The EOS-37PTH DSC in the EOS-HSM-FPS was evaluated in Section 4.9.5. A review of the results in Table 4.9.5-3 concludes that the EOS-HSM-FPS thermal evaluation bounds the generic EOS-HSM evaluation as it has higher FA temperatures. Therefore, this section will evaluate the bounding EOS-HSM-FPS loaded with the EOS-89BTH DSC basket with a maximum heat load of 48.2 kW for normal, off-normal and accident conditions for the bounding HLZC 4. To evaluate the wind impact, the CFD model includes the external air domain that represents the wind conditions. This section also discusses the grid convergence index (GCI) for the thermal model of the EOS-HSM (FPS) with the EOS-89BTH DSC.

4.9.8.2.1 Description of Load Cases

To determine the thermal performance of the EOS-HSM (FPS) loaded with the EOS-89BTH DSC, the load cases (LCs) listed in Table 4.9.8-1 are evaluated for normal, off-normal, and accident conditions using the CFD model described in Section 4.9.8.2.3.

LC 1 is evaluated for storage under normal conditions using HLZC 4 (48.2 kW) with wind deflectors [,] as described in Section 4.9.4.6.1, and with maximum yearly average ambient temperature of 70 °F.

LC 1b is evaluated for storage under normal conditions using HLZC 4 (42 kW) without wind deflectors [] and with daily average ambient temperature of 90 °F. Heat load of 42 kW is conservatively used instead of 41.6 kW.

LC 2 is evaluated for storage under off-normal conditions using HLZC 4 (48.2 kW) with wind deflectors without any wind and with daily average ambient temperature of 103 °F.

LC 3 is evaluated for storage under accident conditions with blocked inlet and outlet vents for 40 hours using HLZC 4 (48.2 kW) with wind deflectors without any wind and with daily average ambient temperature of 103 °F. Initial temperatures are taken from the steady-state results of LC 2.

4.9.8.2.2

Thermal Model of EOS-HSM (FPS) with EOS-89BTH DSC

4.9.8.2.3 CFD Model EOS-HSM (FPS) with EOS-89BTH DSC

Proprietary Information on This Page
Withheld Pursuant to 10 CFR 2.390

Temperature Calculations

The maximum temperatures of fuel cladding and concrete of EOS-HSM loaded with EOS-89BTH DSC for LCs 1, 1b, 2, and 3 are summarized in Table 4.9.8-3.

The maximum temperatures of various components of the EOS-HSM loaded with the EOS-89BTH DSC for LCs 1, 1b, 2, and 3 are summarized in Table 4.9.8-4. The average temperatures of key components of the EOS-HSM loaded with the EOS-89BTH DSC for LCs 1, 1b, 2, and 3 are summarized in Table 4.9.8-5.

Typical temperature plots for the key components in the EOS-HSM loaded with the EOS-89BTH DSC for LCs 1, 1b, 2, and 3 are shown in Figure 4.9.8-1 through Figure 4.9.8-4.

Airflow Calculation

The streamlines for the airflow inside the EOS-HSM loaded with the EOS-89BTH DSC under normal hot storage condition (LC 1) is shown in Figure 4.9.8-5. Cool air enters into the EOS-HSM from the inlet, absorbs the heat from the EOS-89BTH DSC, and leaves the EOS-HSM through the outlet with higher temperatures. Table 4.9.8-6 summarizes the air temperatures and mass flow rates at the inlet and outlet for LCs 1, 1b, and 2.

Internal Pressure Calculation

Chapter 4, Section 4.7.2 reports the maximum internal pressures of the EOS-89BTH DSC during normal, off-normal, and accident storage and transfer operations for HLZCs 1 through 3. Since the same type of EOS-89BTH DSC is stored in the EOS-HSM (FPS), the internal pressure calculation follows the same methodology and computation as in Sections 4.7.2 to calculate the average helium temperatures for the EOS-89BTH DSC stored in EOS-HSM during the bounding storage conditions with HLZCs 4 through 6. As shown in Table 4.9.8-7, the average helium temperatures determined for the EOS-89BTH DSC in the EOS-HSM with bounding HLZC 4 are lower than the temperatures determined for the design basis values in Table 4-46. Therefore, the maximum internal pressures in Chapter 4, Table 4-46 remain bounding for the EOS-89BTH DSC in the EOS-HSM with HLZCs 4 through 6 under normal, off-normal, and accident storage conditions.

4.9.8.3 Transfer Evaluation in HLZCs 4, 5 and 6

This section evaluates the thermal performance of the EOS-89BTH DSC in the EOS-TC125 during transfer operations for normal, off-normal, and accident conditions, based on HLZCs 4, 5 and 6.

4.9.8.3.1 Description of Load Cases

As discussed in Section 4.5.1, the load cases considered for transfer of the EOS-89BTH DSC include the vertical loading condition inside of the fuel handling facility, normal and off-normal horizontal transfer conditions with and without air circulation, and the bounding hypothetical accident scenario of loss of both the air circulation system and the water in the neutron shield.

As shown in Table A.4-45, the maximum temperatures of the fuel cladding and concrete for the EOS-89BTH DSC in the HSM-MX with HLZC 4 bound those with HLZCs 5 and 6. Therefore, it is concluded that the thermal performance of the EOS-89BTH DSC in the EOS-TC125 with HLZC 4 will be bounding for HLZCs 5 and 6. The time limits and the maximum temperatures computed for HLZC 4 are applicable for HLZCs 5 and 6.

Table 4.9.8-8 lists the LCs to determine the bounding thermal performance of the EOS-TC125 with the EOS-89BTH DSC with HLZC 4.

LCs 1, 2, 3 and 4 are used to determine the time limits for the loading operations inside the fuel building or transfer operations outside the fuel building for the bounding HLZC 4. In this evaluation, the maximum component temperatures and time limits for the EOS-TC125 loaded with EOS-89BTH DSC and HLZC 4 are considered to bound the corresponding values for EOS-89BTH DSC with HLZCs 5 and 6. The transient analyses for both the horizontal transfer operations and vertical loading operations in these LCs begin with the initial conditions established from the steady-state thermal analyses with the EOS-89BTH DSC with water in the TC/DSC annulus at 223 °F and a 120 °F ambient temperature within the fuel building. In vertical operation, the bottom surface of EOS-TC125 is fixed at 220 °F to account for the heat dissipation to the floor. For the initial conditions with water in the annulus, a maximum temperature of 223 °F is considered based on the boiling temperature of water. Since the bottom of the TC is located further away from the heat generating region, assuming a temperature of 220 °F is reasonable. A review of the LCs 2, 3 and 4 shows that LC 3 bounds LCs 2 and 4 due to higher ambient temperature. Therefore, the time limits determined for LC 3 are applicable to LCs 2 and 4.

LC 6a (off-normal hot, horizontal, transient, air circulation) is used to determine the minimum duration required to operate the air circulation. If the air circulation is initiated as a recovery operation during transfer, the air circulation needs to be turned off before transferring the DSC into the storage module. However, due to the large thermal mass of the system, the air circulation needs to be operated for a minimum duration before it can be turned off to allow sufficient cooling time. This LC determines the minimum duration required to operate the air circulation before it can be turned off.

LC 6b (off-normal hot, horizontal, steady-state, air circulation) is performed to demonstrate that the maximum component temperatures for the EOS-TC125 TC and EOS-89BTH DSC remain below the allowable limits if the air circulation as the recovery operation is initiated. This LC bounds the maximum temperatures for heat loads less than or equal to 48.2 kW when the air circulation is activated.

LC 5 considers the accident case of the loss of neutron shield, wherein the liquid neutron absorber is replaced with air, combined with the loss of air circulation in a steady-state analysis. Off-normal ambient temperature of 117 °F is considered for this LC.

LC 7 begins at the end of LC 6a, in which the air circulation was in operation, and it applies for an EOS-TC125 with EOS-89BTH DSC with HLZC 4, 5 or 6. If the air circulation is activated as a recovery operation during transfer, the air circulation needs to be turned off before transferring the EOS-89BTH DSC into the EOS-HSM storage module. This condition presents a routine transfer operation.

A condition is also postulated where the air circulation is lost during transfer operation. To minimize the occurrence of this condition, the EOS-TC125 skid is equipped with redundant industrial grade blowers and each one of these blowers is capable of supplying the required minimum airflow rate. These blowers are also powered with a redundant power supply.

Both of the above scenarios (i.e., turning off air circulation to offload the EOS-89BTH DSC to the storage module or failure of the air circulation) will decrease the heat dissipation and result in a gradual increase of the maximum temperatures of the EOS-TC125 and EOS-89BTH DSC components. Therefore, for these conditions, an additional time limit is calculated to complete the transfer of the EOS-89BTH DSC from the EOS-TC125 to the storage module or to restart the air circulation or initiate other recovery operations to ensure that the peak fuel cladding temperature remains below the temperature limit of 752 °F established in [4.9.8-5].

For all the normal, off-normal hot conditions, and accident design LCs considered in Table 4.9.8-8, insulation is considered per 10 CFR 71.71 [4.9.8-6].

4.9.8.3.2

EOS-89BTH DSC - Thermal Model for Transfer in EOS-TC125

4.9.8.3.3

EOS-89BTH DSC - Normal and Off-Normal Conditions of Transfer

Due to the high decay heat loads considered for the EOS-89BTH DSC, certain time limits are applicable to the transfer operations under normal and off-normal conditions. The time limits are established to maintain the fuel cladding and the EOS-TC125 components temperatures below the allowable limits based on various LCs discussed in Section 4.9.8.3.1. An overview of these time limits is provided in Section 4.9.8.3.4 and Table 4.9.8-13.

As described in Section 4.9.8.3.1, the maximum temperatures and time limits determined for the EOS-89BTH DSC with HLZC 4 during transfer in EOS-TC125 bound the maximum temperatures and time limits determined for the EOS-89BTH DSC with HLZCs 5 and 6.

Normal/Off-Normal Transfer Conditions without Air Circulation

For both the normal hot, vertical transient condition (LC 1) and off-normal hot, horizontal transient condition (LC 3), the initial conditions are determined from a steady-state analysis of the EOS-TC125 with EOS-89BTH DSC with 223 °F (379 K) water in the TC/DSC annulus.

For both cases, when the clock starts ($t=0$), the water in the TC/DSC annulus is assumed to be drained, and the TC closure is completed. For LC 1, the TC is assumed to be left inside the fuel building in a vertical position. For LC 3, the TC is moved outdoor in a horizontal orientation.

Based on the transient thermal analyses, a maximum duration of 13 hours is allowed for both the vertical loading operations (LC 1) and also for the off-normal hot horizontal transfer operations (LC 3) for HLZCs 4 through 6.

Table 4.9.8-9 summarizes the maximum temperatures for the EOS-TC125 components for LCs 1 and 3. Table 4.9.8-14 and Table 4.9.8-15 summarize the maximum and average temperatures for the key components of the EOS-89BTH DSC for all LCs listed in Table 4.9.8-8. Figure 4.9.8-6 and Figure 4.9.8-7 show the temperature distribution of the key components in the EOS-TC125 with EOS-89BTH DSC for, respectively, LC 1 (48.2 kW, normal hot, vertical transient transfer operations) and LC 3 (48.2 kW, off-normal hot, horizontal transient transfer operations) at 13 hours after drainage of water in the TC/DSC annulus. Figure 4.9.8-12 shows the temperature history of the fuel cladding during the transfer operation for LCs 1 and 3.

For practical purposes, the time limits for vertical or horizontal transfer operations should be considered after sealing the EOS-89BTH DSC when the water in the TC/DSC annulus starts to drain.

Normal/Off-Normal Transfer Conditions with Air Circulation

Transient (LC 6a) and steady-state (LC 6b) thermal analyses are performed for the EOS-TC125 with EOS-89BTH DSC and HLZC 4 with air circulation for off-normal, hot, horizontal transfer conditions. They demonstrate that the maximum fuel cladding and TC component temperatures remain below the allowable limits once the air circulation is activated. Table 4.9.8-10 summarizes the maximum temperatures for these LCs. The temperature profiles for LC 6a are presented in Figure 4.9.8-9. The streamlines for the airflow within the TC/DSC annulus gap are shown in Figure 4.9.8-14. Based on the transient analysis for LC 6a, if air circulation is initiated as a recovery option, it must be operated for a minimum duration of 8 hours to allow sufficient time for the TC/DSC components to cool down.

Transient thermal analysis is performed for the EOS-TC125 with EOS-89BTH DSC and HLZC 4 without air circulation when the air circulation is turned off or lost (LC 7). This analysis is assumed to begin with TC and DSC temperatures at the end of LC 6a. At time = 0, the fan airflow is turned off or lost and the system starts to heat up.

Based on the transient thermal analysis, a maximum duration of 6 hours is available to complete the transfer of the EOS-89BTH DSC to the EOS-HSM or to re-establish the air circulation. Table 4.9.8-12 summarizes the maximum temperatures for this LC. Figure 4.9.8-13 shows the temperature history of the fuel cladding during the transfer operation for LCs 6a and 7.

4.9.8.3.4 EOS-89BTH DSC - Time Limits for Normal/Off-Normal Transfer Operations

For HLZCs 4, 5 and 6, based on the results for LCs 1 and 3 in Section 4.9.8.3.3, steady-state transfer operations are not permitted, and a time limit of 13 hours is determined to complete both vertical and horizontal transfer operations.

At the end of the 13 hours transient transfer operation, the maximum fuel cladding temperature reaches 718 °F with sufficient margin to the fuel cladding temperature limit of 752 °F. However, to provide an additional margin and to ensure sufficient time for the initiation of recovery actions, a time limit of 8 hours is chosen for all transfer operations for HLZCs 4, 5, and 6. The maximum fuel cladding temperature at 8 hours after start of the transfer operations is 682 °F.

If transfer operations cannot be completed within the time limit of 8 hours and the TC/DSC is in a horizontal orientation, one of the recovery actions is to initiate air circulation within 1 hour as noted in Technical Specifications [4.9.8-7].

If air circulation is initiated as a recovery option, it must be operated for a minimum duration of 8 hours to allow sufficient time for the TC/DSC components to cool down. After 8 hours has elapsed with the blowers in operation, they can be turned off to complete the DSC transfer. The maximum fuel cladding temperature at 4 hours after the air circulation is turned off is 710 °F, which has sufficient margin to the temperature limit of 752 °F as shown in Table 4.9.8-12. Therefore, a time limit of 4 hours is chosen to complete the DSC transfer operations.

If air circulation cannot be initiated within 1 hour of exceeding the 8-hour time limit specified in Table 4.9.8-13, the TC/DSC has to be returned to the cask handling area to be positioned in vertical orientation and then the TC/DSC annulus will be filled with clean water. As specified in the Actions for LCO 3.1.3 of the Technical Specifications [4.9.8-7], a total of 5 hours is available to complete Action A.2 and Action A.3 of the LCO 3.1.3 with a maximum duration of 1 hour for Action A.2. The following evaluation considers the maximum duration allowed for Action A.2 (1 hour) and the remaining duration of 4 hours allowed for Action A.3. However, in this instance, the total time from the beginning of transfer operations is 13 hours as shown below.

Total Time for Transfer = $T1 + T2 + T3 = 8 \text{ hours} + 1 \text{ hour} + 4 \text{ hours} = 13 \text{ hours}$

where:

$T1$ = Transfer Time Limit after draining the water from the TC/DSC annulus
= 8 hours (See Table 4.9.8-13)

$T2$ = Time to Initiate Air Circulation = 1 hour (See Technical Specification)

$T3$ = Time to move the TC/DSC into the cask handling area to be positioned in Vertical orientation and to fill the TC/DSC annulus with clean water =
4 hours (See Technical Specification)

It is very unlikely that air circulation cannot be initiated because of the redundant nature of the air circulation system, which includes redundant blower and power systems. Further, the entire air circulation system is assembled and verified to operate prior to transfer operation as indicated in the Technical Specifications [4.9.8-7] and in Chapter 9, Section 9.1.5.

In the extremely unlikely event that air circulation cannot be initiated, duration to complete the refilling of the TC/DSC annulus with water is 13 hours. The maximum fuel cladding temperature at the end of 13 hours is 718 °F. Even for this worst case condition, the maximum fuel cladding temperature remains below the allowable limit of 752 °F. In addition to the fuel cladding temperature, a review of the maximum temperatures in Table 4.9.8-14 shows large margins for other TC components. Therefore, the temperature limits specified for the TC/DSC in Section 4.2 will be satisfied for this condition.

Table 4.9.8-13 presents an overview of time limits of the transfer operations based on the discussions presented in Section 4.9.8.3.3.

The time limits for transfer operations presented in Table 4.9.8-13 are based on the maximum heat load of 48.2 kW and the bounding ambient conditions noted in Section 4.3. However, if the maximum heat load for a loaded DSC is less than 48.2 kW, the time limits for transfer operations can be recalculated based on the maximum heat load and ambient conditions for that DSC using the methodology/models presented in Sections 4.9.8.3.1 and 4.9.8.3.2 to provide more accurate time limits for transfer operations.

4.9.8.3.5 EOS-89BTH DSC - Hypothetical Accident Conditions of Transfer

As noted in Section 4.5.1, the loss of neutron shield and loss of air circulation is bounding for the fire accident case. The maximum temperatures for the bounding loss of neutron shield and loss of air circulation steady-state accident condition (LC 5) are presented in Table 4.9.8-11 for the EOS-89BTH DSC in EOS-TC125. As shown in Table 4.9.8-11, maximum component temperatures are below the allowable limits. Figure 4.9.8-8 presents the temperature profiles for the loss of neutron shield and loss of air circulation accident condition for the EOS-TC125 TC loaded with the EOS-89BTH DSC and 48.2 kW heat load.

4.9.8.4 References

- 4.9.8-1 J.M. Cuta, U.P. Jenquin, and M.A. McKinnon, "Evaluation of Effect of Fuel Assembly Loading Patterns on Thermal and Shielding Performance of a Spent Fuel Storage/Transportation Cask," PNNL-13583, Pacific Northwest National Laboratory, November 2001.
- 4.9.8-2 ANSYS ICEM CFD, Version 17.1, ANSYS, Inc.
- 4.9.8-3 ANSYS Mechanical APDL, Version 17.1, ANSYS, Inc.
- 4.9.8-4 ANSYS FLUENT, Version 17.1, ANSYS, Inc.
- 4.9.8-5 NUREG-1536, "Standard Review Plan for Spent Fuel Dry Cask Storage Systems at a General License Facility," Revision 1, U.S. Nuclear Regulatory Commission, July 2010.
- 4.9.8-6 Title 10, Code of Federal Regulations, Part 71, "Packaging and Transportation of Radioactive Material," 2003.
- 4.9.8-7 CoC 1042 Appendix A, NUHOMS® EOS System Generic Technical Specifications, Amendment 3.

Table 4.9.8-1
Design Load Cases for EOS-HSM Loaded with EOS-89BTH DSC Basket

LC No.	Operation Condition	Description	Daily Average Ambient Temperature (°F)	HLZC (Heat Load)
1	Normal		70 ⁽¹⁾	4 (48.2 kW)
1b			90 ⁽⁴⁾	4 (42 kW)
2	Off-Normal		103 ⁽²⁾	4 (48.2 kW)
3 ⁽³⁾	Accident		103 ⁽²⁾	4 (48.2 kW)

Notes:

- (1) For storage operations with heat load >41.8 kW for the EOS-89BTH DSC, the maximum yearly average temperature is 70 °F for normal storage conditions.
- (2) A daily average ambient temperature of 103 °F is used in the evaluations, corresponding to a daily maximum temperature of 117 °F for the off-normal and accident hot storage conditions, based on the discussion in Section 4.3 of Chapter 4.
- (3) Initial temperatures are taken from steady-state results of LC 2.
- (4) For storage operations with heat loads ≤41.8 kW for the EOS-89BTH DSC the maximum temperature is 100 °F for normal storage conditions. A daily average ambient temperature of 90 °F is used in the evaluations, corresponding to a daily maximum temperature of 100 °F for the normal hot storage conditions, based in Section 4.3 of Chapter 4.

Proprietary Information on This Page
Withheld Pursuant to 10 CFR 2.390

Table 4.9.8-3
Maximum Fuel Cladding and Concrete Temperatures of EOS-HSM loaded
with EOS-89BTH DSC

LC ⁽¹⁾	Description	Fuel Cladding Temperature (°F)		Concrete Temperature (°F)	
		Maximum	Limit ⁽¹⁾	Maximum	Limit ⁽¹⁾
1		729	752	220	300
1b		723		259	
2		752	1058	253	
3		858		436	500

Notes:

- (1) See Table 4.9.8-1 for the description of the LCs.
(2) The temperature limits are from NUREG-1536 [4.9.8-5].

Table 4.9.8-4
Maximum Temperatures of Key Components of EOS-HSM Loaded with
EOS-89BTH DSC

LC ⁽¹⁾	Temperature (°F)				
	Basket Plate	Transition Rails	DSC Shell	Heat Shield	Support Structure
1	709	487	413	207	323
1b	704	492	422	265	334
2	733	515	428	240	344
3	844	652	584	459	497

Notes:

(1) See Table 4.9.8-1 for the description of the LCs.

Table 4.9.8-5
Average Temperatures of Key Components of EOS-HSM Loaded with EOS-89BTH DSC

LC ⁽¹⁾	Temperature (°F)					
	Fuel Assembly	Cavity Gas	DSC Shell	Basket Plates	Transition Rails	HSM
1	574	360	244	521	408	124
1b	572	379	275	525	418	155
2	596	384	272	544	432	161
3	715	519	413	669	571	218

Notes:

(1) See Table 4.9.8-1 for the description of the LCs.

Table 4.9.8-6
Summary of Air Temperatures and Mass Flow Rates at Inlet and Outlet of
EOS-HSM Loaded with EOS-89BTH DSC

LC ⁽¹⁾	T _{inlet} (°F)	T _{exit} (°F)	T _{exit} -T _{inlet} (°F)	Mass Flow Rate at Inlet (kg/s)		
				Inlet	Outlet	Imbalance
1	70	139	69	8.61E-01	8.48E-01	1.31E-02
1b	90	111	59	5.10E-01	5.03E-01	7.10E-03
2	103	197	94	8.48E-01	8.48E-01	6.72E-05

Notes:

(1) See Table 4.9.8-1 for the description of the LCs.

Table 4.9.8-7
Average Temperatures of Helium Gas in EOS-89BTH DSC Cavity

LC ⁽¹⁾	Average Temperature of Helium in DSC (K)		Temperature Difference (K)
	Bounding Design Basis [See Table 4-46]	HLZC 4 in EOS-HSM-FPS	
1	572	558	-14
1b	572	559	-13
2	572	571	-1
3	671	638	-33

Notes:

(1) See Table 4.9.8-1 for the description of the LCs.

Table 4.9.8-8
Design Load Cases for EOS-TC125 Loaded with EOS-89BTH DSC

LC	Operating Condition	EOS-TC125 Orientation	Description	Ambient Temperature (°F)	Solar Insolation	Notes
1	Normal	Vertical	Normal, hot, indoor, Transient, No air circulation, HLZC 4	120	No	(1), (2)
2	Normal	Horizontal	Normal, hot, outdoor, Transient, No air circulation, HLZC 4	100	Yes	(1), (2), (3)
3	Off-Normal	Horizontal	Off-normal, hot, outdoor, Transient, No air circulation, HLZC 4	117	Yes	(1), (2)
4	Off-Normal	Horizontal	Off-normal, cold, outdoor, Transient, No air circulation, HLZC 4	0	No	(3)
5	Accident	Horizontal	Accident, hot, outdoor, loss of liquid in neutron shield, Steady-state, No air circulation, HLZC 4	117	Yes	(1)
6a	Off-Normal	Horizontal	Off-normal, hot, outdoor, Transient, Air circulation on, HLZC 4	117	Yes	(1), (4), (6)
6b	Off-Normal	Horizontal	Off-normal, hot, outdoor, Steady-state, Air circulation on, HLZC 4	117	Yes	(1), (4)
7	Off-Normal	Horizontal	Off-normal, hot, outdoor, Transient, Air circulation is turned off, HLZC 4	117	Yes	(1), (5)

Notes:

- (1) Daily average temperatures as noted in Section 4.3 are used for normal and off-normal transfer conditions outside the fuel building. No averaging is used for the temperature inside the fuel building and the maximum temperature of 120 °F is used in the thermal evaluation.
- (2) Initial steady-state conditions are calculated assuming water in the TC/DSC annulus is at 223 °F and an ambient temperature of 120 °F.
- (3) LC 3 bounds the LC 2 and LC 4 due to higher ambient temperature.
- (4) Air circulation with 850 cfm.
- (5) Initial temperatures are taken from LC 6a after 8 hours in the transient run. At time=0, the air circulation is assumed to be turned off or lost and the system begins to heat up.
- (6) Initial temperatures are taken from LC 3 after 14 hours in the transient run. At time t=0, the air circulation is assumed to be turned on and the system begins to cool down.

Table 4.9.8-9
Maximum Temperatures of EOS-TC125 with EOS-89BTH DSC at 48.2 kW,
without Air Circulation

	Normal Hot, Vertical (LC 1)			Off-Normal Hot, Horizontal (LC 3)			Max. Allowable Temperature
	Steady	Transient		Steady	Transient		
Heat Load	48.2 kW			48.2 kW			
Time Limit	Initial	8 hrs	13 hrs	Initial	8 hrs	13 hrs	
Components Name	Temperature (°F)						
Fuel Cladding	653	682	718	643	674	709	752
DSC Shell	303	450	477	302	451	478	-
Inner Shell	221	295	320	229	327	353	-
Gamma Shield	220	293	318	227	322	348	620
Structural Shell (outer shell)	208	214	224	199	212	231	-
Neutron Shield (Max/Avg ⁽¹⁾)	200/181	207/196	223/209	191/176	211/189	230/201	259
Neutron Shield Outer Skin (Neutron Shield Panel)	220	221	221	184	202	221	-
Solid Neutron Shield (Max/Avg)	231/223	252/231	261/235	223/198	233/199	244/207	262
Closure Lid (Top End Plate)	170	162	164	169	159	160	-
Top Ring (Inner Shell Assembly)	196	180	185	204	184	189	-
Bottom Ring	220	228	233	215	222	233	-

Notes:

- (1) Bulk average temperature of water in the neutron shield is limited by the 20 psig pressure relief valves on the shield. The equivalent steam saturation temperature at this pressure is approximately 259 °F.

Table 4.9.8-10
Maximum Temperatures of EOS-TC125 with EOS-89BTH DSC at 48.2 kW,
With Air Circulation

	Off-Normal, Hot, Horizontal, Outdoor, Transient, Air Circulation on (LC 6a)	Off-Normal, Hot, Horizontal, Outdoor, Steady State, Air Circulation on (LC 6b)	Max. Allowable Temperature
Heat Load	48.2 kW	48.2 kW	
Time Limit	8 hrs after air circulation is initiated	No Time Limit	
Components Name	Temperature (°F)		
Fuel Cladding	707	683	752
DSC Shell	429	427	-
Inner Shell	360	361	-
Gamma Shield	355	357	620
Structural Shell (outer shell)	240	246	-
Neutron Shield (Max/Avg ⁽¹⁾)	239/187	245/171	259
Neutron Shield Outer Skin (Neutron Shield Panel)	229	234	-
Solid Neutron Shield (Max/Avg)	163/138	142/123	262
Closure Lid (Top End Plate)	229	218	-
Top Ring (Inner Shell Assembly)	244	240	-
Bottom Ring	176	152	-

Notes:

- (1) Bulk average temperature of water in the neutron shield is limited by the 20 psig pressure relief valves on the shield. The equivalent steam saturation temperature at this pressure is approximately 259 °F.

Table 4.9.8-11
Maximum Temperatures of EOS-TC125 with EOS-89BTH DSC at 48.2 kW,
Accident Loss of Neutron Shield with Loss of Air Circulation Accident
Conditions

	Accident, Hot, Horizontal, Steady State Air filled Neutron Shield, (LC 5)	Max. Allowable Temperature
Heat Load	48.2 kW	
Time Limit	-	
Components Name	Temperature (°F)	
Fuel Cladding	935	1058
DSC Shell	651	-
Inner Shell	561	-
Gamma Shield	556	620
Structural Shell (TC Outer Shell)	445	-
Neutron Shield Outer Skin	345	-
Solid Neutron Shield (Max/Avg)	354/292	262
Closure Lid	206	-
Top Ring	262	-
Bottom Ring	341	-

Table 4.9.8-12
Maximum Temperatures of EOS-TC125 with EOS-89BTH DSC at 48.2 kW,
Air Circulation Turned Off / Air Circulation Failure during Transfer
Operations.

	Off-Normal, Hot, Outdoor, Horizontal, Transient, No Air Circulation (LC 7)	Max. Allowable Temperature
Heat Load	48.2 kW	
Time Limit	4 hrs	
Components Name	Temperature (°F)	
Fuel Cladding	710	1058
DSC Shell	448	-
Inner Shell	368	-
Gamma Shield	364	620
Structural Shell (TC Outer Shell)	368	-
Neutron Shield (Max/Avg ⁽¹⁾)	245/191	259
Neutron Shield Outer Skin	235	-
Solid Neutron Shield Avg	187/161	262
Closure Lid	188	-
Top Ring	218	-
Bottom Ring	196	-

Notes:

- (1) Bulk average temperature of water in the neutron shield is limited by the 20 psig pressure relief valves on the shield. The equivalent steam saturation temperature at this pressure is approximately 259 °F.

Table 4.9.8-13
Time Limit Operations

Operating Conditions	HLZC	Heat Load (kW)	Time Limit (hours)
Normal/ Off-normal Transfer	HLZC 4 (LC 1)	48.2	8
	HLZC 4 (LCs 2, 3 and 4)	48.2	8
	HLZC 4 (LC 6b)	48.2	No Time Limit ⁽¹⁾
Insertion of EOS-89BTH DSC into the EOS-HSM or restart of air circulation after its inactivation	HLZC 4 (LC 7)	48.2	4
Loss of Neutron Shield with Loss of Air Circulation, Accident Condition	HLZC 4 (LC 5)	48.2	No Time Limit

Notes:

- (1) If air circulation is initiated as a recovery option, it must be maintained for a minimum duration of 8 hours per LC 6a, before it is turned off.

Table 4.9.8-14
Maximum Temperatures of Key Components in EOS-TC125 loaded with
EOS-89BTH DSC

LC	Fuel Cladding	Basket Plate	Transition Rail	DSC Shell	Lead (Gamma Shield)	Neutron Shield	Bottom Neutron Shield
Temperature Limit (°F)	752 ⁽⁴⁾ / 1058 ⁽⁴⁾	--	--	--	620	259	262
	Temperature (°F)						
1 ⁽¹⁾	682	664	500	450	293	196	231
1 ⁽²⁾	718	701	530	477	318	209	235
2	<709	<694	<536	<478	<348	<201	<207
3 ⁽¹⁾	674	658	506	451	322	189	199
3 ⁽²⁾	709	694	536	478	348	201	207
4	<709	<694	<536	<478	<348	<201	<207
5	935	921	715	651	556	NA ⁽⁵⁾	292
6a ⁽⁶⁾	707	687	496	429	355	187	138
6b	683	666	487	427	357	171	123
7 ⁽³⁾	710	691	514	448	364	191	161

Notes:

- (1) Temperature reported in transient case at 8 hours.
- (2) Temperature reported in transient case at 13 hours.
- (3) Temperature reported in transient case at 4 hours.
- (4) Temperature limits for normal and off-normal conditions are 752 °F and 1058 °F, respectively.
- (5) It is assumed that the water in the neutron shield is lost during the accident condition.
- (6) Temperature reported in transient case at 8 hours.

Table 4.9.8-15
Average Temperatures of Key Components in EOS-TC125 Loaded with
EOS-89BTH DSC

Average Temperature							
LC	Fuel Cladding	Basket Plate	Transition Rail	Helium Gap	DSC Shell	Lead (Gamma Shield)	TC Inner Shell
Temperature (°F)							
1 ⁽¹⁾	561	515	435	379	374	229	263
1 ⁽²⁾	591	545	462	401	395	244	281
2	<578	<530	<445	<382	<376	<239	<276
3 ⁽¹⁾	549	502	420	362	356	223	258
3 ⁽²⁾	578	530	445	382	376	239	276
4	<578	<530	<445	<382	<376	<239	<276
5	767	714	611	532	526	404	448
6a ⁽³⁾	548	497	378	361	297	211	232
6b	517	468	353	345	277	194	214
7 ⁽⁴⁾	563	515	424	380	360	227	261

Notes:

- (1) Temperature reported in transient case at 8 hours.
- (2) Temperature reported in transient case at 13 hours.
- (3) Temperature reported in transient case at 8 hours.
- (4) Temperature reported in transient case at 4 hours.

Proprietary Information on Pages 4.9.8-30 through 4.9.8-53
Withheld Pursuant to 10 CFR 2.390

Stringent design and fabrication requirements ensure that the confinement function of the DSC is maintained. The cylindrical shell and inner bottom cover are pressure tested in accordance with the ASME Code, Section III, Subarticle NB-6300. This pressure test is performed after installation of the inner bottom cover at the fabricator's facility and may be performed concurrently with the leak test, provided the requirements of NB-6300 are met. *This pressure test is not required if the single piece forged bottom is used. See drawing EOS01-1001-SAR, sheet 2, detail 1-alternate 1.*

A leak test of the shell assembly, including the inner bottom cover, is performed in accordance with ANSI N14.5 [5-1] and the ASME Code, Section V, Article 10. These tests are typically performed at the fabricator's facility. The acceptance criteria for the test are "leaktight" as defined in ANSI N14.5.

The process for leak testing the DSC involves temporarily sealing the shell from the top end. The gas-filled envelope and evacuated envelope testing methodologies have the required nominal test sensitivity for leaktight construction and are used for leak testing. A helium mass spectrometer is used to detect any leakage as defined in ANSI N14.5. During final drying and sealing operations of the DSC, the top closure confinement welds are applied to confine radioactive materials within the cavity.

The inner top cover weld is welded to the DSC shell using automated welding equipment. Once the DSC has been vacuum dried, a pressure test is performed by backfilling the DSC cavity with helium. Following the satisfactory completion of the pressure test, the drain port cover and vent *port* plug are welded, and a leak test is performed to verify that the weld between the DSC shell and the inner top cover, drain port cover and vent *port* plug meet the leaktight criteria of ANSI N14.5. The outer top cover plate is also welded in place using automated welding equipment.

72.48

5.1.2 Confinement Penetrations

All penetrations in the DSC confinement boundary are welded closed. The DSC is designed to have no credible leakage as described above.

5.1.3 Seals and Welds

The welds made during fabrication of the DSC that affect the confinement boundary include the weld applied to the shell bottom, and the circumferential and longitudinal seam welds applied to the cylindrical shell. These welds are inspected (radiographic or ultrasonic inspection, and liquid penetrant inspection (PT)) according to the requirements of Subsection NB of the ASME Code.

6.1 Discussions and Results

The following is a summary of the methodology and results of the shielding analysis of the EOS system. More detailed information is presented in the body of the chapter.

The EOS-37PTH DSC stores up to 37 PWR FAs, while the EOS-89BTH stores up to 89 BWR FAs. Each EOS-DSC is configured into heat load zones in order to optimize the system performance for both thermal and shielding considerations. *Eleven* heat load zoning configurations (HLZCs) are available for the EOS-37PTH DSC, and *six* HLZCs are available for the EOS-89BTH DSC. The *PWR* HLZCs are defined in the Technical Specifications (TS) [6-11], *and the BWR HLZCs are defined in Chapter 2*. Fuel to be stored is limited by the decay heat and minimum cooling times defined in the Technical Specifications.

The EOS-37PTH DSC is authorized to store up to eight damaged FAs or four FFCs using HLZC 6 or HLZC 8. *The EOS-37PTH DSC is also authorized to store up to six damaged FAs or two FFCs using HLZC 10 or 11.* Damaged and failed fuel shall not be present in the same DSC.

Source Terms

The ORIGEN-ARP module of the Oak Ridge National Laboratory (ORNL) SCALE6.0 code package [6-1] is used to develop reasonably bounding gamma and neutron source terms. [

]

Control components (CCs) are allowed to be stored within a PWR FA. Examples of CCs include burnable poison rod assemblies (BPRAs) and thimble plug assemblies. Control components typically have a Co-60 source because of its light element activation, which contributes substantially to the dose rates. The CC source term used in the analysis is provided in Table 6-37. Co-60 equivalent activity limits per zone are provided in TS Table 3 [6-11].

BWR fuel does not include CCs other than the fuel channel, which is conservatively included in the source term. The BWR fuel channel is fabricated from zirconium alloy and does not require a Co-60 limit because the contribution to the source term from the fuel channel is negligible.

Dose Rates

The Monte Carlo transport code, MCNP5 [6-5], is used to compute dose fields around the EOS-TCs and EOS-HSM using detailed three-dimensional models for the following normal configurations:

- EOS-37PTH DSC inside the EOS-TC108
- EOS-37PTH DSC inside the EOS-TC125/135
- EOS-37PTH DSC inside the EOS-HSM-Short
- EOS-89BTH DSC inside the EOS-TC108
- EOS-89BTH DSC inside the EOS-TC125 (*minimum lead thickness*)
- EOS-89BTH DSC inside the EOS-HSM-Medium

The computed EOS-HSM dose rates are used to establish TS dose rate limits and support compliance with 72.104 and 72.106 requirements. EOS-TC accident dose rates are used to support compliance with 72.106 requirements. However, normal condition EOS-TC dose rates are used as input to an exposure evaluation but are not used to support compliance with either 72.104 or 72.106 requirements. Therefore, the conservative EOS-TC source terms provided in this chapter may be used directly to compute normal condition EOS-TC dose rates when evaluating modifications to the EOS-TC design.

The EOS-TC125 and EOS-TC135 provide equivalent shielding but accommodate different DSC lengths. The EOS-TC135 is used only with the EOS-37PTH DSC. The EOS-TC125 and EOS-TC135 designs are bounded by the same Monte Carlo N-particle (MCNP) model and are referred to in this chapter as EOS-TC125/135. The EOS-TC108 offers less shielding than the EOS-TC125/135 and features a removable neutron shield. The neutron shield is removed for fuel loading and attached subsequent to fuel loading. The neutron shield for the EOS-TC125/135 is integral to the cask and cannot be removed.

The EOS-37PTH and EOS-89BTH DSCs are custom-built for the fuel to be stored and, therefore, do not have a standard length. BWR fuel is typically longer than PWR fuel, so the EOS-89BTH DSC is longer than the EOS-37PTH DSC in the MCNP models. To accommodate the various DSC lengths, three versions of the EOS-HSM are available: short, medium, and long. In the EOS-HSM models, the EOS-37PTH DSC is paired with the EOS-HSM-Short, while the EOS-89BTH DSC is paired with the EOS-HSM-Medium, as these are the smallest EOS-HSMs that can accommodate the modeled EOS-DSCs.

All EOS-37PTH DSC calculations conservatively include both the FA and CC sources. BWR fuel does not include CC, other than the fuel channel, which is conservatively included in the source term.

Based on the near-field dose rates calculated for the EOS-TCs, a dose assessment is performed for the EOS-TC loading operation. This dose assessment is documented in Chapter 11.

The shielding effectiveness of the EOS-TC and EOS-HSM is not impacted by any off-normal events. Two accident events have been identified:

- Loss of neutron shielding for the EOS-TCs
- Loss of EOS-HSM outlet vent covers due to a tornado or missile event

MCNP cases are developed for the EOS-HSM in which the vent covers are absent. The EOS-HSM accident increases the average dose rate on the roof of the module to 18,800 mrem/hr. The fluxes and dose rates on the surface of the EOS-HSM in an accident condition are used as input to an accident site dose calculation documented in Chapter 11.

6.2 Source Specification

Design basis source terms for PWR and BWR fuels are developed in this section. The source terms are developed to be reasonably bounding consistent with the limits on fuel qualification. A site-specific analysis must evaluate the site-specific used fuel to be stored and determine if the parameters utilized in the UFSAR analysis are bounding and appropriate. Site-specific source terms may be different than the source terms presented herein. However, the source terms presented in this chapter were developed to bound most used fuels and will result in reasonably bounding dose rates.

Fuel types that are authorized for storage are provided in Chapter 2. These fuel types may be divided into PWR and BWR fuel types. The list of authorized fuels is summarized below.

PWR

- Westinghouse (WE) 14x14 class
- WE 15x15 class
- WE 17x17 class
- Babcock & Wilcox (B&W) 15x15 class
- Combustion Engineering (CE) 14x14 class
- CE 15x15 class
- CE 16x16 class

BWR

- 7x7 lattice array type
- 8x8 lattice array type
- 9x9 lattice array type
- 10x10 lattice array type
- *11x11 lattice array type*

[

]

Prior to using ORIGEN-ARP, detailed two-dimensional models of the design basis PWR and BWR FAs are developed in TRITON using the FA design data in Chapter 2. The ENDF/B-VII 238-group cross section library (v7-238) is utilized in the TRITON input files. TRITON is used to generate ORIGEN-ARP data libraries as a function of burnup and enrichment. These libraries are used by ORIGEN-ARP to compute the source terms. *For the EOS-89BTH DSC source terms developed for the EOS-TC125 and EOS-HSM analyses, the default GE 7x7 ORIGEN-ARP library provided with SCALE 6.0 is used.*

ORIGEN-ARP uses interpolated cross section libraries to generate source terms that are essentially equivalent to the detailed TRITON runs. TRITON has been benchmarked against experimentally measured isotopes and results in excellent agreement with the measured data in ORNL/TM-2010 SCALE 5.1 [6-2]. As part of the code validation, the TRITON benchmark cases from SCALE 5.1 are rerun using the ENDF/B-VII 238-group cross section library. The isotopes important for shielding for which benchmark data are available include Cs-137/Ba-137m, Cs-134, Eu-154, Ce-144/Pr-144, Ru-106/Rh-106, Sr-90/Y-90, and Cm-244. The average ratio of the measured to calculated concentration for these nuclides is close to unity, indicating that TRITON/ORIGEN-ARP is an acceptable program for source term generation.

6.2.2

PWR and BWR Source Terms

Sources are developed for a variety of different enrichments. For a particular U-235 enrichment, the uranium fuel loading is distributed according to the following relationship from the SCALE 6.0 manual:

- $\text{wt. \% U-234} = 0.0089 * \text{wt. \% U-235}$
- $\text{wt. \% U-236} = 0.0046 * \text{wt. \% U-235}$
- $\text{wt. \% U-238} = 100 - \text{wt. \% U-234} - \text{wt. \% U-235} - \text{wt. \% U-236}$

6.2.2.1 Bounding HLZCs

The EOS-DSC baskets are zoned by heat load. Heat load zoning allows hotter FAs, which generally have larger neutron and gamma source terms, to be placed in the inner zones and be shielded by FAs in the outer zone. The EOS-TC108 and EOS-TC125/135 have different heat load zone configurations because the EOS-TC125/135 is more heavily shielded than the EOS-TC108 and can therefore be loaded with stronger sources.

Eleven HLZCs are available for the EOS-37PTH DSC and six HLZCs are available for the EOS-89BTH DSC. The PWR HLZCs are defined in the TS [6-11], and the BWR HLZCs are defined in Chapter 2. All PWR HLZCs may be transferred in the EOS-TC125/135, while the EOS-TC108 is limited to HLZCs 2 through 9. All BWR HLZCs may be transferred in the EOS-TC125/135, while the EOS-TC108 is limited to BWR HLZC 2 and 3. The EOS-HSM may store PWR HLZCs 1 through 6, 10, 11 and all BWR HLZCs.

The bounding HLZCs are used for dose rate analysis. For each zone within a DSC, higher heat loads result in stronger source terms and larger dose rates if the minimum cooling time is the same.

EOS-89BTH DSC

The bounding HLZCs used in the EOS-89BTH DSC analyses are:

- EOS-89BTH DSC transferred in the EOS-TC125 and stored in the EOS-HSM: “Shielding HLZC” that bounds HLZC 1 through 6, as described below.
- EOS-89BTH DSC transferred in the EOS-TC108: HLZC 2

Rather than justify which HLZC is bounding, an EOS-89BTH DSC “shielding HLZC” is developed to bound HLZC 1 through 6 when transferred in the EOS-TC125 and stored in the EOS-HSM. Each basket location in the shielding HLZC bounds the corresponding heat load at that location allowed in HLZC 1 through 6. The shielding HLZC is provided in Figure 6-18 and is identical to the MHLC, Figure 11 of the TS [6-11]. The shielding HLZC is highly conservative for dose rate analysis, as the shielding HLZC features 42.8 kW on the periphery and 82.8 kW within the entire DSC. The peripheral fuel assemblies are defined in TS Figure 8 [6-11]. The minimum cooling time associated with the shielding HLZC is 1.0 year.

Only the EOS-89BTH DSC HLZC 2 and 3 may be transferred in the EOS-TC108. The minimum cooling time of 3 years is applicable to zones 1 and 2. HLZC 2 has larger heat loads in each zone compared to HLZC 3. When HLZC 2 or 3 is used with the EOS-TC108, the minimum cooling time in zone 3 is 9.7 years and 9.0 years, respectively. While the EOS-89BTH DSC HLZC 2 zone 3 has a slightly longer minimum cooling time than HLZC 3 zone 3, the minimum cooling time difference (0.7 years) is small compared to the large difference in decay heat (0.1 kW/FA). Therefore, EOS-89BTH DSC HLZC 2 is bounding for EOS-TC108 analysis.

EOS-37PTH DSC

The bounding HLZCs used in the EOS-37PTH DSC analyses are:

- EOS-37PTH DSC transferred in the EOS-TC125/135 and stored in the EOS-HSM: HLZCs 4 and 10
- EOS-37PTH DSC transferred in the EOS-TC108: HLZCs 4 and 5

HLZC 10 features eight 3.5 kW FAs in the peripheral region. For PWR fuel in the EOS-TC125/135, HLZC 10 is bounding at the cask side in the active fuel region because the heat load in the peripheral region is the largest for HLZC 10. HLZC 10 is also bounding for the EOS-HSM because vent dose rates are dominated by gamma radiation emitted from the peripheral region. However, the inner regions of HLZC 10 are limited to generally low values of 0.5 kW/FA or 0.7 kW/FA. For this reason, it is expected that HLZC 1 or HLZC 4 would result in higher dose rates on the bottom or top cover plate (lid) of the EOS-TC125/135 because the inner regions allow fuel with higher heat loads than HLZC 10. Based on MCNP calculations, HLZC 4 bounds HLZC 1 on the ends of the EOS-TC125/135, although the dose rates are similar. Therefore, EOS-TC125/135 and EOS-HSM source terms are provided only for HLZC 4 and HLZC 10.

Only HLZC 2 through 9 may be transferred in the EOS-TC108, and both HLZC 4 and 5 are analyzed for the EOS-TC108 and bound the remaining HLZCs. HLZC 5 features eight 2.4 kW fuel assemblies.

Note that up to eight damaged PWR fuel assemblies or up to four FFCs are authorized for HLZC 6 and HLZC 8. Source terms are also developed for a damaged/failed fuel HLZC that bounds both HLZC 6 and 8. These source terms are derived for 1.0 kW/FA in Zone 1, 1.5 kW/FA in Zone 2, 1.5 kW/FA for intact fuel in Zone 3, and 0.85 kW/FA for failed fuel in Zone 3. *The EOS-37PTH DSC is also authorized for storage of up to six damaged FAs or two FFCs using HLZC 10 or 11. For failed fuel analysis using HLZC 10, the same 0.85 kW/FA source terms used in the HLZC 6/8 analysis are utilized.* The ORIGEN-ARP methodology for developing damaged/failed fuel source terms is the same as used for developing intact fuel source terms. Reconfiguration of damaged/failed fuel source terms is addressed in Section 6.3.2.

6.2.2.2 Source Term Generation for Limited Burnup, Enrichment, and Cooling Time Combinations

Source term generation outlined in this section is applicable to source terms generated for the EOS-37PTH DSC (all sources) and the EOS-89BTH DSC transferred within the EOS-TC108. A limited number of burnup, enrichment, and cooling time (BECT) combinations (typically 3 to 5) are used to select bounding BECT combinations for each zone. Source terms for the EOS-89BTH DSC transferred within the EOS-TC125 and stored in the EOS-HSM are developed in Section 6.2.2.3.

The EOS-TC108 and EOS-TC125/135 feature reduced lead thickness next to the top nozzle region of the fuel assembly. For this reason, the maximum dose rate at the side of the EOS-TC occurs next to the top nozzle rather than the active fuel. The dose rate at this location is due almost entirely to Co-60 in the top nozzle and plenum regions of the FA. Therefore, to be conservative, the burnup/enrichment/cooling time combination that maximizes Co-60 activity is used to develop the top nozzle, plenum, and bottom nozzle sources. The computed Co-60 activity for each burnup/enrichment/cooling time is provided in the last column of Table 6-8 and Table 6-9 and represents the total Co-60 present in the FA. These Co-60 activities are only used for ranking the sources. For the active fuel region, the burnup/enrichment/cooling time combination that maximizes dose rate next to the active fuel is used to develop the active fuel region sources. The final “hybrid” sources are very conservative because the hardware is integral to the FA and the hardware and active fuel cannot be at different burnups/cooling times.

Based on EOS-TC and EOS-HSM dose rates (for the active fuel) and Co-60 activity (for the end hardware), reasonably bounding burnup/enrichment/cooling time combinations are determined. For these burnup/enrichment/cooling time combinations, the sources in the bottom nozzle, active fuel, plenum, and top nozzle are computed using the appropriate light elements from Table 6-5 and Table 6-6.

During an EOS-TC accident, it is postulated that the water in the neutron shield is lost. In this scenario, there is no hydrogenous neutron shield and the neutron dose rate dominates the primary gamma dose rate. Therefore, the burnup/enrichment/cooling time combination that results in the maximum neutron source is used in accident calculations with no neutron shield. In many cases, the normal condition and accident condition sources are the same.

PWR source terms are reported in the following tables:

- PWR sources terms for EOS-TC108 :
HLZC 4: Table 6-10 through Table 6-13
HLZC 5: Table 6-13a through Table 6-13f
- PWR source terms for EOS-TC125/135
 Intact fuel (HLZC 4): Table 6-14 through Table 6-16
 Damaged/failed fuel (HLZC 6/8): Table 6-14, Table 6-16a through Table 6-16c
 Intact fuel (HLZC 10): Table 6-16d through *Table 6-16i*
- PWR source terms for EOS-HSM:
 HLZC 4: Table 6-17 through Table 6-19
 HLZC 10: Table 6-19a through *Table 6-19c*

BWR source terms are reported in the following tables:

- BWR sources terms for EOS-TC108 (HLZC 2):
 Table 6-20 through Table 6-22

In these tables, the “raw” neutron source computed by ORIGEN-ARP is provided, as well as neutron sources that include neutron peaking factors and subcritical neutron multiplication. These factors are derived in Section 6.2.3. The scaled neutron sources are used in the detailed MCNP dose rate calculations. Only the total neutron source magnitude is reported because the Cm-244 spectrum is used in all dose rate calculations for simplicity because the neutron source is almost entirely due to Cm-244 decay. For example, for the 62 GWd/MTU, 10.25 year cooled PWR source, 95% of the neutron source is due to spontaneous fission of Cm-244. Cm-244 is also the dominant neutron source for shorter cooling times. For instance, for a 36.178 GWd/MTU, three-year cooled PWR source, Cm-244 represents 97% of the total neutron source. The effect on the neutron spectrum of neutron source isotopes with shorter half-lives, such as Cm-242 and Cf-252, is negligible.

6.2.2.3 *Source Term Generation for Comprehensive Burnup, Enrichment, and Cooling Time Combinations*

Source term generation outlined in this section is applicable to source terms generated for the EOS-89BTH DSC transferred within the EOS-TC125 and stored in the EOS-HSM. The overall methodology is the same as the methodology outlined in Section 6.2.2.2, with minor changes as noted below.

- 1. Candidate source terms over a range of BECT combinations are generated to match the decay heat of each zone of the EOS-89BTH DSC shielding HLZC provided in Figure 6-18. The ORIGEN-ARP module of SCALE 6.0 is used in the analysis. However, while only a limited number of BECT combinations are considered in Section 6.2.2.2, a comprehensive set of 142 burnup and enrichment combinations are considered for the EOS-89BTH DSC shielding HLZC. The burnup and enrichment combinations considered correspond to the fuel qualification table (FQT) provided in TS Table 21 [6-11].*
- 2. Using MCNP, response functions are generated for the side of the EOS-TC125 and outlet vent opening of the EOS-HSM (the vent cover is not modeled). The response functions when multiplied by a source term generate a dose rate. These dose rates are used to rank the source terms and select bounding BECT combinations in the active fuel region.*
- 3. The source in the bottom nozzle, plenum, and top nozzle are due almost entirely to Co-60. As an added conservatism, the bounding BECT of the hardware regions is selected to optimize Co-60 activation and may differ from the bounding BECT of the active fuel region.*
- 4. Using the bounding BECT combinations developed in steps 2 and 3, design basis source terms are generated for each zone. Separate bounding source terms are generated for EOS-TC125 and EOS-HSM analysis.*

A constant specific power of 25 MW/MTU is used for all calculations. This specific power is also used in the 61BTH Type 2 DSC analysis documented in Chapter B.6.

Because reconstituted fuel with irradiated stainless steel rods is an allowed content, candidate source terms are generated for both standard fuel (i.e., without irradiated stainless steel rods) and reconstituted fuel (i.e., with five irradiated stainless steel rods). Standard fuel light element inputs are provided in Table 6-6, and reconstituted fuel light element inputs are derived in Section 6.2.6 and provided in Table 6-39b.

Response functions for EOS-HSM and EOS-TC125 analysis are provided in Table 6-62 and Table 6-63, respectively. The EOS-TC125 response functions are based on a minimum lead thickness of 3.07 inches. The bounding BECT combinations, response function results, and Co-60 activities are summarized in Table 6-9a and Table 6-9b for standard and reconstituted fuel, respectively. The following observations are made based on these results:

- EOS-HSM vent dose rates are approximately 5-7% larger for reconstituted fuel.*
- EOS-TC125 side dose rates are approximately 15% larger for reconstituted fuel.*

Because modeling all fuel as reconstituted results in higher dose rates than modeling all fuel as standard, all reported EOS-89BTH DSC source terms for EOS-HSM and EOS-TC125 analysis include five irradiated steel rods, or $89 \times 5 = 445$ irradiated stainless steel rods per DSC. The bounding BECT combinations are:

Hardware (i.e., bottom nozzle, plenum, top nozzle)

- Zone 1: BU = 35 GWd/MTU, E = 1.7 wt.% U-235, CT = 4.38 years*
- Zone 2: BU = 35 GWd/MTU, E = 1.7 wt.% U-235, CT = 3.00 years*
- Zone 3: BU = 35 GWd/MTU, E = 1.7 wt.% U-235, CT = 1.37 years*
- Zone 4: BU = 62 GWd/MTU, E = 3.8 wt.% U-235, CT = 1.48 years*

EOS-HSM (active fuel, normal and accident conditions)

- Zone 1: BU = 35 GWd/MTU, E = 1.7 wt.% U-235, CT = 4.38 years*
- Zone 2: BU = 50 GWd/MTU, E = 3.1 wt.% U-235, CT = 4.00 years*
- Zone 3: BU = 62 GWd/MTU, E = 3.8 wt.% U-235, CT = 2.09 years*
- Zone 4: BU = 62 GWd/MTU, E = 3.8 wt.% U-235, CT = 1.48 years*

EOS-TC125 (active fuel normal conditions)

- Zone 1: BU = 62 GWd/MTU, E = 3.8 wt.% U-235, CT = 12.22 years*
- Zone 2: BU = 62 GWd/MTU, E = 3.8 wt.% U-235, CT = 5.41 years*
- Zone 3: BU = 35 GWd/MTU, E = 1.7 wt.% U-235, CT = 1.37 years*
- Zone 4: BU = 35 GWd/MTU, E = 1.7 wt.% U-235, CT = 1.00 years*

Source terms are developed based on the bounding BECTs listed above. EOS-TC125 source terms are provided in Table 6-23 through Table 6-26, and EOS-HSM source terms are provided in Table 6-27 through Table 6-29a.

As noted in Section 6.2.2.2, EOS-TC125 accident cases should use maximum neutron sources because the loss of the neutron shield increases neutron dose rates more than gamma dose rates. To minimize the number of sources generated, the accident cases conservatively use the gamma sources generated for reconstituted fuel, which has a much larger Co-60 component. However, the accident neutron sources are the maximum values over all BECT combinations for both standard and reconstituted fuel, as standard fuel typically has a larger neutron source than reconstituted fuel. The accident neutron sources are provided in the last row of Table 6-23 through Table 6-26.

6.2.3 Axial Source Distributions and Subcritical Neutron Multiplication

ORIGEN-ARP is used to compute source terms for the average assembly burnup. However, an FA will exhibit an axial burnup profile in which the fuel is more highly burned near the axial center of the fuel assembly and less burned near the ends. This axial burnup profile must be taken into account when performing dose rate calculations, as the dose rate will typically peak near the maximum of this distribution.

The PWR axial burnup profile is taken from NUREG/CR-6801 [6-6] for fuel in the burnup range 26-30 GWd/MTU and is provided in Table 6-30. As fuel is more highly peaked for lower burnups, this distribution is more conservative than a flatter high-burnup distribution. The gamma source term varies proportionally to axial burnup, while neutron source terms vary exponentially with burnup by a power of 4.0 to 4.2 [6-7]. Therefore, the burnup profile is used as the gamma axial source distribution, while the neutron axial source distribution is derived as the burnup profile raised to the power of 4.2.

The average value of the neutron source distribution is 1.215, as shown in Table 6-30. This value has a physical meaning, as it is the ratio of the total neutron source from an FA with the given axial burnup profile to an assembly with a flat burnup profile. The neutron source term as computed by ORIGEN-ARP is for a flat burnup profile (average assembly burnup). Therefore, the “raw” PWR neutron source computed by ORIGEN-ARP is scaled by the factor 1.215 to account for the burnup profile.

For clarity, both the gamma and neutron axial source distributions are renormalized to sum to 1.0, as shown in Table 6-30. When normalized in this manner, the source distribution is the fraction of the source in each axial segment. For example, the fraction of the neutron source in axial segment 10 is 0.0781, or 7.81%.

6.2.5 Blended Low Enriched Uranium Fuel

6.2.6 Reconstituted Fuel

6.2.6.1 EOS-37PTH DSC (EOS-TC125/135 and EOS-TC108) and EOS-89BTH DSC (EOS-TC108 Only)

The dose rate effect of reconstituted fuel assemblies containing irradiated stainless steel rods is addressed in this section for the EOS-37PTH DSC when transferred in either the EOS-TC125/135 or EOS-TC108 and the EOS-89BTH DSC when transferred in the EOS-TC108. For the EOS-89BTH DSC transferred in the EOS-TC125, the dose rate effect of reconstituted fuel assemblies containing irradiated stainless steel rods is addressed in Section 6.2.6.2.

Proprietary Information on Pages 6-23 and 6-24
Withheld Pursuant to 10 CFR 2.390

[

]

For the EOS-89BTH DSC, GE 7x7 fuel with 49 fuel rods is used as the design basis. Other BWR fuel classes (i.e., 8x8, 9x9, 10x10, and 11x11) have larger numbers of fuel rods per fuel assembly. For instance, 5 steel rods in the GE 7x7 represents $\approx 10\%$ of the fuel assembly, while 7 steel rods in a 9x9 would also represent $\approx 10\%$ of the fuel assembly. Therefore, limits on the number of irradiated stainless steel rods per fuel assembly are developed for each class of BWR fuel to maintain the same $\sim 10\%$ fraction as GE 7x7 fuel.

The number of fuel rods for each fuel assembly is defined in Chapter 2, Table 2-3 and Table 2-4. The minimum numbers of fuel rods (N_F) for each class are:

- 8x8: $N_F = 59$ fuel rods (minimum)
- 9x9: $N_F = 72$ fuel rods (minimum)
- 10x10: $N_F = 82$ fuel rods (minimum)

- 11×11 : $N_F = 112$ fuel rods (minimum)

The maximum number of irradiated stainless steel rods per fuel assembly for different fuel classes is N_{SS} , where $N_{SS} = 5/49 \cdot N_F$. The maximum number of irradiated stainless steel rods per DSC is N_{DSC} , where $N_{DSC} = 20 \cdot N_{SS}$, based on the 20 reconstituted fuel assemblies modeled in the EOS-89BTH DSC analysis. Values of N_{SS} and N_{DSC} as a function of BWR fuel assembly class are provided in TS Table 23 [6-11].

6.2.6.2 EOS-89BTH DSC Transferred in the EOS-TC125

The methodology for addressing dose rates due to reconstituted fuel for transfer of the EOS-89BTH DSC within the EOS-TC125 is different than the EOS-TC108 methodology described in Section 6.2.6.1. Major differences are:

- In the EOS-TC108 analysis, reconstituted fuel with irradiated stainless steel rods is not modeled on the periphery. However, the baseline source terms for EOS-TC125 and EOS-HSM analysis are developed with 5 irradiated stainless steel rods in all fuel assemblies, including peripheral fuel assemblies (see Section 6.2.2.3). Therefore, for up to 5 irradiated stainless steel rods per fuel assembly (for 7×7 class fuel), there are no additional restrictions for reconstituted fuel compared to standard fuel.
- In the EOS-TC108 analysis, a maximum of 5 irradiated stainless steel rods per fuel assembly and 100 rods per DSC (for 7×7 class fuel) is defined. However, in the EOS-TC125 analysis, > 5 irradiated stainless steel rods per fuel assembly are allowed, but with a cooling time penalty to result in comparable dose rates.

EOS-HSM and EOS-TC125 response functions are described in Section 6.2.2.3 and provided in Table 6-62 and Table 6-63. These response functions are used to generate ranking dose rates for 142 BECT combinations for each zone. The bounding ranking dose rates with 5 irradiated stainless steel rods are provided in Table 6-9b. The approach is to allow > 5 irradiated stainless steel rods per fuel assembly but increase the minimum cooling time so that response function dose rates are comparable (maximum dose rate increase of 2%) to the baseline results with 5 irradiated stainless steel rods.

The number of irradiated stainless steel rods per fuel assembly is varied from 10 to 45 in increments of 5. Light element masses and uranium loadings are adjusted for each case, as appropriate.

Dose rate results are summarized in Table 6-64. The percent change of the dose rate from the base case is provided for the EOS-HSM (zones 3 and 4) and the EOS-TC125 (total). EOS-HSM zones 1 and 2 response function results are provided for completeness, although zones 1 and 2 contribute negligibly to vent dose rates.

EOS-TC125 dose rates are more limiting than EOS-HSM dose rates. While the EOS-TC125 response function dose rates with > 5 irradiated stainless steel rods are comparable to the baseline dose rates for the indicated minimum cooling times, EOS-HSM response function dose rates are typically much less than the baseline dose rates. The minimum cooling time ranges from 2.0 years for 10 irradiated stainless steel rods to 3.25 years for 45 irradiated stainless steel rods. The baseline case has a minimum cooling time of 1.0 year.

The minimum cooling times in Table 6-64 are used as the basis for the limits provided in TS Table 22 [6-11]. The TS limits are provided as ranges in the numbers of irradiated stainless steel rods. Numbers of irradiated steel rods between those analyzed are conservatively assigned to the next higher analyzed value. For instance, the minimum cooling time developed for 20 irradiated stainless steel rods is conservatively applied to 16, 17, 18, or 19 irradiated stainless steel rods.

Also, consistent with the discussion in Section 6.2.6.1, limits on the number of irradiated stainless steel rods per fuel assembly developed for GE 7x7 fuel are adjusted for 8x8, 9x9, 10x10, and 11x11 fuel. The maximum number of irradiated stainless steel rods per fuel assembly for different fuel classes is N_{SS} . In this analysis, $N_{SS} = G_{SS}/49 \cdot N_F$, where G_{SS} is the number of irradiated stainless steel rods in the GE 7x7 analysis ($G_{SS} = 5, 10, 15$, etc.) and N_F is the minimum number of fuel rods for each fuel assembly class (as defined in Section 6.2.6.1). For instance, if $G_{SS} = 25$ rods, for 8x8 class fuel, $N_F = 59$ rods, and $N_{SS} = 25/49 \cdot 59 = 30$ rods. These limits are summarized in TS Table 22 [6-11].

6.2.7 Irradiation Gases

During irradiation in a reactor, a FA will generate gases due to fission, alpha decay, and light element activation. The moles of gas generated are needed for subsequent pressure calculations documented in Chapter 4, Section 4.7, and are computed using ORIGEN-ARP. The noble gases (He, Ne, Ar, Kr, Xe, and Rn) are of primary interest as these gases do not react with other elements. The elements H, N, F, and Cl generated during irradiation are conservatively assumed to be present in a gaseous state, although these elements may have formed solid compounds and may not be present as a gas. Bromine and iodine are also assumed to be present as a gas because the boiling points of these elements are low. Oxygen is not treated as a gas because it is present primarily in the compound UO_2 .

The quantities of irradiation gases increase with burnup. Therefore, the quantity of gas is maximized for a burnup of 62 GWd/MTU.

Integral fuel burnable absorber rods (IFBA) are used in some Westinghouse PWR designs. IFBA contains B-10, which results in helium gas generation due to the reaction $B-10 + n \rightarrow Li-7 + He-4$. While the design basis B&W 15x15 FA does not contain IFBA, the effect of an IFBA FA is conservatively included by considering 450 g boron.

Proprietary Information on This Page
Withheld Pursuant to 10 CFR 2.390

Proprietary Information on This Page
Withheld Pursuant to 10 CFR 2.390

PWR source terms (without CCs) are provided in Table 6-17 through *Table 6-19c*, and the CC source provided in Table 6-37 is added to these PWR source terms for all FAs. BWR source terms are provided in Table 6-27 through *Table 6-29a*. For the active fuel regions, an axial source distribution is applied per Table 6-30 and Table 6-31 for PWR and BWR fuel, respectively. For the top nozzle, plenum, and bottom nozzle regions, the source is evenly distributed throughout the region.

The EOS-HSMs are modeled explicitly, including the inlet (front) and outlet (roof) vents. Key dimensions used to develop the EOS-HSM models are summarized in Table 6-50, and figures illustrating the basic MCNP model are provided in Figure 6-11 through Figure 6-13. The figures illustrate the EOS-HSM-Medium with the EOS-89BTH DSC, although the geometry of the EOS-HSM-Short with the EOS-37PTH DSC is similar.

The EOS-HSM design consists of a base module that includes the door and 1-foot thick shield walls on the sides and rear. A 3-foot-8-inch thick roof block that matches the length and width of the base rests on the base module. The modules may be positioned either side-by-side in a single row or back-to-back in a double row. When positioned in a single row the rear of the base module is shielded by a 3-foot thick rear shield wall. An end (side) shield wall, which is also 3 feet thick, is placed beside the last module in the row. The end shield wall is comprised of two pieces mated with a Z-joint to prevent direct streaming through the joint. A corner shield wall is placed at the interface of the rear and end shield walls. When the modules are positioned back-to-back, no rear or corner shield walls are used.

Air inlet vents are located on the front and air outlet vents are located on the roof. Because little radiation directly penetrates the thick concrete shielding, essentially all of the dose rate is due to gamma radiation streaming from the vents. Radiation streaming through the outlet vents is mitigated by the use of vent covers. The vent covers feature a 1-inch thick steel plate and approximately 11 inches of concrete. The vent covers are 4 feet wide and are placed between adjacent EOS-HSMs or between an EOS-HSM and the end shield wall. Under normal and off-normal conditions the vent covers are always in place.

[

]

6.4 Shielding Analysis

6.4.1 Computer Codes

MCNP5 v1.40 is used in the shielding analysis [6-5]. MCNP5 is a Monte Carlo transport program that allows full three-dimensional modeling of the EOS-TC and EOS-HSM. Therefore, no geometrical approximations are necessary when developing the shielding models.

6.4.2 Flux-to-Dose Rate Conversion

MCNP5 is used to compute the neutron or gamma flux at the location of interest and the flux is converted to a dose rate using ANSI/ANS-6.1.1-1977 flux-to-dose rate conversion factors [6-10]. These factors are provided in Table 6-51. Results are computed in the units mrem/hr.

6.4.3 EOS-TC Dose Rates

Intact Fuel, Normal and Off-Normal Conditions

[

]

Proprietary Information on Pages 6-45 through 6-49
Withheld Pursuant to 10 CFR 2.390

The results are presented in Table 6-59. With no grout, the dose rate is 1.4 mrem/hr, while with 6 inches of grout, the dose rate is 2.2 mrem/hr. Therefore, the use of lower density grout to repair concrete is acceptable because the localized dose rate remains small. For example, the average dose rate on the end shield wall of the EOS-HSM is 2.53 mrem/hr (see Table 6-55), and if 6 inches of grout were used, the dose rate would increase to only $2.53 \times 2.2 / 1.4 = 4.0$ mrem/hr. Dose rates are dominated by streaming from the vents because little radiation penetrates the thick concrete shield walls, and repairing the EOS-HSM with grout in localized areas will have no effect on worker exposure or site dose rates.

6.5 Supplemental Information

6.5.1 PWR Fuel Qualification

6.5.1.1 EOS-37PTH DSC

Chapter 6 presents the shielding analysis for design basis fuel. For the EOS-37PTH DSC, HLZC 10 results in bounding *EOS-HSM vent* dose rates. HLZC 10 features 1.6 kW fuel in the peripheral region. The peripheral region is illustrated in TS Figure 3/6-11].

To provide additional assurance that TS dose rate limits will be met, a relationship between decay heat, burnup, enrichment, cooling time, and source terms is developed for 3.5 kW fuel and provided as a fuel qualification table (FQTs. The methodology to develop *this* FQT is the same as used to develop the design basis source terms.

The purpose of the FQT is solely to provide an additional dose rate constraint. Decay heat for each fuel assembly to be loaded is determined using NRC Regulatory Guide 3.54, ORIGEN-ARP, or other acceptable method.

The FQT developed based on 3.5 kW is a global constraint and is applied to every PWR fuel assembly to be loaded. This FQT is provided as TS Table 7B/6-11].

A range of burnup, enrichment, and cooling time combinations are considered for the inner regions of HLZC 10, as documented in Table 6-8. The design basis source terms in the inner regions are optimized to maximize dose rates. However, dose rates, both transfer cask and storage, are dominated by thermally hot fuel in the peripheral region because inner locations are heavily self-shielded by peripheral fuel assemblies. For HLZC 4, the peripheral region (zone 3) contributes approximately 80% of the dose rate on the side of the EOS-TC125/135. For the EOS-HSM, the peripheral region (zone 3) contributes approximately 95% of the vent dose rate. *The peripheral contribution for HLZC 10 would be similar.* Because the inner basket locations do not contribute appreciably to the total dose rate, an FQT constraint on the inner basket locations *in addition to TS Table 7B* is not imposed.

The burnup in the FQT is expressed in units of GWd/FA rather than GWd/MTU. The burnup in GWd/FA is the burnup in GWd/MTU multiplied by the MTU of the fuel assembly. The minimum cooling times are obtained *this* table tables using linear interpolation.

- Linearly interpolating for $BU = 22.5$ GWd/FA between $CT = 2.15$ years and $CT = 2.38$ years, the minimum cooling time is $CT = 2.18$ years.

Because 4 years > 2.18 years, the fuel assembly meets the TS Table 7B requirements. Because it is the only LEOF assembly in the DSC, it may be stored in the basket location of interest.

6.5.1.2 EOS-89BTH DSC

Chapter 6 presents the shielding analysis for design basis fuel. For the EOS-89BTH DSC, a shielding HLZC is developed that bounds HLZC 1 through 6. Consistent with HLZC 5, the shielding HLZC features 1.7 kW fuel assemblies in the peripheral region. The 1.7 kW fuel assemblies are the dominant fuel assemblies in the as-modeled peripheral region. The peripheral region is illustrated in TS Figure 8 [6-11].

To provide additional assurance that TS dose rate limits will be met, a relationship between decay heat, burnup, enrichment, cooling time, and source terms is developed for 1.7 kW fuel and provided as a fuel qualification table (FQT). The methodology to develop this FQT is the same as used to develop the design basis source terms.

The purpose of the FQT is solely to provide an additional dose rate constraint. Decay heat for each fuel assembly to be loaded is determined using NRC Regulatory Guide 3.54, ORIGEN-ARP, or another acceptable method.

The FQT developed based on 1.7 kW is a global constraint and is applied to every BWR fuel assembly to be loaded. This FQT is provided as TS Table 21 [6-11]. Because the inner basket locations do not contribute appreciably to the total dose rate, an FQT constraint on the inner basket locations in addition to TS Table 21 is not imposed.

The burnup in the FQT is expressed in units of GWd/FA rather than GWd/MTU. The burnup in GWd/FA is the burnup in GWd/MTU multiplied by the MTU of the fuel assembly. The minimum cooling times are obtained for this table using linear interpolation.

As documented in Section 6.2.8, a small percentage (<0.5%) of fuel assemblies are low-enrichment outlier fuel (LEOF). LEOF is rare, occurring at a rate of approximately 1 per 200 fuel assemblies. To determine if a fuel assembly is LEOF, the enrichment is compared to the minimum value specified in TS Table 18. LEOF would not affect storage dose rates, which are gamma dominated, but could have a small effect (generally < 5%) on transfer cask dose rates. Based on these considerations, up to 4 LEOFs are allowed in the peripheral region. A minimum of six non-LEOFs shall circumferentially separate LEOFs within the peripheral region. There are no limitations on the number and location of LEOF stored in the inner region.

Because LEOF, by definition, is below the minimum enrichments provided in the FQT, minimum cooling times for LEOF are obtained by extrapolating the FQT cooling times using an appropriate method. Because minimum cooling times increase with lower enrichments, this extrapolation provides an additional cooling time penalty.

The overall method for application of this FQT and qualification of LEOF is provided below.

- 1. Determine the decay heat of all fuel to be loaded in an EOS-89BTH DSC using NRC Regulatory Guide 3.54, ORIGEN-ARP, or another acceptable method. Confirm the decay heat limit is met for each basket location.*
- 2. Determine if LEOF is present in the fuel to be loaded by application of TS Table 18.*
 - a) Up to 4 LEOF are allowed in the peripheral region. A minimum of six non-LEOFs shall circumferentially separate LEOFs within the peripheral region.*
 - b) There are no limitations on the number and location of LEOF stored in the inner region.*
- 3. Verify all fuel to be loaded meets the minimum cooling time of TS Table 21. Fuel that does not meet the cooling time limitations of this table cannot be loaded.*

This FQT provides an additional constraint to ensure compliance with the dose rate limitations in TS 5.1.2(c).

6.5.2 References

- 6-1 Oak Ridge National Laboratory, “A Modular Code System for Performing Standardized Computer Analyses for Licensing Evaluation,” ORNL/TM-2005/39, Version 6, SCALE, January 2009.
- 6-2 Oak Ridge National Laboratory, “Predictions of PWR Spent Nuclear Fuel Isotopic Compositions,” ORNL/TM-2010/44, SCALE 5.1, March 2010.
- 6-3 Oak Ridge National Laboratory, “Standard- and Extended-Burnup PWR and BWR Reactor Models for the ORIGEN2 Code,” ORNL/TM-11018, December 1989.
- 6-4 Pacific Northwest Laboratory, “Spent Fuel Assembly Hardware: Characterization and 10 CFR 61 Classification for Waste Disposal, Volume 1 – Activation Measurements and Comparison with Calculations for Spent Fuel Assembly Hardware,” PNL-6906, Vol. 1, June 1989.
- 6-5 Oak Ridge National Laboratory, “MCNP/MCNPX – Monte Carlo N-Particle Transport Code System Including MCNP5 1.40 and MCNPX 2.5.0 and Data Libraries,” CCC-730, RSICC Computer Code Collection, January 2006.

- 6-6 NUREG/CR-6801, “Recommendations for Addressing Axial Burnup in PWR Burnup Credit Analyses,” March 2003.
- 6-7 NUREG-1536, Rev. 1, “Standard Review Plan for Spent Fuel Dry Storage Systems at a General License Facility,” July 2010.
- 6-8 Design Data Document DI-81001-02, NOK Document, “Technical Specification for the Supply of Transportable Casks for the Storage of Kernkraftwerk Leibstardt (KKL) Spent Fuel in ZWILAG,” TS 07/01, Rev. 1.
- 6-9 Pacific Northwest National Laboratory, “Compendium of Material Composition Data for Radiation Transport Modeling,” PNNL-15870, Rev. 1, March 2011.
- 6-10 ANSI/ANS-6.1.1-1977, “American National Standard Neutron and Gamma-Ray Flux-to-Dose-Rate Factors,” American National Standards Institute, Inc., New York, New York.
- 6-11 CoC 1042 Appendix A, NUHOMS® EOS System Generic Technical Specifications, Amendment 3.
- 6-12 NUREG/CR-6999, “Technical Basis for a Proposed Expansion of Regulatory Guide 3.54 - Decay Heat Generation in an Independent Spent Fuel Storage Installation,” February 2010.
- 6-13 U.S. Energy Information Administration (EIA), Spent Nuclear Fuel GC-859 Database, Accessed January 20, 2019. URL: https://www.eia.gov/nuclear/spent_fuel/
- 6-14 *ADVANTG - An Automated Variance Reduction Parameter Generator, Oak Ridge National Laboratory, August 2015.*
- 6-15 Interagency Agreement DE-SA09-01 SR18976/TVA No. P-01 N8A-249655-001 between the Department of Energy (DOE) and the Tennessee Valley Authority (TVA) for the Off-Specification Fuel Project, April 5, 2001.

Proprietary Information on This Page
Withheld Pursuant to 10 CFR 2.390

Table 6-9a**Source Term Ranking for the EOS-89BTH DSC Shielding HLZC, Standard Fuel**

EOS-HSM				
Zone	BU (GWd/MTU)	E (%)	CT (years)	Max RF-HSM (rmem/hr)
<i>1</i>	36	2.2	4.72	12193
<i>2</i>	50	3.7	4.22	18270
<i>3</i>	62	3.8	2.34	37757
<i>4</i>	62	3.8	1.68	46730
EOS-TC125				
Zone	BU (GWd/MTU)	E (%)	CT (years)	Max RF-TC125 (rmem/hr)
<i>1</i>	62	3.8	15.57	45
<i>2</i>	62	3.8	6.23	144
<i>3</i>	35	1.7	1.53	944
<i>4</i>	35	1.7	1.11	2090
<i>Total</i>	-	-	-	3221
Co-60 Activity				
Zone	BU (GWd/MTU)	E (%)	CT (years)	Max Co-60 (Ci)
<i>1</i>	30	1.5	4.05	242.7
<i>2</i>	35	1.7	3.23	292.0
<i>3</i>	35	1.7	1.53	365.1
<i>4</i>	62	3.8	1.68	389.3

Table 6-9b
Source Term Ranking for the EOS-89BTH DSC Shielding HLZC,
Reconstituted Fuel

EOS-HSM				
Zone	BU (GWd/MTU)	E (%)	CT (years)	Max RF-HSM (rmem/hr)
<i>1</i>	<i>35</i>	<i>1.7</i>	<i>4.38</i>	<i>14196</i>
<i>2</i>	<i>50</i>	<i>3.1</i>	<i>4.00</i>	<i>20364</i>
<i>3</i>	<i>62</i>	<i>3.8</i>	<i>2.09</i>	<i>40225</i>
<i>4</i>	<i>62</i>	<i>3.8</i>	<i>1.48</i>	<i>49092</i>
EOS-TC125				
Zone	BU (GWd/MTU)	E (%)	CT (years)	Max RF-TC125 (rmem/hr)
<i>1</i>	<i>62</i>	<i>3.8</i>	<i>12.22</i>	<i>45</i>
<i>2</i>	<i>62</i>	<i>3.8</i>	<i>5.41</i>	<i>147</i>
<i>3</i>	<i>35</i>	<i>1.7</i>	<i>1.37</i>	<i>1115</i>
<i>4</i>	<i>35</i>	<i>1.7</i>	<i>1.00</i>	<i>2385</i>
<i>Total</i>	<i>-</i>	<i>-</i>	<i>-</i>	<i>3693</i>
Co-60 Activity				
Zone	BU (GWd/MTU)	E (%)	CT (years)	Max Co-60 (Ci)
<i>1</i>	<i>35</i>	<i>1.7</i>	<i>4.38</i>	<i>1137</i>
<i>2</i>	<i>35</i>	<i>1.7</i>	<i>3.00</i>	<i>1363</i>
<i>3</i>	<i>35</i>	<i>1.7</i>	<i>1.37</i>	<i>1688</i>
<i>4</i>	<i>62</i>	<i>3.8</i>	<i>1.48</i>	<i>1808</i>

Table 6-23
BWR Source Term for the EOS-TC125, *Shielding* HLZC Zone 1 (Normal and Accident)

Burnup (GWD/MTU)			35	62	35	35
Enrichment (wt. % U-235)			1.7	3.8	1.7	1.7
Cooling Time (years)			4.38	12.22	4.38	4.38
Gamma Source Term, γ/(sec*FA)						
E_{min}, MeV	to	E_{max}, MeV	Bottom Nozzle	In-core	Plenum	Top Nozzle
1.00E-02	to	5.00E-02	5.241E+10	4.146E+14	8.172E+10	2.293E+10
5.00E-02	to	1.00E-01	8.380E+09	1.123E+14	5.831E+09	3.172E+09
1.00E-01	to	2.00E-01	2.924E+09	8.078E+13	5.917E+09	1.355E+09
2.00E-01	to	3.00E-01	1.626E+08	2.390E+13	3.907E+08	7.951E+07
3.00E-01	to	4.00E-01	3.392E+08	1.551E+13	1.168E+09	1.886E+08
4.00E-01	to	6.00E-01	4.672E+09	4.442E+13	2.414E+10	3.113E+09
6.00E-01	to	8.00E-01	2.443E+09	8.000E+14	1.259E+10	1.661E+09
8.00E-01	to	1.00E+00	4.843E+10	2.482E+13	3.176E+10	1.536E+10
1.00E+00	to	1.33E+00	2.411E+12	4.169E+13	1.605E+12	9.089E+11
1.33E+00	to	1.66E+00	6.809E+11	9.026E+12	4.532E+11	2.567E+11
1.66E+00	to	2.00E+00	9.791E+02	4.255E+10	6.295E+02	7.160E+02
2.00E+00	to	2.50E+00	1.629E+07	4.736E+09	1.084E+07	6.141E+06
2.50E+00	to	3.00E+00	1.392E+04	3.964E+08	9.264E+03	5.247E+03
3.00E+00	to	4.00E+00	2.387E-07	5.480E+07	2.201E-08	1.347E-06
4.00E+00	to	5.00E+00	8.487E-15	1.100E+07	8.488E-15	8.489E-15
5.00E+00	to	6.50E+00	2.446E-15	4.415E+06	2.446E-15	2.446E-15
6.50E+00	to	8.00E+00	3.111E-16	8.661E+05	3.111E-16	3.111E-16
8.00E+00	to	1.00E+01	4.151E-17	1.839E+05	4.152E-17	4.152E-17
Total Gamma, γ /(sec*FA)			3.212E+12	1.567E+15	2.221E+12	1.213E+12
Total Neutron Source Term, n/(sec*FA)						
Raw ORIGEN-ARP source for uniform burnup, <i>normal</i>						3.168E+08
Treated with peaking factor 1.232 and $k_{eff}=0.4$ (dry), <i>normal</i>						6.505E+08
Treated with peaking factor 1.232 and $k_{eff}=0.65$ (wet), <i>normal</i>						1.115E+09
Raw ORIGEN-ARP source for reconstituted fuel, uniform burnup, accident (BU = 62 GWd/MTU, E = 3.8 wt.% U-235, CT = 12.22 years)						3.168E+08
Treated with peaking factor 1.232 and $k_{eff}=0.4$ (dry), accident						6.505E+08

Table 6-24
BWR Source Term for the EOS-TC125, *Shielding* HLZC Zone 2 (Normal and Accident)

Burnup (GWD/MTU)			35	62	35	35
Enrichment (wt. % U-235)			1.7	3.8	1.7	1.7
Cooling Time (years)			3.00	5.41	3.00	3.00
Gamma Source Term, γ/(sec*FA)						
E_{min}, MeV	to	E_{max}, MeV	Bottom Nozzle	In-core	Plenum	Top Nozzle
1.00E-02	to	5.00E-02	6.966E+10	6.255E+14	1.332E+11	3.200E+10
5.00E-02	to	1.00E-01	1.008E+10	1.717E+14	7.091E+09	3.821E+09
1.00E-01	to	2.00E-01	3.715E+09	1.354E+14	8.121E+09	1.760E+09
2.00E-01	to	3.00E-01	2.105E+08	3.874E+13	5.480E+08	1.057E+08
3.00E-01	to	4.00E-01	4.922E+08	2.602E+13	1.843E+09	2.831E+08
4.00E-01	to	6.00E-01	6.645E+09	3.479E+14	3.430E+10	4.428E+09
6.00E-01	to	8.00E-01	3.496E+09	1.241E+15	1.804E+10	2.363E+09
8.00E-01	to	1.00E+00	1.485E+11	1.590E+14	9.739E+10	4.704E+10
1.00E+00	to	1.33E+00	2.892E+12	9.932E+13	1.925E+12	1.090E+12
1.33E+00	to	1.66E+00	8.168E+11	2.875E+13	5.436E+11	3.079E+11
1.66E+00	to	2.00E+00	1.369E+05	3.534E+11	8.938E+04	1.001E+05
2.00E+00	to	2.50E+00	1.954E+07	5.047E+11	1.301E+07	7.367E+06
2.50E+00	to	3.00E+00	1.670E+04	2.493E+10	1.111E+04	6.294E+03
3.00E+00	to	4.00E+00	2.457E-07	2.348E+09	2.266E-08	1.387E-06
4.00E+00	to	5.00E+00	1.063E-13	1.426E+07	1.063E-13	1.064E-13
5.00E+00	to	6.50E+00	3.064E-14	5.722E+06	3.064E-14	3.064E-14
6.50E+00	to	8.00E+00	3.897E-15	1.123E+06	3.897E-15	3.898E-15
8.00E+00	to	1.00E+01	5.201E-16	2.383E+05	5.201E-16	5.202E-16
Total Gamma, γ /(sec*FA)			3.952E+12	2.874E+15	2.769E+12	1.490E+12
Total Neutron Source Term, n/(sec*FA)						
Raw ORIGEN-ARP source for uniform burnup, <i>normal</i>						4.105E+08
Treated with peaking factor 1.232 and $k_{eff}=0.4$ (dry), <i>normal</i>						8.429E+08
Treated with peaking factor 1.232 and $k_{eff}=0.65$ (wet), <i>normal</i>						1.445E+09
Raw ORIGEN-ARP source for standard fuel, uniform burnup, accident (BU = 62 GWd/MTU, E = 3.8 wt.% U-235, CT = 6.23 years)						4.483E+08
Treated with peaking factor 1.232 and $k_{eff}=0.4$ (dry), accident						9.205E+08

Table 6-25
BWR Source Term for the EOS-TC125, *Shielding* HLZC Zone 3 (Normal and Accident)

Burnup (GWD/MTU)			35	35	35	35
Enrichment (wt. % U-235)			1.7	1.7	1.7	1.7
Cooling Time (years)			1.37	1.37	1.37	1.37
Gamma Source Term, γ/(sec*FA)						
E_{min}, MeV	to	E_{max}, MeV	Bottom Nozzle	In-core	Plenum	Top Nozzle
1.00E-02	to	5.00E-02	1.137E+11	2.284E+15	3.053E+11	5.790E+10
5.00E-02	to	1.00E-01	1.277E+10	7.456E+14	9.615E+09	4.919E+09
1.00E-01	to	2.00E-01	5.109E+09	7.087E+14	1.217E+10	2.511E+09
2.00E-01	to	3.00E-01	3.770E+08	1.910E+14	1.168E+09	2.098E+08
3.00E-01	to	4.00E-01	2.154E+09	1.499E+14	1.014E+10	1.377E+09
4.00E-01	to	6.00E-01	1.290E+10	1.076E+15	5.356E+10	8.789E+09
6.00E-01	to	8.00E-01	2.307E+10	1.586E+15	1.193E+11	1.541E+10
8.00E-01	to	1.00E+00	5.616E+11	3.502E+14	3.678E+11	1.812E+11
1.00E+00	to	1.33E+00	3.581E+12	1.829E+14	2.383E+12	1.350E+12
1.33E+00	to	1.66E+00	1.011E+12	6.346E+13	6.729E+11	3.811E+11
1.66E+00	to	2.00E+00	4.570E+07	4.991E+12	3.388E+07	3.336E+07
2.00E+00	to	2.50E+00	2.436E+07	1.357E+13	1.699E+07	9.233E+06
2.50E+00	to	3.00E+00	2.081E+04	3.669E+11	1.448E+04	7.885E+03
3.00E+00	to	4.00E+00	2.543E-07	3.360E+10	2.345E-08	1.435E-06
4.00E+00	to	5.00E+00	2.066E-12	6.437E+06	2.066E-12	2.066E-12
5.00E+00	to	6.50E+00	5.952E-13	2.583E+06	5.953E-13	5.953E-13
6.50E+00	to	8.00E+00	7.571E-14	5.068E+05	7.571E-14	7.572E-14
8.00E+00	to	1.00E+01	1.010E-14	1.076E+05	1.010E-14	1.011E-14
Total Gamma, g/(sec*FA)			5.323E+12	7.357E+15	3.935E+12	2.003E+12
Total Neutron Source Term, n/(sec*FA)						
Raw ORIGEN-ARP source for uniform burnup, <i>normal</i>						1.850E+08
Treated with peaking factor 1.232 and $k_{\text{eff}}=0.4$ (dry), <i>normal</i>						3.799E+08
Treated with peaking factor 1.232 and $k_{\text{eff}}=0.65$ (wet), <i>normal</i>						6.512E+08
Raw ORIGEN-ARP source for standard fuel, uniform burnup, accident (BU = 62 GWd/MTU, E = 3.8 wt.% U-235, CT = 2.34 years)						5.251E+08
Treated with peaking factor 1.232 and $k_{\text{eff}}=0.4$ (dry), accident						1.078E+09

Table 6-26
**BWR Source Term for the EOS-TC125, *Shielding* HLZC Zone 4 (*Normal*
and Accident)**

Burnup (GWD/MTU)			62	35	62	62
Enrichment (wt. % U-235)			3.8	1.7	3.8	3.8
Cooling Time (years)			1.48	1.00	1.48	1.48
Gamma Source Term, γ /(sec*FA)						
E _{min} , MeV	to	E _{max} , MeV	Bottom Nozzle	In-core	Plenum	Top Nozzle
1.00E-02	to	5.00E-02	1.198E+11	2.970E+15	3.175E+11	6.106E+10
5.00E-02	to	1.00E-01	1.359E+10	9.742E+14	1.014E+10	5.284E+09
1.00E-01	to	2.00E-01	5.635E+09	9.374E+14	1.411E+10	2.822E+09
2.00E-01	to	3.00E-01	3.902E+08	2.503E+14	1.218E+09	2.161E+08
3.00E-01	to	4.00E-01	1.908E+09	1.976E+14	8.866E+09	1.213E+09
4.00E-01	to	6.00E-01	1.411E+10	1.304E+15	6.300E+10	9.545E+09
6.00E-01	to	8.00E-01	1.758E+10	2.106E+15	9.086E+10	1.177E+10
8.00E-01	to	1.00E+00	5.536E+11	4.084E+14	3.627E+11	1.779E+11
1.00E+00	to	1.33E+00	3.833E+12	2.068E+14	2.547E+12	1.464E+12
1.33E+00	to	1.66E+00	1.082E+12	7.352E+13	7.192E+11	4.133E+11
1.66E+00	to	2.00E+00	3.482E+07	6.555E+12	2.704E+07	2.540E+07
2.00E+00	to	2.50E+00	2.606E+07	1.863E+13	1.806E+07	9.999E+06
2.50E+00	to	3.00E+00	2.226E+04	4.745E+11	1.539E+04	8.539E+03
3.00E+00	to	4.00E+00	4.147E-07	4.335E+10	3.824E-08	2.340E-06
4.00E+00	to	5.00E+00	1.569E-12	6.743E+06	1.569E-12	1.569E-12
5.00E+00	to	6.50E+00	4.521E-13	2.706E+06	4.521E-13	4.522E-13
6.50E+00	to	8.00E+00	5.751E-14	5.308E+05	5.751E-14	5.752E-14
8.00E+00	to	1.00E+01	7.675E-15	1.127E+05	7.675E-15	7.676E-15
Total Gamma, g/(sec*FA)			5.642E+12	9.454E+15	4.135E+12	2.147E+12
Total Neutron Source Term, n/(sec*FA)						
Raw ORIGEN-ARP source for uniform burnup, normal						1.943E+08
Treated with peaking factor 1.232 and k _{eff} =0.4 (dry), normal						3.990E+08
Treated with peaking factor 1.232 and k _{eff} =0.65 (wet), normal						6.839E+08
Raw ORIGEN-ARP source for standard fuel, uniform burnup, accident (BU = 62 GWd/MTU, E = 3.8 wt.% U-235, CT = 1.68 years)						5.450E+08
Treated with peaking factor 1.232 and k _{eff} =0.4 (dry), accident						1.119E+09

Table 6-27
BWR Source Term for the EOS-HSM, *Shielding* HLZC Zone 1 (Normal and Accident)

Burnup (GWD/MTU)			35	35	35	35
Enrichment (wt. % U-235)			1.7	1.7	1.7	1.7
Cooling Time (years)			4.38	4.38	4.38	4.38
Gamma Source Term, γ /(sec*FA)						
E _{min} , MeV	to	E _{max} , MeV	Bottom Nozzle	In-core	Plenum	Top Nozzle
1.00E-02	to	5.00E-02	5.241E+10	5.002E+14	8.172E+10	2.293E+10
5.00E-02	to	1.00E-01	8.380E+09	1.450E+14	5.831E+09	3.172E+09
1.00E-01	to	2.00E-01	2.924E+09	1.208E+14	5.917E+09	1.355E+09
2.00E-01	to	3.00E-01	1.626E+08	3.431E+13	3.907E+08	7.951E+07
3.00E-01	to	4.00E-01	3.392E+08	2.476E+13	1.168E+09	1.886E+08
4.00E-01	to	6.00E-01	4.672E+09	2.916E+14	2.414E+10	3.113E+09
6.00E-01	to	8.00E-01	2.443E+09	8.086E+14	1.259E+10	1.661E+09
8.00E-01	to	1.00E+00	4.843E+10	1.183E+14	3.176E+10	1.536E+10
1.00E+00	to	1.33E+00	2.411E+12	9.120E+13	1.605E+12	9.089E+11
1.33E+00	to	1.66E+00	6.809E+11	2.711E+13	4.532E+11	2.567E+11
1.66E+00	to	2.00E+00	9.791E+02	6.126E+11	6.295E+02	7.160E+02
2.00E+00	to	2.50E+00	1.629E+07	1.103E+12	1.084E+07	6.141E+06
2.50E+00	to	3.00E+00	1.392E+04	4.673E+10	9.264E+03	5.247E+03
3.00E+00	to	4.00E+00	2.387E-07	4.346E+09	2.201E-08	1.347E-06
4.00E+00	to	5.00E+00	8.487E-15	5.499E+06	8.488E-15	8.489E-15
5.00E+00	to	6.50E+00	2.446E-15	2.207E+06	2.446E-15	2.446E-15
6.50E+00	to	8.00E+00	3.111E-16	4.330E+05	3.111E-16	3.111E-16
8.00E+00	to	1.00E+01	4.151E-17	9.193E+04	4.152E-17	4.152E-17
Total Gamma, g/(sec*FA)			3.212E+12	2.164E+15	2.221E+12	1.213E+12
Total Neutron Source Term, n/(sec*FA)						
Raw ORIGEN-ARP source for uniform burnup						1.576E+08
Treated with peaking factor 1.232 and k _{eff} =0.4 (dry)						3.236E+08

Table 6-28
BWR Source Term for the EOS-HSM, *Shielding* HLZC Zone 2 (Normal and Accident)

Burnup (GWD/MTU)			35	50	35	35
Enrichment (wt. % U-235)			1.7	3.1	1.7	1.7
Cooling Time (years)			3.00	4.00	3.00	3.00
Gamma Source Term, γ /(sec*FA)						
E _{min} , MeV	to	E _{max} , MeV	Bottom Nozzle	In-core	Plenum	Top Nozzle
1.00E-02	to	5.00E-02	6.966E+10	7.260E+14	1.332E+11	3.200E+10
5.00E-02	to	1.00E-01	1.008E+10	2.108E+14	7.091E+09	3.821E+09
1.00E-01	to	2.00E-01	3.715E+09	1.760E+14	8.121E+09	1.760E+09
2.00E-01	to	3.00E-01	2.105E+08	4.979E+13	5.480E+08	1.057E+08
3.00E-01	to	4.00E-01	4.922E+08	3.560E+13	1.843E+09	2.831E+08
4.00E-01	to	6.00E-01	6.645E+09	4.659E+14	3.430E+10	4.428E+09
6.00E-01	to	8.00E-01	3.496E+09	1.208E+15	1.804E+10	2.363E+09
8.00E-01	to	1.00E+00	1.485E+11	1.966E+14	9.739E+10	4.704E+10
1.00E+00	to	1.33E+00	2.892E+12	1.101E+14	1.925E+12	1.090E+12
1.33E+00	to	1.66E+00	8.168E+11	3.413E+13	5.436E+11	3.079E+11
1.66E+00	to	2.00E+00	1.369E+05	8.192E+11	8.938E+04	1.001E+05
2.00E+00	to	2.50E+00	1.954E+07	1.571E+12	1.301E+07	7.367E+06
2.50E+00	to	3.00E+00	1.670E+04	6.138E+10	1.111E+04	6.294E+03
3.00E+00	to	4.00E+00	2.457E-07	5.700E+09	2.266E-08	1.387E-06
4.00E+00	to	5.00E+00	1.063E-13	9.179E+06	1.063E-13	1.064E-13
5.00E+00	to	6.50E+00	3.064E-14	3.684E+06	3.064E-14	3.064E-14
6.50E+00	to	8.00E+00	3.897E-15	7.227E+05	3.897E-15	3.898E-15
8.00E+00	to	1.00E+01	5.201E-16	1.534E+05	5.201E-16	5.202E-16
Total Gamma, g/(sec*FA)			3.952E+12	3.215E+15	2.769E+12	1.490E+12
Total Neutron Source Term, n/(sec*FA)						
Raw ORIGEN-ARP source for uniform burnup						2.635E+08
Treated with peaking factor 1.232 and k _{eff} =0.4 (dry)						5.411E+08

Table 6-29
BWR Source Term for the EOS-HSM, *Shielding* HLZC Zone 3 (Normal and Accident)

Burnup (GWD/MTU)			35	62	35	35
Enrichment (wt. % U-235)			1.7	3.8	1.7	1.7
Cooling Time (years)			1.37	2.09	1.37	1.37
Gamma Source Term, γ/(sec*FA)						
E_{min}, MeV	to	E_{max}, MeV	Bottom Nozzle	In-core	Plenum	Top Nozzle
1.00E-02	to	5.00E-02	1.137E+11	1.803E+15	3.053E+11	5.790E+10
5.00E-02	to	1.00E-01	1.277E+10	5.632E+14	9.615E+09	4.919E+09
1.00E-01	to	2.00E-01	5.109E+09	5.099E+14	1.217E+10	2.511E+09
2.00E-01	to	3.00E-01	3.770E+08	1.403E+14	1.168E+09	2.098E+08
3.00E-01	to	4.00E-01	2.154E+09	1.063E+14	1.014E+10	1.377E+09
4.00E-01	to	6.00E-01	1.290E+10	1.227E+15	5.356E+10	8.789E+09
6.00E-01	to	8.00E-01	2.307E+10	2.128E+15	1.193E+11	1.541E+10
8.00E-01	to	1.00E+00	5.616E+11	4.817E+14	3.678E+11	1.812E+11
1.00E+00	to	1.33E+00	3.581E+12	1.887E+14	2.383E+12	1.350E+12
1.33E+00	to	1.66E+00	1.011E+12	6.746E+13	6.729E+11	3.811E+11
1.66E+00	to	2.00E+00	4.570E+07	3.244E+12	3.388E+07	3.336E+07
2.00E+00	to	2.50E+00	2.436E+07	7.853E+12	1.699E+07	9.233E+06
2.50E+00	to	3.00E+00	2.081E+04	2.421E+11	1.448E+04	7.885E+03
3.00E+00	to	4.00E+00	2.543E-07	2.229E+10	2.345E-08	1.435E-06
4.00E+00	to	5.00E+00	2.066E-12	1.637E+07	2.066E-12	2.066E-12
5.00E+00	to	6.50E+00	5.952E-13	6.570E+06	5.953E-13	5.953E-13
6.50E+00	to	8.00E+00	7.571E-14	1.289E+06	7.571E-14	7.572E-14
8.00E+00	to	1.00E+01	1.010E-14	2.737E+05	1.010E-14	1.011E-14
Total Gamma, γ /(sec*FA)			5.323E+12	7.228E+15	3.935E+12	2.003E+12
Total Neutron Source Term, n/(sec*FA)						
Raw ORIGEN-ARP source for uniform burnup						4.722E+08
Treated with peaking factor 1.232 and $k_{\text{eff}}=0.4$ (dry)						9.696E+08

Table 6-29a
BWR Source Term for the EOS-HSM, Shielding HLZC Zone 4 (Normal and Accident)

Burnup (GWD/MTU)			62	62	62	62
Enrichment (wt. % U-235)			38	38	38	38
Cooling Time (years)			1.48	1.48	1.48	1.48
Gamma Source Term, γ (sec*FA)						
E_{min} , MeV	to	E_{max} , MeV	Bottom Nozzle	In-core	Plenum	Top Nozzle
1.00E-02	to	5.00E-02	1.198E+11	2.533E+15	3.175E+11	6.106E+10
5.00E-02	to	1.00E-01	1.359E+10	8.079E+14	1.014E+10	5.284E+09
1.00E-01	to	2.00E-01	5.635E+09	7.511E+14	1.411E+10	2.822E+09
2.00E-01	to	3.00E-01	3.902E+08	2.038E+14	1.218E+09	2.161E+08
3.00E-01	to	4.00E-01	1.908E+09	1.570E+14	8.866E+09	1.213E+09
4.00E-01	to	6.00E-01	1.411E+10	1.586E+15	6.300E+10	9.545E+09
6.00E-01	to	8.00E-01	1.758E+10	2.513E+15	9.086E+10	1.177E+10
8.00E-01	to	1.00E+00	5.536E+11	6.002E+14	3.627E+11	1.779E+11
1.00E+00	to	1.33E+00	3.833E+12	2.223E+14	2.547E+12	1.464E+12
1.33E+00	to	1.66E+00	1.082E+12	8.299E+13	7.192E+11	4.133E+11
1.66E+00	to	2.00E+00	3.482E+07	4.976E+12	2.704E+07	2.540E+07
2.00E+00	to	2.50E+00	2.606E+07	1.307E+13	1.806E+07	9.999E+06
2.50E+00	to	3.00E+00	2.226E+04	3.665E+11	1.539E+04	8.539E+03
3.00E+00	to	4.00E+00	4.147E-07	3.362E+10	3.824E-08	2.340E-06
4.00E+00	to	5.00E+00	1.569E-12	1.699E+07	1.569E-12	1.569E-12
5.00E+00	to	6.50E+00	4.521E-13	6.818E+06	4.521E-13	4.522E-13
6.50E+00	to	8.00E+00	5.751E-14	1.337E+06	5.751E-14	5.752E-14
8.00E+00	to	1.00E+01	7.675E-15	2.840E+05	7.675E-15	7.676E-15
Total Gamma, g/(sec*FA)			5.642E+12	9.476E+15	4.135E+12	2.147E+12
Total Neutron Source Term, n/(sec*FA)						
Raw ORIGEN-ARP source for uniform burnup						4.906E+08
Treated with peaking factor 1.232 and k_{eff} =0.4 (dry)						1.007E+09

Proprietary Information on This Page
Withheld Pursuant to 10 CFR 2.390

Table 6-48
EOS-TC108 and EOS-TC125/135 Key As-Modeled Dimensions (Inches)

Item	EOS-TC108	EOS-TC125/135
Cask inner diameter	76.25	76.25
Carbon steel inner shell thickness	0.75	0.75
Stainless steel side lead minimum thickness	2.4	3.51 ⁽¹⁾
Carbon steel outer shell thickness	1.0	1.0
Neutron shield water thickness	2.5	4.0
Ram port inner diameter	22.0	22.0
Carbon steel ram plate thickness	1.25	1.25
Carbon steel bottom panel thickness	0.75	0.75
Borated polyethylene thickness	2.13	2.13
Carbon steel bottom end plate thickness	2.0	2.0
Carbon steel bottom ring height	9.0	9.0
Carbon steel top ring height	16.25	16.25
Top ring lead height	5.65	5.65
Top ring lead minimum thickness	0.85	0.85
Top ring thickness (at top nozzle)	4.63	5.38
Top cover plate (lid) thickness	2.0 (Aluminum)	3.2 (Carbon Steel)

(1) In the EOS-37PTH DSC models, the lead thickness is modeled at the indicated value. In the EOS-89BTH DSC models, the lead thickness is modeled at 3.07 inches, which is the minimum value of the variable lead EOS-TC125/135 design.

Proprietary Information on This Page
Withheld Pursuant to 10 CFR 2.390

Proprietary Information on Pages 6-151 through 6-152
Withheld Pursuant to 10 CFR 2.390

Proprietary Information on Pages 6-154 through 6-158
Withheld Pursuant to 10 CFR 2.390

Proprietary Information on This Page
Withheld Pursuant to 10 CFR 2.390

Table 6-62
EOS-HSM Response Function for the EOS-89BTH DSC Shielding HLZC

	$E_{upper} \text{ (MeV)}$	$Dose \text{ Rate (mrem/hr)}$
<i>Primary Gamma</i>	0.05	0.00E+00
	0.1	0.00E+00
	0.2	8.42E-15
	0.3	2.21E-13
	0.4	8.98E-13
	0.6	2.99E-12
	0.8	8.25E-12
	1	1.64E-11
	1.33	3.09E-11
	1.66	5.32E-11
	2	7.65E-11
	2.5	1.08E-10
	3	1.47E-10
	4	2.02E-10
	5	2.69E-10
	6.5	3.45E-10
	8	4.28E-10
	10	5.13E-10
<i>Secondary Gamma</i>	-	8.20E-09
<i>Neutron</i>	-	8.48E-08

Table 6-63
EOS-TC125 Response Functions for the EOS-89BTH DSC Shielding HLZC

		Zone 1	Zone 2	Zone 3	Zone 4
	$E_{upper} \text{ (MeV)}$	Dose Rate (mrem/hr)	Dose Rate (mrem/hr)	Dose Rate (mrem/hr)	Dose Rate (mrem/hr)
Primary Gamma	0.05	0.00E+00	0.00E+00	0.00E+00	0.00E+00
	0.1	0.00E+00	0.00E+00	0.00E+00	0.00E+00
	0.2	0.00E+00	0.00E+00	0.00E+00	0.00E+00
	0.3	0.00E+00	0.00E+00	0.00E+00	0.00E+00
	0.4	0.00E+00	0.00E+00	0.00E+00	0.00E+00
	0.6	0.00E+00	0.00E+00	2.80E-17	8.03E-17
	0.8	0.00E+00	2.64E-16	5.68E-15	1.19E-14
	1	5.35E-17	5.61E-15	9.23E-14	1.98E-13
	1.33	1.61E-15	8.81E-14	1.01E-12	1.97E-12
	1.66	1.52E-14	5.64E-13	4.94E-12	9.09E-12
	2	6.32E-14	1.77E-12	1.31E-11	2.31E-11
	2.5	1.92E-13	4.40E-12	2.83E-11	4.73E-11
	3	4.32E-13	8.32E-12	4.93E-11	7.92E-11
	4	8.57E-13	1.46E-11	7.87E-11	1.22E-10
	5	1.30E-12	2.07E-11	1.08E-10	1.63E-10
	6.5	1.60E-12	2.46E-11	1.28E-10	1.90E-10
	8	1.69E-12	2.74E-11	1.41E-10	2.08E-10
	10	1.73E-12	2.84E-11	1.50E-10	2.22E-10
Secondary Gamma	-	3.95E-08	6.40E-08	8.94E-08	7.62E-08
Neutron	-	2.96E-08	7.50E-08	1.44E-07	1.59E-07

Table 6-64
EOS-89BTH DSC Reconstituted Fuel Minimum Cooling Time Results

<i>Stainless Steel Rods →</i>	<i>5 (Base)</i>	<i>10</i>	<i>15</i>	<i>20</i>	<i>25</i>	<i>30</i>	<i>35</i>	<i>40</i>	<i>45</i>
<i>Minimum Cooling Time (years) →</i>	<i>1.0</i>	<i>2.0</i>	<i>2.0</i>	<i>2.25</i>	<i>2.50</i>	<i>2.75</i>	<i>3.00</i>	<i>3.25</i>	<i>3.25</i>
<i>Maximum EOS-HSM Response Function Dose Rate (mrem/hr)</i>									
<i>Zone 1</i>	<i>14196</i>	<i>16197</i>	<i>18498</i>	<i>20934</i>	<i>23480</i>	<i>25911</i>	<i>29071</i>	<i>26357</i>	<i>22204</i>
<i>Zone 2</i>	<i>20364</i>	<i>22708</i>	<i>25212</i>	<i>27912</i>	<i>31124</i>	<i>31393</i>	<i>29071</i>	<i>26357</i>	<i>22204</i>
<i>Zone 3</i>	<i>40225</i>	<i>40543</i>	<i>39753</i>	<i>36519</i>	<i>33791</i>	<i>31393</i>	<i>29071</i>	<i>26357</i>	<i>22204</i>
<i>Zone 4</i>	<i>49092</i>	<i>40543</i>	<i>39753</i>	<i>36519</i>	<i>33791</i>	<i>31393</i>	<i>29071</i>	<i>26357</i>	<i>22204</i>
<i>Zone 3 (% change from base)</i>	<i>-</i>	<i>1%</i>	<i>-1%</i>	<i>-9%</i>	<i>-16%</i>	<i>-22%</i>	<i>-28%</i>	<i>-34%</i>	<i>-45%</i>
<i>Zone 4 (% change from base)</i>	<i>-</i>	<i>-17%</i>	<i>-19%</i>	<i>-26%</i>	<i>-31%</i>	<i>-36%</i>	<i>-41%</i>	<i>-46%</i>	<i>-55%</i>
<i>Maximum EOS-TC125 Response Function Dose Rate (mrem/hr)</i>									
<i>Zone 1</i>	<i>45</i>	<i>44</i>	<i>41</i>	<i>36</i>	<i>31</i>	<i>25</i>	<i>19</i>	<i>11</i>	<i>5</i>
<i>Zone 2</i>	<i>147</i>	<i>153</i>	<i>159</i>	<i>166</i>	<i>176</i>	<i>172</i>	<i>157</i>	<i>140</i>	<i>116</i>
<i>Zone 3</i>	<i>1115</i>	<i>1213</i>	<i>1285</i>	<i>1267</i>	<i>1263</i>	<i>1264</i>	<i>1258</i>	<i>1221</i>	<i>1094</i>
<i>Zone 4</i>	<i>2385</i>	<i>2070</i>	<i>2238</i>	<i>2244</i>	<i>2271</i>	<i>2306</i>	<i>2322</i>	<i>2277</i>	<i>2057</i>
<i>Total</i>	<i>3693</i>	<i>3479</i>	<i>3722</i>	<i>3713</i>	<i>3741</i>	<i>3767</i>	<i>3756</i>	<i>3648</i>	<i>3272</i>
<i>Total (% change from base)</i>	<i>-</i>	<i>-6%</i>	<i>1%</i>	<i>1%</i>	<i>1%</i>	<i>2%</i>	<i>2%</i>	<i>-1%</i>	<i>-11%</i>

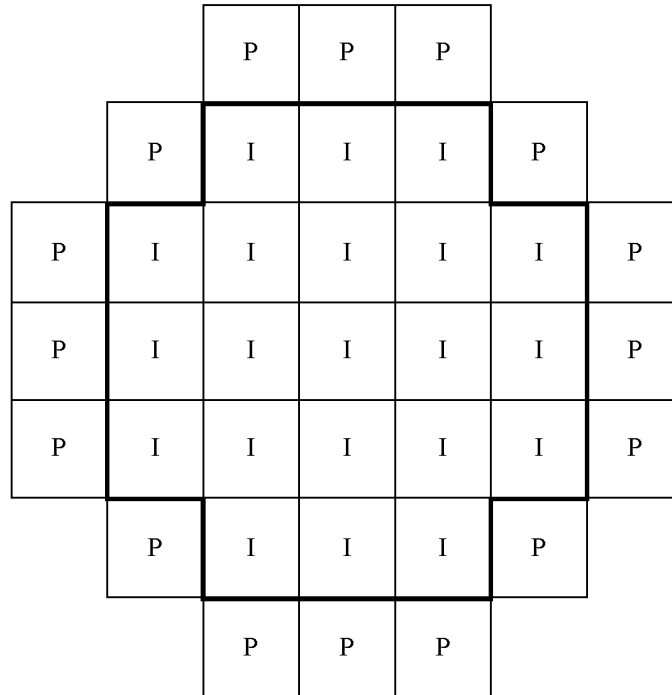


Figure 6-1
Peripheral and Inner Fuel Locations for the EOS-37PTH DSC

Figure 6-2
Deleted

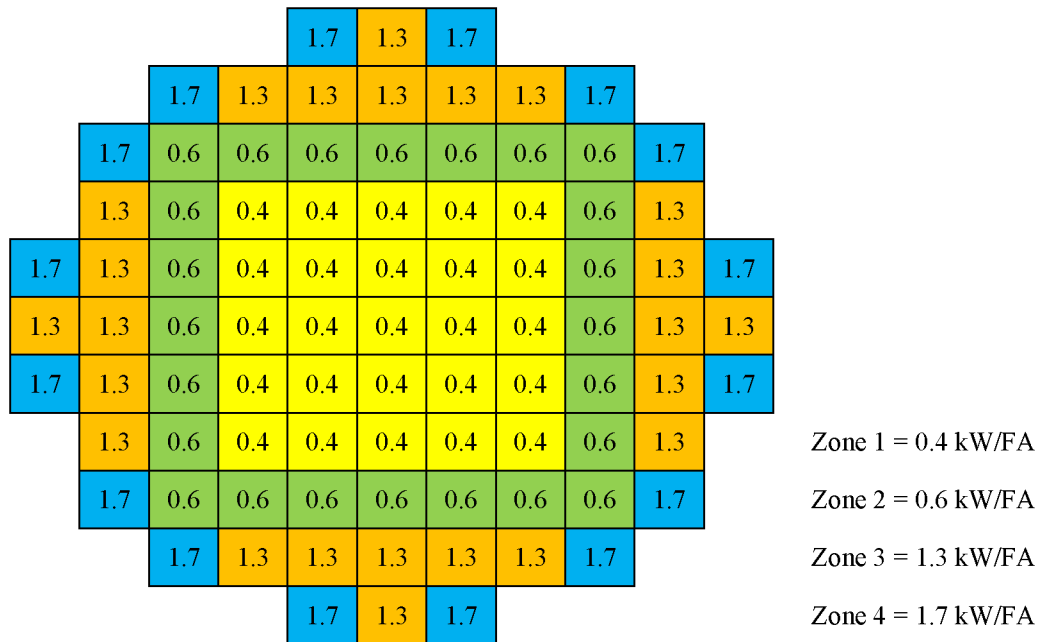


Figure 6-18
Shielding HLZC for the EOS-89BTH DSC

EOS-89BTH

The EOS-89BTH DSC consists of a shell assembly, which provides confinement and shielding, and an internal basket assembly, which locates and supports the BWR FAs. A detailed description of the DSC and Basket is found in Chapter 1, Section 1.2.1.2.

The FAs evaluated for storage in the EOS-89BTH DSC are considered intact. The authorized FAs are presented in Chapter 2. Reconstituted fuel assemblies with replacement rods that displace an equal or greater amount of water as the original rods are also authorized for storage and are bounded by the intact fuel, for criticality purposes.

The criticality analysis performed uses the most reactive configuration to determine the maximum allowable enrichment for the representative BWR FA design as a function of basket type. *The GNF2 fuel assembly type is used to bound all fuel assembly types with the exception of ABB-10-C and ATRIUM 11 class fuel, which are treated separately. Enrichment limits are developed for 89, 88, 87, and 84 fuel assemblies.* The results are presented in Table 7-4.

Computer models for the EOS-37PTH DSC and EOS-89BTH DSC are discussed in Section 7.3. The SCALE 6.0 [7-1] computer code package is employed to perform the criticality calculations. The criticality evaluation is presented in Section 7.4. The criticality benchmarks are described in Section 7.5.

7.2 Package Fuel Loading

EOS-37PTH

The EOS-37PTH DSC is designed to accommodate the FAs listed in Chapter 2. Since the assemblies listed represent a wide range of fuel types and configurations, it is demonstrated first that the most reactive case is obtained for each fuel class. In this context, the fuel class is defined as a set of fuel assembly designs with the same array size and rod pitch or rod outer diameter. The most reactive case for each class is used to determine the maximum allowable enrichments for intact, damaged, and failed fuel.

The payload of the EOS-37PTH DSC may include CCs that are contained within the FA. The authorized CCs are listed in Chapter 2. The only change to the package fuel loading required to evaluate the addition of the CCs is to replace the borated water in the water holes with CC materials. Since the CCs displace the borated moderator in the assembly guide and/or the instrument tubes, an evaluation is performed to determine the potential impact of the storage of CCs that extend into the active fuel region on the system reactivity. CCs that extend into the active fuel regions, such as burnable poison rod assemblies (BPRAs), control rod assemblies (CRAs), axial power shaping rod assemblies (APSRAs), control element assemblies (CEAs), and neutron source assemblies (NSAs) are conservatively assumed to exhibit the neutronic properties of $^{11}\text{B}_4\text{C}$ (no credit taken for B-10 content).

Since the criticality analysis models simulate only the active fuel height, any CC that is inserted into the FA in such a way that it does not extend into the active fuel region is considered as authorized for storage without adjustment to the soluble boron content or initial enrichment, as required for CCs that extend into the active fuel region.

EOS-89BTH

The EOS-89BTH DSC is designed to accommodate the FAs listed in Chapter 2. Since the assemblies listed represent a wide range of fuel types and configurations, a representative FA is determined by comparing k_{eff} values for the FAs listed, with and without various thicknesses of channels. The representative FA is used to obtain the maximum allowable enrichment as a function of basket type.

The maximum allowable enrichment is obtained using the GNF2 10x10 FA, except for the KKL-BWR 11/16 and SVEA-96Opt2 FAs, classified with a BWR fuel identification of ABB-10-C in Table 7-39, and *ATRIUM 11*. The maximum allowable enrichment requirements for these *three* assembly *classes* are also specified in Table 7-4.

7.4.3 EOS-89BTH Fuel Loading Optimization

As described in Section 7.3.1, the base model is employed to perform criticality calculations to determine the MRF design. A representative FA design is chosen based on the MRF analysis to determine the MRC of the system. By using the representative fuel and the MRC, maximum allowable and enrichment as a function of basket type (B-10 loading) for BWR FAs in the EOS-89BTH DSC are determined to ensure the system k_{eff} is below the USL. *In addition, the maximum allowable enrichment as a function of basket type is determined for three short-loading scenarios (i.e., 88, 87, and 84 fuel assemblies).*

C. Determination of the Maximum Initial Enrichment for 89 BWR Fuel Assemblies

The design basis KENO model with the GNF2 fuel assembly design is employed to determine the maximum allowable initial enrichment for the three allowable fixed poison loadings. The KENO model employed herein incorporates the bounding modeling features evaluated in the previous evaluations and also is consistent with the actual design dimensions as discussed in the Section 7.3.1. The results of the criticality analyses are shown in Table 7-43. These results demonstrate that the maximum k_{eff} of the system remains below the USL.

ABB-10-C and ATRIUM 11 fuel assembly classes are more reactive than the GNF2 fuel assembly used to bound all other fuel assembly types and are addressed separately. ATRIUM 11 fuel assembly design characteristics are provided in Chapter 2, Table 2-3, and the ATRIUM 11 KENO model is illustrated in Figure 7-27. The ATRIUM 11 channel thickness is modelled consistent with the most reactive GNF2 channel thickness determined in Table 7-40. Enrichment limits for ABB-10-C and ATRIUM 11 class fuel with 89 fuel assemblies are provided in Table 7-43. Of the three fuel assembly classes, ABB-10-C is the most reactive and has the lowest enrichment limits.

D. Determination of Maximum Allowable Enrichment for Short-Loading Scenarios

Higher enrichments may be achieved when considering less than 89 BWR fuels loaded in the 89BTH DSC (i.e., short-loading). For M1-A and M1-B basket types, higher enrichment limits are developed for three short loading scenarios of 88, 87, and 84 fuel assemblies. Because ABB-10-C and ATRIUM 11 fuel classes are more reactive than the GNF2 fuel used to bound all other fuel assembly classes, separate enrichment limits are developed for each fuel assembly class. The KENO models employed herein incorporate the bounding modelling features evaluated in the 89 fuel assembly analysis.

The short-loading scenarios are illustrated in Figure 7-28 through Figure 7-30. The empty locations indicated in these figures must remain empty when taking credit for a reduced number of fuel assemblies (i.e., dummy fuel assemblies are not allowed in these locations). The results for the GNF2, ABB-10-C, and ATRIUM 11 fuel assembly classes are presented in Table 7-43a.

E. Summary of Enrichment Limits

The enrichment limits from Table 7-43 (for 89 fuel assemblies) and from Table 7-43a (for short-loading) are consolidated in Table 7-4. Because ABB-10-C fuel bounds ATRIUM 11 fuel, the ABB-10-C enrichment limit for 89 fuel assemblies (4.60 wt. % U-235) developed using the M2-A basket type is conservatively applied to ATRIUM 11 fuel.

7.4.4 Criticality Results

In Table 7-44, a summary of the bounding scenarios that exist for both the EOS-37PTH and EOS-89BTH are presented. These are: dry storage condition, applicable to the DSC and placed in the EOS-HSM, normal loading or unloading operation where the DSC is in the fuel pool with 100% internal moderator density, and condition where the internal moderator density is at the optimum calculated for maximum reactivity.

For the EOS-37PTH, loading of intact fuels only, the most reactive case for the normal loading or unloading condition is calculated for the CE 15x15 class FA with 4.75 wt. % U-235, Type B basket, without CCs and 2000 ppm of soluble boron 100% internal moderator density, which is also the most optimum density. For the dry storage condition, this CE 15x15 case is modified by changing the internal and external moderator density to air, because this results in a bounding dry condition scenario.

For the EOS-37PTH, loading of damaged or failed fuels balanced with intact fuels, the most reactive case for the normal loading or unloading condition is calculated for the WE 17x17 class FA with 4.85 wt. % U-235 for intact fuels and 4.85 wt. % U-235 for failed fuels, (Basket Type B, without CCs and 2300 ppm of soluble boron 90% internal moderator density).

For the EOS-89BTH the most reactive case for the normal loading or unloading condition is calculated for the GNF2 FA with 88 FAs at 4.45 wt. % U-235, Type MI-A basket and 100% internal moderator density, which is also the optimum density. *The dry storage condition is based on 89 GNF2 FAs at 4.85 wt. % U-235. The dry model is developed from the equivalent moderated model by changing the internal and external moderator density to void (i.e., water with density of 1E-07 g/cm³), as this results in a bounding dry condition scenario.*

72.48

The criterion for subcriticality is that:

$$k_{\text{keno}} + 2\sigma_{\text{keno}} < \text{USL}$$

where USL is the upper subcriticality limit established by an analysis of benchmark criticality experiments. From Section 7.5 the USL for the EOS-37PTH DSC is 0.9404 while the USL for the EOS-89BTH DSC is 0.9418.

From Table 7-44, the most reactive case determined for PWR intact fuel storage only is:

$$k_{\text{keno}} + 2\sigma_{\text{keno}} = 0.9371 + 2 \times 0.0007 = 0.9385 < 0.9404,$$

From Table 7-44, the most reactive case determined for the storage of a maximum of up to eight damaged PWR FAs or up to four FFCs containing failed PWR fuel balanced with intact PWR FAs:

$$k_{\text{keno}} + 2\sigma_{\text{keno}} = 0.9370 + 2 \times 0.0007 = 0.9384 < 0.9404,$$

From Table 7-44, the most reactive case determined for BWR fuel storage is:

$$k_{\text{keno}} + 2\sigma_{\text{keno}} = 0.9388 + 2 * 0.0005 = 0.9398 < 0.9418.$$

7.5.3 Results of the Benchmark Calculations

The k_{eff} values of the 92 experiments are examined to determine correlation against the independent parameters listed in Section 7.5.2. The results in Table 7-47 indicate that there is no close correlation. The k_{eff} values are normally distributed and therefore, a single-sided lower tolerance limit USL is computed according to the methodology described in NUREG/CR-6698. The USL for the EOS-37PTH DSC is 0.9404. The results are summarized in Table 7-48.

The highest k_{eff} obtained for fuels loaded in the EOS-37PTH DSC is $0.9371 + 2 * 0.0007 = 0.9385$, which is less than the USL of 0.9404.

The k_{eff} values of the 51 experiments are examined to determine correlation against the independent parameters listed in Section 7.5.2. The results in Table 7-47 indicate that there is no close correlation. The k_{eff} values are normally distributed and, therefore, a single-sided lower tolerance limit USL is computed according to the methodology described in NUREG/CR 7109. The USL for the EOS-89BTH DSC is 0.9418. The results are summarized in Table 7-48.

The highest k_{eff} obtained for fuels loaded in the EOS-89BTH DSC is $0.9388 + 2 * 0.0005 = 0.9398$, which is less than the USL of 0.9418.

7.6 References

- 7-1 SCALE 6: Modular Code System for Performing Standardized Computer Analyses for Licensing Evaluation for Workstations and Personal Computers, Oak Ridge National Laboratory, Radiation Shielding Information Center Code Package CCC-750, February 2009.
- 7-2 U.S. Nuclear Regulatory Commission, “Standard Review Plan for Spent Fuel Dry Storage Systems at a General License Facility,” NUREG-1536, Revision 1, July 2010.
- 7-3 Scaglione, J.M., Mueller, D.E., Wagner, J.C., and Marshall, W.J., “An Approach for Validating Actinide and Fission Product Burnup Credit Criticality Safety Analyses – Criticality (k_{eff}) Predictions,” NUREG/CR 7109, U.S. Nuclear Regulatory Commission, April 2012.
- 7-4 International Criticality Safety Benchmark Evaluation Project (ICSBEP), “International Handbook of Evaluated Criticality Safety Benchmark Experiments,” NEA/NSC/DOC(95)03, NEA Nuclear Science Committee, September 2009, <http://icsbep.inel.gov/>.
- 7-5 USLSTATS: A Utility to Calculate Upper Subcritical Limits for Criticality Safety Applications, Version 6, Oak Ridge National Laboratory, January 26, 2009.
- 7-6 Dean, J.C., Tayloe Jr., R.W., “Guide for Validation of Nuclear Criticality Safety Calculational Methodology,” NUREG/CR-6698, January 2001.
- 7-7 *TN Americas LLC, “Updated Final Safety Analysis Report for the Standardized NUHOMS® Horizontal Modular Storage System for Irradiated Nuclear Fuel,” Revision 18, USNRC Docket Number 72-1004, January 2019.*
- 7-8 CoC 1042 Appendix A, NUHOMS® EOS System Generic Technical Specifications, Amendment 3.

Table 7-4
EOS-89BTH Maximum Lattice Average Initial Enrichment

<i>Basket Type</i>	<i>Number of Assemblies⁽¹⁾</i>	<i>Maximum Lattice Average Initial Enrichment (wt. % U-235)</i>		
		<i>All fuel Except ABB-10-C and ATRIUM 11</i>	<i>ABB-10-C Fuel</i>	<i>ATRIUM 11 Fuel</i>
<i>M1-A (A1/A2/A3)</i>	89	4.20	4.05	4.15
	88	4.45	4.20	4.35
	87	4.55	4.35	4.50
	84	5.00	4.75	4.90
<i>M1-B (B1/B2/B3)</i>	89	4.55	4.35	4.45
	88	4.75	4.55	4.70
	87	4.90	4.70	4.85
	84	5.00	5.00	5.00
<i>M2-A (C1/C2/C3)</i>	89	4.85	4.60	4.60

Note:

1. When short-loading the basket, allowable loading patterns are defined in Figure 7-28, Figure 7-29, and Figure 7-30. Locations marked as empty in these figures shall not contain fuel or dummy fuel.

Table 7-8
Material Property Data

Material	ID	Density g/cm ³	Element	Wt. %	Atom Density (atoms/b-cm)
UO ₂ (Enrichment – 1.0 to 5.0 wt. %) ⁽¹⁾	1	10.686	U-235	4.41	1.20668E-03
			U-238	83.74	2.26374E-02
			O	11.85	4.76881E-02
Zircaloy-4	2	6.56	Zr	98.23	4.2541E-02
			Sn	1.45	4.8254E-04
			Fe	0.21	1.4856E-04
			Cr	0.10	7.5978E-05
			Hf	0.01	2.2133E-06
Water (Pellet Clad Gap)	3	0.998	H	11.1	6.6769E-02
			O	88.9	3.3385E-02
Stainless Steel (SS304)	4	7.94	C	0.080	3.1877E-04
			Si	1.000	1.7025E-03
			P	0.045	6.9468E-05
			Cr	19.000	1.7473E-02
			Mn	2.000	1.7407E-03
			Fe	68.375	5.8545E-02
			Ni	9.500	7.7402E-03
Borated Water (2000 – 2500 ppm Boron) ⁽²⁾	5	1.00	H	11.163	6.67515E-02
			O	88.587	3.33757E-02
			B-10	0.046	2.77126E-05
			B-11	0.204	1.11547E-04
¹¹ B ₄ C in CC	7	2.52	B-11	78.57	1.08305E-01
			C	21.43	2.70763E-02
Aluminum	8	2.702	Al	100.0	6.0307E-02
Water	10	0.998	H	11.1	6.6769E-02
			O	88.9	3.3385E-02
Lead	11	11.344	Pb	100.0	3.2969E-02

Note:

- (1) The composition for maximum enrichment evaluated at 5.0 wt. % U-235 is provided for the EOS-37PTH DSC. For the EOS-89BTH DSC, a density of 10.576 g/cm³ is used in the GNF2 and ABB-10-C models, and a density of 10.696 g/cm³ is used in the ATRIUM 11 models.
- (2) Applies to EOS-37PTH only. EOS-89BTH evaluated with 100% internal moderator density. The composition for the maximum soluble boron concentration at 100 % internal moderator density is provided.

Table 7-43
Determination of Minimum Poison Loading Requirement, 89 Fuel Assemblies

<i>Basket Type</i>	<i>Enrichment (wt% of U-235)</i>	<i>As-Modeled B-10 Content (mg/cm²)</i>	<i>k_{keno}</i>	<i>σ_{keno}</i>	<i>k_{eff}</i>
<i>All Fuel Except ABB-10-C and ATRIUM 11</i>					
<i>MMC</i>	<i>4.20</i>	<i>29.4</i>	<i>0.9375</i>	<i>0.0005</i>	<i>0.9385</i>
	<i>4.55</i>	<i>37.2</i>	<i>0.9383</i>	<i>0.0005</i>	<i>0.9393</i>
<i>BORAL®</i>	<i>4.85</i>	<i>45.0</i>	<i>0.9380</i>	<i>0.0005</i>	<i>0.9390</i>
<i>ABB-10-C Fuel</i>					
<i>MMC</i>	<i>4.05</i>	<i>29.4</i>	<i>0.9386</i>	<i>0.0005</i>	<i>0.9396</i>
	<i>4.35</i>	<i>37.2</i>	<i>0.9380</i>	<i>0.0005</i>	<i>0.9390</i>
<i>BORAL®</i>	<i>4.60</i>	<i>45.0</i>	<i>0.9375</i>	<i>0.0005</i>	<i>0.9385</i>
<i>ATRIUM 11 Fuel</i>					
<i>MMC</i>	<i>4.15</i>	<i>29.4</i>	<i>0.9363</i>	<i>0.0005</i>	<i>0.9373</i>
	<i>4.45</i>	<i>37.2</i>	<i>0.9363</i>	<i>0.0003</i>	<i>0.9369</i>

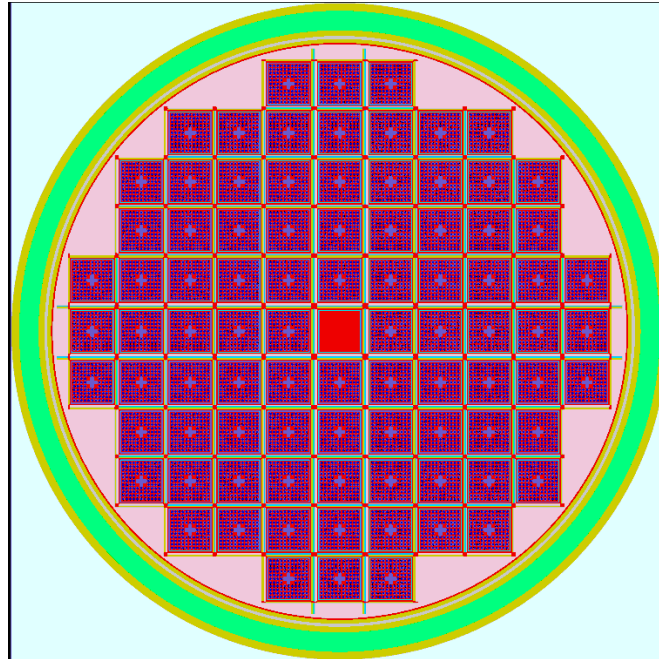
Table 7-43a
Maximum Allowable Enrichment Values, EOS-89BTH DSC Short-Loading

<i>As-Modeled B-10 Content (mg/cm²)</i>	<i>Number of Assemblies</i>	<i>Enrichment (wt. % U-235)</i>	<i>k_{keno}</i>	<i>σ_{keno}</i>	<i>k_{eff}</i>
<i>All Fuel Except ABB-10-C and ATRIUM 11</i>					
29.4	88	4.45	0.9388	0.0005	0.9398
	87	4.55	0.9382	0.0005	0.9392
	84	5.00	0.9376	0.0005	0.9386
37.2	88	4.75	0.9372	0.0005	0.9382
	87	4.90	0.9376	0.0005	0.9386
	84	5.00	0.9220	0.0005	0.9230
<i>ABB-10-C Fuel</i>					
29.4	88	4.20	0.9365	0.0005	0.9375
	87	4.35	0.9376	0.0005	0.9386
	84	4.75	0.9383	0.0005	0.9393
37.2	88	4.55	0.9383	0.0005	0.9393
	87	4.70	0.9387	0.0005	0.9397
	84	5.00	0.9324	0.0005	0.9334
<i>ATRIUM 11 Fuel</i>					
29.4	88	4.35	0.9359	0.0005	0.9369
	87	4.50	0.9368	0.0005	0.9378
	84	4.90	0.9367	0.0005	0.9377
37.2	88	4.70	0.9368	0.0005	0.9378
	87	4.85	0.9379	0.0005	0.9389
	84	5.00	0.9243	0.0005	0.9253

Table 7-44
Criticality Results

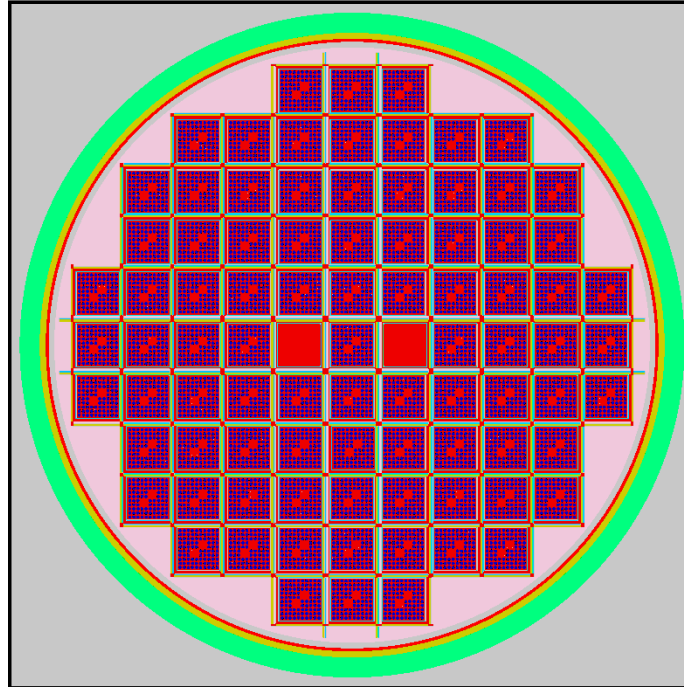
EOS-37PTH: Regulatory Requirements for Storage			
Configuration	k_{keno}	σ_{keno}	k_{eff}
Dry Storage (Bounded by infinite array of undamaged storage casks) for intact fuel assemblies	0.6203	0.0003	0.6209
Normal Loading and Unloading Conditions (Optimum Moderator Density) for intact fuel assemblies	0.9371	0.0007	0.9385
Normal Loading and Unloading Conditions (Optimum Moderator Density) for damaged and failed fuels balanced with intact fuels	0.9370	0.0007	0.9384
USL = 0.9404			
EOS-89BTH: Regulatory Requirements for Storage			
Configuration	k_{keno}	σ_{keno}	k_{eff}
Dry Storage (Bounded by infinite array of undamaged storage casks)	0.4909	0.0004	0.4917
Normal Loading and Unloading Conditions (Optimum Moderator Density)	0.9388	0.0005	0.9398
USL = 0.9418			

Proprietary Information on This Page
Withheld Pursuant to 10 CFR 2.390



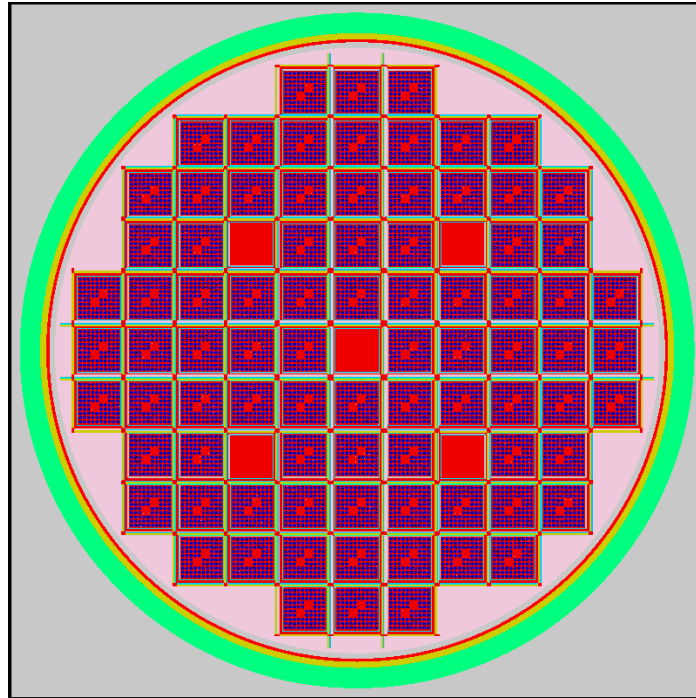
(ATRIUM 11 fuel depicted)

Figure 7-28
Cross-sectional View of NUHOMS® EOS-89BTH DSC Loaded with 88 Fuel Assemblies



(GNF2 Fuel Depicted)

Figure 7-29
Cross-sectional View of NUHOMS® EOS-89BTH DSC Loaded with 87 Fuel Assemblies



(GNF2 Fuel Depicted)

Figure 7-30
Cross-sectional View of NUHOMS® EOS-89BTH DSC Loaded with 84 Fuel Assemblies

8.6 DSC Closure Weld Testing

The field closure weld of the inner top cover plate to the shell is pressure tested as described in Section 10.1.1.1. The confinement boundary field welds are examined by root and final PT, and the structural weld of the outer top cover plate to the shell is examined by progressive PT as shown on the drawings in Chapter 1, and as described in the Code Alternatives, Section 4 of the Technical Specifications [8-41]. PT acceptance criteria are those of ASME Code, Section III, Subsection NB, Subarticle 5350. *The OTCP-to-shell weld may instead be examined by UT with the acceptance criteria specified in Section 10.1.3.1.*

The weld between the DSC shell and inner top cover and the *drain port cover* and *vent port plug* welds are leak tested to an acceptance criterion of 1×10^{-7} ref cm³/s at the field after the FAs are loaded in the canister. The testing is described in more detail in Chapter 10.

72.48

8.6.1 Periodic Inspections

The NUHOMS® EOS System is designed to be totally passive with minimal maintenance requirements. During fuel storage, the system requires only periodic inspection of the air inlets and outlets to ensure that no blockage has occurred, unless a means of thermal performance monitoring is employed.

The TC is designed to require only minimal maintenance. Transfer cask maintenance is limited to periodic inspection of critical components, inspection and repair of coatings, and replacement of damaged or nonfunctioning components.

Note: If applicable to the planned DSC heat *load* zone configuration per Figure 1A, 1B, 1D, 1E, 1F of the Technical Specifications [9-5] or Figure 2-2a, 2b, and 2d through 2f of Chapter 2, the air circulation system shall be assembled and verified operational within 7 days prior to initiating transfer operations per Technical Specification LCO 3.1.3 [9-5].

Note: The operating procedures for the NUHOMS 61BTH Type 2 DSC and the OS197 TC are provided in Chapter B.9.

12. *NOT USED.*
13. Position the TC lifting yoke and engage the TC lifting trunnions.
14. Visually inspect the yoke lifting arms to ensure that they are properly positioned and engaged on the TC lifting trunnions.
15. Move the scaffolding away from the TC as necessary.
16. Lift the TC just far enough to allow the weight of the TC to be distributed onto the yoke lifting arms. Reinspect the lifting arms to insure that they are properly positioned on the TC trunnions.
17. Optionally, secure a sheet of suitable material to the bottom of the TC to minimize the potential for ground-in contamination. This may also be done prior to initial placement of the TC in the designated area.
18. Prior to the TC being lifted into the fuel pool, the water level in the pool should be adjusted, as necessary, to accommodate the TC/DSC volume. If the water placed in the DSC cavity was obtained from the fuel pool, a level adjustment may not be necessary.

9.1.2 DSC Fuel Loading

1. Lift the TC/DSC and position it over the TC loading area of the spent fuel pool in accordance with the plant's 10 CFR Part 50 TC handling procedures.
2. Lower the TC into the fuel pool until the bottom of the TC is at the height of the fuel pool surface. As the TC is lowered into the pool, spray the exterior surface of the TC with clean water.
3. Place the TC in the location of the fuel pool designated as the TC loading area.
4. Disengage the lifting yoke from the TC lifting trunnions and move the yoke clear of the TC. Spray the lifting yoke with clean water if it is raised out of the fuel pool.
5. The potential for fuel misloading is essentially eliminated through the implementation of procedural and administrative controls. The controls instituted to ensure that intact FAs and CCs, if applicable, are placed into a known cell location within a DSC, will typically consist of the following:
 - A TC/DSC loading plan is developed to verify that the damaged/failed fuel and/or intact FAs, *empty slot locations*, and CCs, if applicable, meet the burnup, enrichment and cooling time parameters of Section 2.1 (EOS-37PTH DSC) or Section 2.2 (EOS-89BTH DSC) of the Technical Specifications [9-5].
 - The loading plan is independently verified and approved before the fuel load.

- A fuel movement schedule is then written, verified, and approved based upon the loading plan. All fuel movements from any rack location are performed under strict compliance of the fuel movement schedule.
 - If loading damaged/failed fuel, verify that the required number of bottom end caps for damaged fuel or FFCs for failed fuel are installed in appropriate fuel compartment locations before fuel load.
 - *If a short-loading configuration is required to load to a maximum lattice average initial enrichment of up to 5.0 wt %, verify the compartments that should be left empty for the short loading configuration per Technical Specifications Figure 10 [9-5]. Empty compartments may utilize storage cell blocking devices prior to fuel loading to prevent misloading scenarios. Storage cell blocking devices are intended to allow for water flow through the basket compartment.*
6. Prior to loading of a FA and CC, if applicable, into the DSC, the identity of the assembly and CC, if applicable, is to be verified by two individuals using an underwater video camera or other means. Verification of CC identification is optional if the CC has not been moved from the host FA since its last verification. Read and record the identification number from the FA and CCs, if applicable, and check this identification number against the DSC loading plan, which indicates which FAs and CCs, if applicable, are acceptable for dry storage.
7. Position the FA for insertion into the selected DSC storage cell and load the FA. Repeat Steps 6 and 7 for each FA loaded into the DSC. After the DSC has been fully loaded, check and record the identity and location of each FA and CCs, if applicable, in the DSC. If loading damaged FAs, place top end caps over each damaged FA placed into the basket. If loading failed fuel, place *FFC top lids* over each FFC placed into the basket.
8. After all the FAs and CCs, if applicable, have been placed into the DSC and their identities verified, position the lifting yoke and the top shield plug and lower the shield plug onto the DSC.

CAUTION: Verify that all the lifting height restrictions as a function of temperature specified in Section 5.2.1 of the Technical Specifications [9-5] can be met in the following steps that involve lifting of the TC.

9. Visually verify that the top shield plug is properly seated onto the DSC.
10. Position the lifting yoke with the TC trunnions and verify that it is properly engaged.
11. Raise the TC to the pool surface.
12. Inspect the top shield plug to verify that it is properly seated onto the DSC. If not, lower the TC and reposition the top shield plug. Repeat Steps 8 to 12 as necessary.

1. Disconnect the VDS from the DSC. Seal weld the prefabricated cover plate over the drain port, inject helium into blind space just prior to completing welding, and perform root and final dye penetrant weld examinations in accordance with Section 4.4.4 of the Technical Specification [9-5] requirements.
2. Temporary shielding may be installed as necessary to minimize personnel exposure. *Place the outer top cover plate (OTCP) onto the DSC. Verify proper fit up of the OTCP with the DSC shell. Install the welding machine onto the OTCP.* 72.48
3. Tack weld the OTCP to the DSC shell. Place the OTCP weld. *If the weld will be inspected by multi-layer PT, place only the root pass.*
4. Helium leak test the inner top cover plate and vent/drain port plug/plate welds using the leak test port in the OTCP in accordance with Sections 4.4.4 and 5.1.2.f of the Technical Specification [9-5] limits. Verify that the personnel performing the leak test are qualified in accordance with SNT-TC-1A [9-3]. Alternatively, this can be done with a test head prior to installing and welding the OTCP. 72.48
5. If a leak is found, remove the OTCP weld, the drain port cover and vent port plug welds, and repair the ITCP welds. Repeat procedure steps from Section 9.1.3 Step 14. 72.48
6. Perform dye penetrant examination of the OTCP root pass weld. Weld out the OTCP to the DSC shell. Perform root and multilayer dye penetrant examination in accordance with Section 4.4.4 of the Technical Specifications [9-5]. *The OTCP-to-shell weld may instead be examined by UT per Section 4.4.4 of the Technical Specifications [9-5].* 72.48
7. Seal weld the prefabricated plug over the OTCP test port and perform root and final dye penetrant weld examinations. 72.48
8. Remove the welding machine from the DSC.
9. Open the TC drain port valve and drain the water from the TC/DSC annulus.

CAUTION: *For the EOS-TC108, verify the neutron shield is filled with water and continuously monitor water in the neutron shield during the first five minutes of TC/DSC annulus draining as specified in Section 5.1.2.e of the Technical Specifications [9-5].* 72.48

Note: The time limit for Transfer Operations, if any, starts from initiation of this step. *This step may be performed at any time from this point until lifting the TC to the transfer trailer.*

CAUTION: Monitor the applicable time limits of Section 3.1.3 of the Technical Specifications [9-5] until the completion of DSC transfer Step 16 of Section 9.1.6, or Step 17 of Section A.9.1.6.

8. Inspect the *TC* to ensure that *it is* properly seated onto the skid.
9. If used, remove the aluminum TC top cover plate and replace with the steel TC top cover plate.

72.48

9.a Install the TC retainers to secure the TC to the transfer skid.

10. Optionally, remove the bottom ram access cover plate from the TC and install the air flow adaptor, if a time limit for transfer is specified in Section 3.1.3 of the Technical Specifications [9-5] *or Table 2-10 of Chapter 2. This step can be performed at any time from this point until the time limit is reached.*

72.48

Note: This step is only applicable if the DSC and HLZC combination results in a time limit for completion of transfer per LCO 3.1.3 of the Technical Specifications [9-5].

72.48

9.1.6 DSC Transfer to the EOS-HSM

1. Prior to transporting the TC to the ISFSI, verify that the wind deflectors are in place, if needed per Section 5.5 of the Technical Specifications [9-5], remove the EOS-HSM door, inspect the cavity of the EOS-HSM, removing any debris and ready the EOS-HSM to receive a DSC. The doors on adjacent EOS-HSMs should remain in place.

CAUTION: The insides of empty modules have the potential for high does rates due to adjacent loaded modules. Proper ALARA practices should be followed for operations inside these modules and in the areas outside these modules whenever the door from the empty EOS-HSM has been removed.

2. Inspect the EOS-HSM air inlet and outlets to ensure that they are clear of debris. Inspect the screens on the air inlet and outlets for damage.
3. Verify specified lubrication of the DSC support structure rails.
4. Transport the TC from the plant's fuel/reactor building to the ISFSI along the designated transfer route.
5. Once at the ISFSI, position the transfer trailer to within a few feet of the EOS-HSM.
6. Check the position of the trailer to ensure the centerline of the EOS-HSM and TC approximately coincide. If the trailer is not properly oriented, reposition the trailer, as necessary.
7. Unbolt and remove the TC top cover plate.
8. Back the trailer to within a few inches of the EOS-HSM, set the trailer brakes and disengage the tractor, if applicable. Extend the transfer trailer vertical jacks.

9.3 References

- 9-1 U.S. Nuclear Regulatory Commission, Office of the Nuclear Material Safety and Safeguards, “Safety Evaluation of VECTRA Technologies’ Response to Nuclear Regulatory Commission Bulletin 96-04 For the NUHOMS®-24P and NUHOMS®-7P.
- 9-2 U.S. Nuclear Regulatory Commission Bulletin 96-04, “Chemical, Galvanic or Other Reactions in Spent Fuel Storage and Transportation Casks,” July 5, 1996.
- 9-3 SNT-TC-1A, “American Society for Nondestructive Testing, Personnel Qualification and Certification in Nondestructive Testing,” 2006.
- 9-4 U.S. Nuclear Regulatory Commission, Regulatory Guide 3.61 “Standard Format and Content for a Topical Safety Analysis Report for a Spent Fuel Dry Storage Container,” February 1989.
- 9-5 CoC 1042 Appendix A, NUHOMS® EOS System Generic Technical Specifications, Amendment 3.
- 9-6 U.S. Nuclear Regulatory Commission, Interim Staff Guidance (ISG-22), “Potential Rod Splitting due to Exposures to an Oxidizing Atmosphere during Short-term Cask Loading Operations in LWR of Other Uranium Oxide Based Fuel.”

10.1 Acceptance Tests

10.1.1 Structural and Pressure Tests

10.1.1.1 DSC

The DSC confinement boundary is fabricated, inspected, and tested in accordance with American Society of Mechanical Engineers (ASME) Code Subsection NB [10-1] with alternatives specified in Section 4.4.4 of the Technical Specifications [10-32]. The shell and inner bottom cover plate *or the optional Alternate 1-Bottom Forging* assembly is pneumatically tested during fabrication in accordance with ASME Article NB-6300. *If using a single piece bottom forging, the fabrication leak test may be waived. The pressure test at 18 to 23 psig does not stress a single piece bottom and bottom-to-shell weld sufficiently to cause pre-existing defects to propagate into leaks. For the purpose of finding leaks, the helium leak test of Section 10.1.2 is far more sensitive than the pressure test.* The inner top cover plate and its weld to the shell are pneumatically tested in the field, in accordance with the above-cited ASME Code alternatives. Per ASME Article NB-6300, the pneumatic test pressure shall be 1.1 times the design pressure, which results in a test pressure of 16.5 psig. For conservatism, a *minimum* test pressure of 18.0 psig is selected to bound potential conditions for transportation under 10 CFR Part 71.

72.48

72.48

DSC	Normal Pressure (psig)	Design Pressure (psig)	Test Pressure Range (psig)
EOS37PTH	10.5	15 ⁽¹⁾	18.0-23.0
EOS89BTH	10.8	15 ⁽¹⁾	18.0-23.0

72.48

- (1) A pressure of 20 psig is used for structural evaluations under normal and off-normal conditions as noted in Section 3.9.1.2.7.3. *The DSC is backfilled with helium to more than 18 psig, but not to exceed 23 psig as noted in Section 9.1.3.19*

72.48

Mechanical properties of materials are tested in accordance with the American Society for Testing and Materials (ASTM), ASME, AMS, or other material specification called out on the drawings in Chapter 1. Weld procedures and welders are qualified in accordance with ASME Code Section IX. Additional material and welding requirements of ASME Code Articles NB-2000 and NB-4000 apply to the confinement boundary unless an ASME Code alternative governs.

Acceptance testing for the high-strength low-alloy steel used in the DSC baskets is specified in 10.1.7. There is no welding on the baskets.

10.1.2 Leak Tests

Confinement welds in the DSC shell and bottom are leak tested during fabrication to the ANSI N14.5 [10-6] leaktight acceptance criterion 1×10^{-7} ref cm³/s. Personnel performing the leak test are qualified in accordance with American Society for Nondestructive Testing (ASNT) SNT-TC-1A [10-7]. The DSC inner top cover plate, port covers, and their welds are leak-tested in the field to the same acceptance criterion after the fuel assemblies are loaded. Leak testing procedures follow ASME Code Section V, Article 10, Appendix IX, ASTM E1603 [10-8], or equivalent standard that provides the sensitivity required by ANSI N14.5.

10.1.3 Visual Inspection and Non-Destructive Examinations

Visual inspections are performed at the fabricator's facility to ensure that the DSC, the HSM, and the TC conform to the drawings and specifications. The visual inspections include weld, dimensional, surface finish, and cleanliness inspections. Visual inspections specified by codes applicable to a component are performed in accordance with the requirements and acceptance criteria of those codes. Requirements specific to each component follow.

10.1.3.1 DSC

Non-destructive examination (NDE) requirements for welds are specified on the drawings provided in Chapter 1. The confinement welds on the DSC are inspected in accordance with ASME Boiler and Pressure Vessel Code Subsection NB, including alternatives to ASME Code cited in Section 4.4.4 of the Technical Specifications.

The outer top cover plate (OTCP) is a structural weld, but not a confinement weld, and may be examined by ultrasonic testing (UT) to meet the following criteria:

- 1. Rounded flaws are evaluated by the acceptance criteria of NB-5331(a).*
- 2. Planar flaws, including root-penetrating flaws, are allowable up to the limit $(W - \sum h_i) \geq 0.30$ inch at any location, where $\sum h_i$ is the sum of the depth of aligned planar defects, and W is the measured thickness of the weld.*
- 3. Laminar flaws are allowable.*
- 4. Planar flaws that penetrate the surface of the weld are not allowable.*

The limit 0.30 inch is based on the minimum weld size with a weld quality factor = 1.0, as shown in Section 3.9.1.6.

Non-destructive examination personnel are qualified in accordance with SNT-TC-1A.

- 10-17 ASTM E1461, “Standard Test Method for Thermal Diffusivity by the Flash Method,” ASTM International, West Conshohocken, PA, 2014.
- 10-18 USNRC SFST-ISG-23, Application of ASTM Standard Practice C1671-07 when performing technical reviews of spent fuel storage and transportation packaging licensing actions
- 10-19 ASTM B557, “Standard Test Methods for Tension Testing Wrought and Cast Aluminum- and Magnesium-Alloy Products,” ASTM International, West Conshohocken, PA, 2014.
- 10-20 ASTM E290-14, “Standard Test Methods for Bend Testing of Material for Ductility,” ASTM International, West Conshohocken, PA, 2014.
- 10-21 NUREG-0933, “Resolution of Generic Safety Issues: Issue 196: Boral Degradation, (Main Report with Supplements 1–34), U.S. Nuclear Regulatory Commission, December 2011.
- 10-22 ASTM A829, “Standard Specification for Alloy Structural Steel Plates,” ASTM International, West Conshohocken, PA, 2014.
- 10-23 []
- 10-24 ASTM A370, “Standard Test Methods and Definitions for Mechanical Testing of Steel Products,” ASTM International, West Conshohocken, PA, 2014.
- 10-25 ASTM E604, “Standard Test Method for Dynamic Tear Testing of Metallic Materials,” ASTM International, West Conshohocken, PA, 2014.
- 10-26 Not used.
- 10-27 ACI 201.1R, “Guide for Conducting a Visual Inspection of Concrete in Service,” American Concrete Institute, 2008.
- 10-28 U.S. Nuclear Regulatory Commission, Regulatory Guide 7.11, “Fracture Toughness Criteria of Base Metal for Ferritic Steel Shipping Cask Containment Vessels with a Maximum Wall Thickness of 4 Inches (0.1 m),” June 1991.
- 10-29 ASTM B311, “Standard Test Method for Density of Powder Metallurgy (PM) Materials Containing Less Than Two Percent Porosity,” ASTM International, West Conshohocken, PA, 2014.
- 10-30 ASTM B963, “Standard Test Methods for Oil Content, Oil-Impregnation Efficiency, and Surface-Connected Porosity of Sintered Powder Metallurgy (PM) Products Using Archimedes' Principle,” ASTM International, West Conshohocken, PA, 2014.
- 10-31 []
- 10-32 CoC 1042 Appendix A, “NUHOMS® EOS System Generic Technical Specifications,” Amendment 3.

The estimated occupational exposures to ISFSI personnel during loading, transfer, and storage operations using the EOS-TC108 (time and number of workers may vary depending on individual ISFSI practices) are provided in Table 11-2 and Table 11-3 for the EOS-37PTH DSC and EOS-89BTH DSC, respectively. Similar operations for the EOS-TC125/135 are provided in Table 11-4 and Table 11-5. The task times, number of personnel required, and total doses are listed in these tables. The total exposure results are as follows:

- EOS-TC108 with EOS-37PTH DSC: 6504 person-mrem (~6.5 person-rem)
- EOS-TC108 with EOS-89BTH DSC: 3270 person-mrem (~3.3 person-rem)
- EOS-TC125/135 with EOS-37PTH DSC: 3205 person-mrem (~3.2 person-rem)
- EOS-TC125 with EOS-89BTH DSC: 6980 person-mrem (~7.0 person-rem)

For equivalent sources, the EOS-TC108 results in larger exposures than the EOS-TC125/135 because it is a lighter cask and provides less shielding. For the EOS-TC108 and the EOS-TC125 with the EOS-89BTH DSC, the exposure due to a crane hang-up off-normal event is also considered. The additional dose due to a crane hang-up event is provided in the footnotes of Table 11-2, Table 11-3, and Table 11-5.

The EOS-TC125/135 may utilize an optional aluminum top cover plate that is exchanged for a steel top cover plate after downending. For the EOS-TC135, this option is applicable only to the EOS-TC135 with the EOS-37PTH DSC, since the EOS-89BTH DSC is not an allowed content in the EOS-TC135. The exposure calculations in Table 11-4 and Table 11-5 are based on a steel top cover plate. If the aluminum top cover plate option is used, the total exposure will increase by approximately 130 person-mrem.

The exposures provided above are bounding estimates. Measured exposures from typical NUHOMS® System loading campaigns have been 600 mrem or lower per canister for normal operations, and exposures for the NUHOMS® EOS System are expected to be similar.

Regulatory Guide 8.34 [11-4] is to be used to define the onsite occupational dose and monitoring requirements.

11.2.2 EOS-DSC Retrieval Operations

Occupational exposures to ISFSI personnel during EOS-DSC retrieval are similar to those exposures calculated for EOS-DSC insertion. Dose rates for retrieval operations will be lower than those for insertion operations due to radioactive decay of the spent fuel inside the EOS-HSM. Therefore, the dose rates for EOS-DSC retrieval are bounded by the dose rates calculated for insertion.

11.3 Offsite Dose Calculations

Calculated dose rates in the immediate vicinity of the NUHOMS® EOS System are presented in Chapter 6, which provides a detailed description of source term configuration, analysis models, and bounding dose rates. Offsite dose rates and annual exposures are presented in this section. Neutron and gamma-ray offsite dose rates are computed, including skyshine, in the vicinity of the two generic ISFSI layouts containing design-basis contents.

11.3.1 Normal Conditions (10 CFR 72.104)

Offsite dose rates from the NUHOMS® EOS System are a result of direct radiation from the ISFSI. The operation of loading an EOS-HSM occurs over a very short time period and contributes negligibly to the offsite dose rates. Therefore, normal condition offsite dose rate calculations are computed only for a loaded ISFSI. No off-normal conditions have been identified that affect offsite dose rates.

Two generic ISFSI designs are considered, a 2x10 back-to-back array and a two 1x10 front-to-front array. In the 2x10 back-to-back array, the rear and corner shield walls are absent because the rears of the EOS-HSMs are in contact. In the two 1x10 front-to-front arrays, the EOS-HSMs are aligned with the rear shield walls facing outward and the front of the EOS-HSMs facing inward, separated by approximately 35 ft. This configuration has the advantage of minimizing the dose rate near the ISFSI because the inlet vents are directed inward in an area that would not normally be occupied.

It is demonstrated in Chapter 6 that EOS-HSM *average surface* dose rates are larger for the EOS-89BTH DSC compared to the EOS-37PTH DSC. Therefore, offsite dose rates *under normal conditions* are *reported* only for the bounding EOS-89BTH DSC. This evaluation provides results for distances ranging from 6.1 to 600 m from each face of the two configurations.

The Monte Carlo computer code MCNP5 [11-5] is used to calculate the dose rates at the specified locations around the arrays of EOS-HSMs. The results of this calculation provide an example of how to demonstrate compliance with the relevant radiological requirements of 10 CFR 20, 10 CFR 72, and 40 CFR 190 for a specific site. Each user must perform site-specific calculations to account for the actual layout of the EOS-HSMs and fuel source.

The total annual exposure for each ISFSI layout as a function of distance from each face is given in Table 11-6 and plotted in Figure 11-2. The total annual exposure estimates are based on 100% occupancy for 365 days. At large distances, the annual exposure from the 2x10 back-to-back array is similar to the two 1x10 front-to-front array configuration. Per 10 CFR 72.104, the annual whole-body dose to an individual at the site boundary is limited to 25 mrem. Based on the data shown in Table 11-6, the offsite dose rate drops below 25 mrem at a distance of approximately 450 m from the ISFSI. Therefore, 450 m is the minimum distance with design basis fuel to the site boundary for a 20-cask array with the NUHOMS® EOS System, however a shorter distance can be demonstrated in a site-specific calculation. [

]

The methodology, inputs, and assumptions for the Monte Carlo N-Particle (MCNP) analyses are summarized in the following paragraphs.

- The 20 EOS-HSMs in the 2x10 back-to-back array are modeled as a box enveloping the 2x10 array of EOS-HSMs, including the 3-foot shield walls on the two ends of the array. Source particles are started on the surfaces of the box. A sketch of this geometry is shown in Figure 11-3. The interiors of the EOS-HSMs and shield walls are modeled as air. Most particles that enter the interiors of the EOS-HSMs and shield walls will, therefore, pass through unhindered.
- The 20 EOS-HSMs in the two 1x10 front-to-front arrays are modeled as two boxes that envelop each 1x10 array of EOS-HSMs, including the 3-foot shield walls on the two ends and back of each array. Source particles are started on the surfaces of one of the 1x10 arrays, which is modeled as air. The opposite 1x10 array is modeled as solid concrete. A sketch of this geometry is shown in Figure 11-4. The dose field is then created for a source in both arrays by accounting for model symmetry, as indicated in Figure 11-4.
- The ISFSI approach slab is modeled as concrete. Because the ground composition has, at best, only a secondary impact on the dose rates at the detectors, any differences between this assumed layout and the actual layout would not have a significant effect on the site dose rates.
- The “universe” is a sphere surrounding the ISFSI. To account for skyshine, the radius of this sphere ($r=500,000$ cm) is more than 10 mean free paths for neutrons and 50 mean free paths for gammas in air, thus ensuring that the model is of a sufficient size to include all interactions, including skyshine, affecting the dose rate at the detectors.
- The 2x10 and two 1x10 surface sources are input to reproduce the average dose rate and spectrum on the surface of the EOS-HSM, as computed in Chapter 6. The surface average fluxes on the front, roof, side, and rear of the EOS-HSM are explicitly computed, and are provided in *Table 6-56 through Table 6-58*. The primary and secondary gamma fluxes are simply summed in the gamma input file. These surface spectra are directly input to MCNP for each face.

- Source particles on the ISFSI array surface are specified with a cosine distribution. For a cosine distribution, the outward particle current is equal to half of the flux. The MCNP source description requires the number of source particles per second emitted on each face (particle current). Because the current is half of the flux for a cosine distribution, and the flux at each face is known, the input current for each face (particles/s) is computed as $A \cdot F/2$, where A is the area of the face (cm^2) and F is the total flux on each face ($\text{particles}/\text{cm}^2\text{-s}$). The surface source calculations are summarized in Table 11-7.
- ANSI/ANS 6.1.1-1977 flux-to-dose rate factors are utilized [11-6]. These factors are provided in Table 6-51.
- For the 2x10 back-to-back array with end shield walls, the “box” dimensions are 1361 cm wide, 3129 cm long, and 564 cm high. For the two 1x10 front-to-front arrays with end and back shield walls, the “box” dimensions for each array are 772 cm wide, 3129 cm long, and 564 cm high. The two 1x10 arrays are 1067 cm (35 ft) apart.
- Dose rates are calculated for distances of 6.1 m (20 ft) to 600 m from the edges of the two ISFSI configurations. Point detectors are placed at the following locations, as measured from each face of the “box”: 6.095 m (20 ft), 10 m, 20 m, 30 m, 40 m, 50 m, 60 m, 70 m, 80 m, 90 m, 100 m, 200 m, 300 m, 400 m, 500 m, and 600 m. Each point detector is placed 91 cm (~3 ft) above the ground.

The MCNP results for the 2x10 back-to-back and two 1x10 front-to-front configurations are summarized in Table 11-8 and Table 11-9, respectively. At near distances, the 2x10 configuration results in larger front dose rates than the outward rear of the two 1x10 configuration. For example, the 6.1 m front dose rate is 27.0 mrem/hr for the 2x10 array compared to 10.9 mrem/hr for the two 1x10 array. However, at near distances, the two 1x10 configuration results in nominally larger side dose rates than the 2x10 array.

At large distances, the dose rates are approximately the same, regardless of configuration or direction from the ISFSI, as the dose rate at large distances is dominated by skyshine from the radiation streaming from the roof outlet vents. Also, note that the neutron dose rate is negligible compared to the gamma dose rate at all dose rate locations.

The Monte Carlo convergence is excellent due to the low uncertainty (<5%) for most dose rate locations. The annual exposures reported in Table 11-6 are simply the computed dose rates multiplied by 8760 hours (1 year).

The preceding analyses and results are intended to provide high estimates of dose rates for generic ISFSI layouts. The written evaluations performed by a general licensee for the actual ISFSI must consider the type and number of storage units, layout, characteristics of the irradiated fuel to be stored, site characteristics (e.g., berms, distance to the controlled area boundary, etc.), and reactor operations at the site in order to demonstrate compliance with 10 CFR 72.104.

11.3.2 Accident Conditions (10 CFR 72.106)

Per 10 CFR 72.106, the exposure to an individual at the site boundary due to an accident is limited to 5 rem. In an accident, the EOS-HSM outlet vent covers and wind deflectors (if required) may be lost. Only the dose rates on the roof are affected, since the front, rear, and side dose rates remain the same. As the dose rates at large distances are mostly due to skyshine from the roof, the dose rates at the site boundary are directly affected. The average EOS-HSM roof dose rates and surface fluxes in an accident are computed in Chapter 6, Tables 6-56 through 6-58 *for the EOS-89BTH DSC and Tables 6-58a through 6-58c for the EOS-37PTH DSC*. Under accident conditions, the roof dose rate for the EOS-89BTH DSC is larger than the roof dose rate for the EOS-37PTH DSC (18,800 mrem/hr vs. 7090 mrem/hr). Therefore, accident dose rates are reported only for the EOS-89BTH DSC.

Table 11-10 shows the bounding dose rate as a function of distance from a 2x10 back-to-back array of EOS-HSMs for the accident configuration described above. These dose rates are calculated assuming that the outlet vent covers and wind deflectors (if required) for the entire array are lost.

MCNP inputs for a 2x10 ISFSI accident configuration are prepared using the same method as described for the normal condition models. At a distance of 200 m and 450 m from the ISFSI, the accident dose rate is approximately 2.6 mrem/hr and 0.1 mrem/hr, respectively. It is assumed that the recovery time for this accident is five days (120 hours). Therefore, the total exposure to an individual at a distance of 200 m and 450 m is 312 mrem and 12 mrem respectively. This is significantly less than the 10 CFR 72.106 limit of 5 rem.

The EOS-TC may also be damaged in an accident during transfer operations, which would result in an offsite dose. For accident conditions, it is assumed that the neutron shield, including the steel or aluminum shell, is absent. The EOS-TC accident calculations are documented in Section 6.4.3 and the results presented in Table 6-54. *Per Section 6.4.3, the estimated dose to an offsite individual is significantly below the 10 CFR 72.106 limit of 5 rem.* This dose is also conservatively large because it is calculated as a distance of 100 m from the EOS-TC.

Table 11-1
Occupational Dose Rates

			Dose Rate (mrem/hr)			
			EOS-TC108		EOS-TC125/135	
Dose Rate Location	Averaged Segments	Config.	EOS-37PTH DSC HLZC 4	EOS-89BTH DSC HLZC 2	EOS-37PTH DSC HLZC 10	EOS-89BTH DSC Shielding HLZC
DRL1	A1-18, R11	Decon.	496	194	142	389
DRL2	A3-16, R10	Decon.	-	-	431	1139
		Transfer	1534	747	342	1221
DRL3	A17, R9	Decon.	-	-	339	161
		Welding	384	198	179	209
		Transfer	358	199	-	-
DRL4	A3-11, R9	Decon.	2467	1050	-	-
DRL5	A1-18, R10	Transfer	1162	586	267	931
DRL6	A17-18, R9	Transfer	183	100	66	84
DRL7	A17-18, R10	Transfer	361	189	131	191
DRL8	A2, R9	Transfer	92	165	38	147
DRL9	A19, R0	Transfer	69	137	46	164
DRL10	A1, R10	Transfer	113	121	31	126
EOS-HSM (HSM)	Front face surface average	-	25	22	25	60

Table 11-5
Occupational Exposure, EOS-TC125 with EOS-89BTH DSC
 (2 Pages)

No.	Operation	Configuration	Dose Rate Location	No. of People	Duration (hr)	Dose Rate (mrem/hr)	Dose (person-mrem)	% of Total Dose
1	Drain neutron shield if necessary. Place an empty EOS-DSC into an EOS-TC and prepare the EOS-TC for placement into the spent fuel pool.	N/A	N/A	6	4.00	0	0	0%
2	Move the EOS-TC containing an EOS-DSC without fuel into the spent fuel pool.	N/A	N/A	6	1.50	0	0	0%
3	Remove a loaded EOS-TC from the fuel pool and place in the decontamination area. Refill neutron shield tank if necessary.	Decon.	DRL1	2	0.25	389	195	3%
4	Decontaminate the EOS-TC and prepare welds.	Decon.	DRL2	2	1.75	1139	3987	57%
		Decon.	DRL3	2	0.50	161	161	2%
5	Weld inner top cover plate.	Welding	DRL3	2	0.75	209	314	4%
6	Vacuum dry and backfill with helium.	Welding	DRL3	2	0.50	209	209	3%
7	Weld outer top cover plate and port covers, perform non-destructive examination.	Welding	DRL3	2	0.50	209	209	3%
8	Drain annulus. Install EOS-TC top cover. Ready the support skid and transfer trailer.	Transfer	DRL5	1	0.50	931	466	7%
9	Place the EOS-TC onto the skid and trailer. Secure the EOS-TC to the skid.	Transfer	DRL2	2	0.33	1221	814	12%
10	Ready the skid and trailer for service. Transfer the EOS-TC to ISFSI. Position the EOS-TC in close proximity with the EOS-HSM.	N/A	N/A	6	1.83	0	0	0%
11	Remove the EOS-TC top cover.	Transfer	HSM+DRL6	2	0.67	144	192	3%

Table 11-5
Occupational Exposure, EOS-TC125 with EOS-89BTH DSC
 (2 Pages)

No.	Operation	Configuration	Dose Rate Location	No. of People	Duration (hr)	Dose Rate (mrem/hr)	Dose (person-mrem)	% of Total Dose
12	Align and dock the EOS-TC with the EOS-HSM.	Transfer	HSM+DRL7	2	0.25	251	126	2%
13	Position and align ram with EOS-TC.	Transfer	HSM+DRL8	2	0.50	207	207	3%
14	Remove ram access cover plate.	Transfer	DRL9	1	0.08	164	14	0.2%
15	Transfer the EOS-DSC from the EOS-TC to the EOS-HSM.	N/A	N/A	3	0.50	0	0	0%
16	Lift the ram back onto the trailer and undock the EOS-TC from the EOS-HSM.	Transfer	HSM+DRL10	2	0.08	186	31	0.4%
17	Install EOS-HSM access door.	Transfer	HSM	2	0.50	60	60	1%
						Total ⁽¹⁾	6980	

Notes:

(1) Use of aluminum cask lid increases total occupational dose by approximately 2% (~130 person-mrem).

(2) A crane hang-up off-normal event adds 1556 person-mrem (DRL1/decon * 4 workers * 1 hour).

Table 11-6
Total Annual Exposure from ISFSI

Distance (m)	2x10		Two 1x10	
	Front Total Dose (mrem)	Side Total Dose (mrem)	Back Total Dose (mrem)	Side Total Dose (mrem)
6.1	2.37E+05	8.33E+04	9.53E+04	1.20E+05
10	1.57E+05	6.36E+04	7.45E+04	8.33E+04
20	7.54E+04	3.86E+04	4.64E+04	4.60E+04
30	4.51E+04	2.64E+04	3.19E+04	3.06E+04
40	3.00E+04	1.91E+04	2.31E+04	2.19E+04
50	2.13E+04	1.44E+04	1.73E+04	1.64E+04
60	1.57E+04	1.11E+04	1.33E+04	1.25E+04
70	1.20E+04	8.73E+03	1.05E+04	9.85E+03
80	9.32E+03	6.89E+03	8.27E+03	7.85E+03
90	7.36E+03	5.58E+03	6.66E+03	6.27E+03
100	5.87E+03	4.53E+03	5.39E+03	5.08E+03
200	9.06E+02	7.52E+02	8.96E+02	8.46E+02
300	1.95E+02	1.67E+02	1.91E+02	1.84E+02
400	4.79E+01	4.11E+01	4.86E+01	4.63E+01
500	1.36E+01	1.20E+01	1.40E+01	1.42E+01
600	4.35E+00	3.79E+00	4.58E+00	4.65E+00

Table 11-7
ISFSI Surface Sources

2x10 Back-to-Back Array			
Source	Area (cm²)	Neutron Source (n/s)	Gamma Source (γ/s)
Roof	4.260E+06	8.635E+08	2.619E+12
Front 1	1.765E+06	7.046E+07	1.388E+11
Front 2	1.765E+06	7.046E+07	1.388E+11
Side 1	7.677E+05	3.351E+06	5.019E+09
Side 2	7.677E+05	3.351E+06	5.019E+09
Total	9.325E+06	1.011E+09	2.906E+12
Two 1x10 Front-to-Front Arrays			
Source	Area (cm²)	Neutron Source (n/s)	Gamma Source (γ/s)
Roof	2.416E+06	4.898E+08	1.485E+12
Front	1.765E+06	7.046E+07	1.388E+11
Back	1.765E+06	4.887E+06	1.991E+10
Side 1	4.354E+05	1.901E+06	2.847E+09
Side 2	4.354E+05	1.901E+06	2.847E+09
Total	6.816E+06	5.689E+08	1.650E+12

Table 11-8
2x10 Back-to-Back Dose Rates
 (2 Pages)

In Front of ISFSI				
Distance (m)	Gamma Dose Rate (mrem/hr)	Neutron Dose Rate (mrem/hr)	Total Dose Rate (mrem/hr)	σ
6.1	2.67E+01	3.51E-01	2.70E+01	0.04%
10	1.77E+01	2.46E-01	1.79E+01	0.05%
20	8.48E+00	1.23E-01	8.60E+00	0.1%
30	5.07E+00	7.34E-02	5.15E+00	0.2%
40	3.37E+00	4.80E-02	3.42E+00	0.1%
50	2.40E+00	3.33E-02	2.43E+00	0.1%
60	1.77E+00	2.42E-02	1.79E+00	0.1%
70	1.35E+00	1.80E-02	1.37E+00	0.2%
80	1.05E+00	1.38E-02	1.06E+00	0.2%
90	8.29E-01	1.08E-02	8.40E-01	0.2%
100	6.62E-01	8.43E-03	6.70E-01	0.3%
200	1.02E-01	1.44E-03	1.03E-01	0.4%
300	2.19E-02	3.98E-04	2.23E-02	1.1%
400	5.34E-03	1.31E-04	5.47E-03	1.0%
500	1.51E-03	4.94E-05	1.55E-03	1.8%
600	4.76E-04	2.09E-05	4.97E-04	2.8%

Table 11-8
2x10 Back-to-Back Dose Rates
 (2 Pages)

At Side of ISFSI				
Distance (m)	Gamma Dose Rate (mrem/hr)	Neutron Dose Rate (mrem/hr)	Total Dose Rate (mrem/hr)	σ
6.1	9.33E+00	1.74E-01	9.51E+00	0.1%
10	7.13E+00	1.32E-01	7.26E+00	0.1%
20	4.33E+00	7.64E-02	4.41E+00	0.1%
30	2.97E+00	4.95E-02	3.02E+00	0.2%
40	2.15E+00	3.40E-02	2.19E+00	0.1%
50	1.62E+00	2.46E-02	1.64E+00	0.2%
60	1.25E+00	1.82E-02	1.27E+00	0.2%
70	9.83E-01	1.39E-02	9.97E-01	0.3%
80	7.76E-01	1.09E-02	7.87E-01	0.2%
90	6.28E-01	8.52E-03	6.37E-01	0.3%
100	5.10E-01	6.91E-03	5.17E-01	0.3%
200	8.46E-02	1.25E-03	8.58E-02	0.4%
300	1.86E-02	4.08E-04	1.90E-02	1.5%
400	4.56E-03	1.27E-04	4.69E-03	0.8%
500	1.33E-03	4.30E-05	1.37E-03	1.7%
600	4.15E-04	1.76E-05	4.32E-04	1.6%

Table 11-9
Two 1x10 Front-to-Front Dose Rates
 (2 Pages)

In Back of ISFSI				
Distance (m)	Gamma Dose Rate (mrem/hr)	Neutron Dose Rate (mrem/hr)	Total Dose Rate (mrem/hr)	σ
6.1	1.07E+01	1.74E-01	1.09E+01	0.1%
10	8.36E+00	1.43E-01	8.50E+00	0.1%
20	5.20E+00	8.83E-02	5.29E+00	0.1%
30	3.59E+00	5.80E-02	3.64E+00	0.1%
40	2.60E+00	4.01E-02	2.64E+00	0.1%
50	1.95E+00	2.89E-02	1.98E+00	0.2%
60	1.50E+00	2.16E-02	1.52E+00	0.2%
70	1.18E+00	1.63E-02	1.19E+00	0.2%
80	9.31E-01	1.26E-02	9.44E-01	0.2%
90	7.50E-01	9.95E-03	7.60E-01	0.2%
100	6.07E-01	8.07E-03	6.15E-01	0.2%
200	1.01E-01	1.44E-03	1.02E-01	0.5%
300	2.14E-02	4.00E-04	2.18E-02	0.6%
400	5.40E-03	1.45E-04	5.55E-03	0.9%
500	1.55E-03	5.19E-05	1.60E-03	1.9%
600	5.00E-04	2.23E-05	5.22E-04	3.0%

Table 11-9
Two 1x10 Front-to-Front Dose Rates
 (2 Pages)

At Side of ISFSI				
Distance (m)	Gamma Dose Rate (mrem/hr)	Neutron Dose Rate (mrem/hr)	Total Dose Rate (mrem/hr)	σ
6.1	1.35E+01	2.09E-01	1.37E+01	0.1%
10	9.35E+00	1.53E-01	9.51E+00	0.1%
20	5.17E+00	8.56E-02	5.25E+00	0.1%
30	3.44E+00	5.46E-02	3.50E+00	0.2%
40	2.47E+00	3.79E-02	2.50E+00	0.2%
50	1.84E+00	2.73E-02	1.87E+00	0.2%
60	1.41E+00	2.00E-02	1.43E+00	0.2%
70	1.11E+00	1.53E-02	1.12E+00	0.2%
80	8.84E-01	1.19E-02	8.96E-01	0.3%
90	7.06E-01	9.45E-03	7.16E-01	0.3%
100	5.72E-01	7.56E-03	5.79E-01	0.3%
200	9.51E-02	1.46E-03	9.66E-02	0.6%
300	2.06E-02	3.93E-04	2.10E-02	1.3%
400	5.15E-03	1.35E-04	5.29E-03	1.2%
500	1.57E-03	5.25E-05	1.63E-03	3.9%
600	5.09E-04	2.24E-05	5.31E-04	5.8%

Table 11-10
2x10 Back-to-Back Accident Dose Rates
 (2 Pages)

Accident Front Dose Rate				
Distance (m)	Gamma Dose Rate (mrem/hr)	Neutron Dose Rate (mrem/hr)	Total Dose Rate (mrem/hr)	σ
6.1	2.43E+02	1.41E+00	2.44E+02	0.1%
10	1.94E+02	1.13E+00	1.95E+02	0.1%
20	1.23E+02	6.71E-01	1.24E+02	0.1%
30	8.47E+01	4.40E-01	8.51E+01	0.1%
40	6.17E+01	3.06E-01	6.20E+01	0.1%
50	4.64E+01	2.24E-01	4.66E+01	0.1%
60	3.56E+01	1.70E-01	3.58E+01	0.1%
70	2.82E+01	1.31E-01	2.83E+01	0.2%
80	2.24E+01	1.04E-01	2.25E+01	0.2%
90	1.81E+01	8.26E-02	1.82E+01	0.2%
100	1.48E+01	6.73E-02	1.49E+01	0.2%
200	2.59E+00	1.30E-02	2.60E+00	0.4%
300	5.98E-01	3.69E-03	6.02E-01	0.7%
400	1.64E-01	1.22E-03	1.66E-01	1.5%
500	4.62E-02	4.59E-04	4.66E-02	1.3%
600	1.55E-02	1.91E-04	1.57E-02	2.1%

Table 11-10
2x10 Back-to-Back Accident Dose Rates
 (2 Pages)

Accident Side Dose Rate				
Distance (m)	Gamma Dose Rate (mrem/hr)	Neutron Dose Rate (mrem/hr)	Total Dose Rate (mrem/hr)	σ
6.1	1.78E+02	1.02E+00	1.79E+02	0.1%
10	1.46E+02	8.15E-01	1.47E+02	0.1%
20	9.53E+01	5.03E-01	9.58E+01	0.1%
30	6.72E+01	3.40E-01	6.75E+01	0.1%
40	4.98E+01	2.42E-01	5.01E+01	0.1%
50	3.80E+01	1.82E-01	3.82E+01	0.2%
60	2.97E+01	1.38E-01	2.98E+01	0.2%
70	2.36E+01	1.08E-01	2.37E+01	0.3%
80	1.90E+01	8.65E-02	1.91E+01	0.2%
90	1.54E+01	7.06E-02	1.55E+01	0.3%
100	1.26E+01	5.81E-02	1.27E+01	0.2%
200	2.27E+00	1.18E-02	2.28E+00	0.4%
300	5.34E-01	3.31E-03	5.37E-01	0.8%
400	1.43E-01	1.15E-03	1.44E-01	0.8%
500	4.24E-02	4.41E-04	4.29E-02	1.3%
600	1.32E-02	2.08E-04	1.34E-02	1.4%

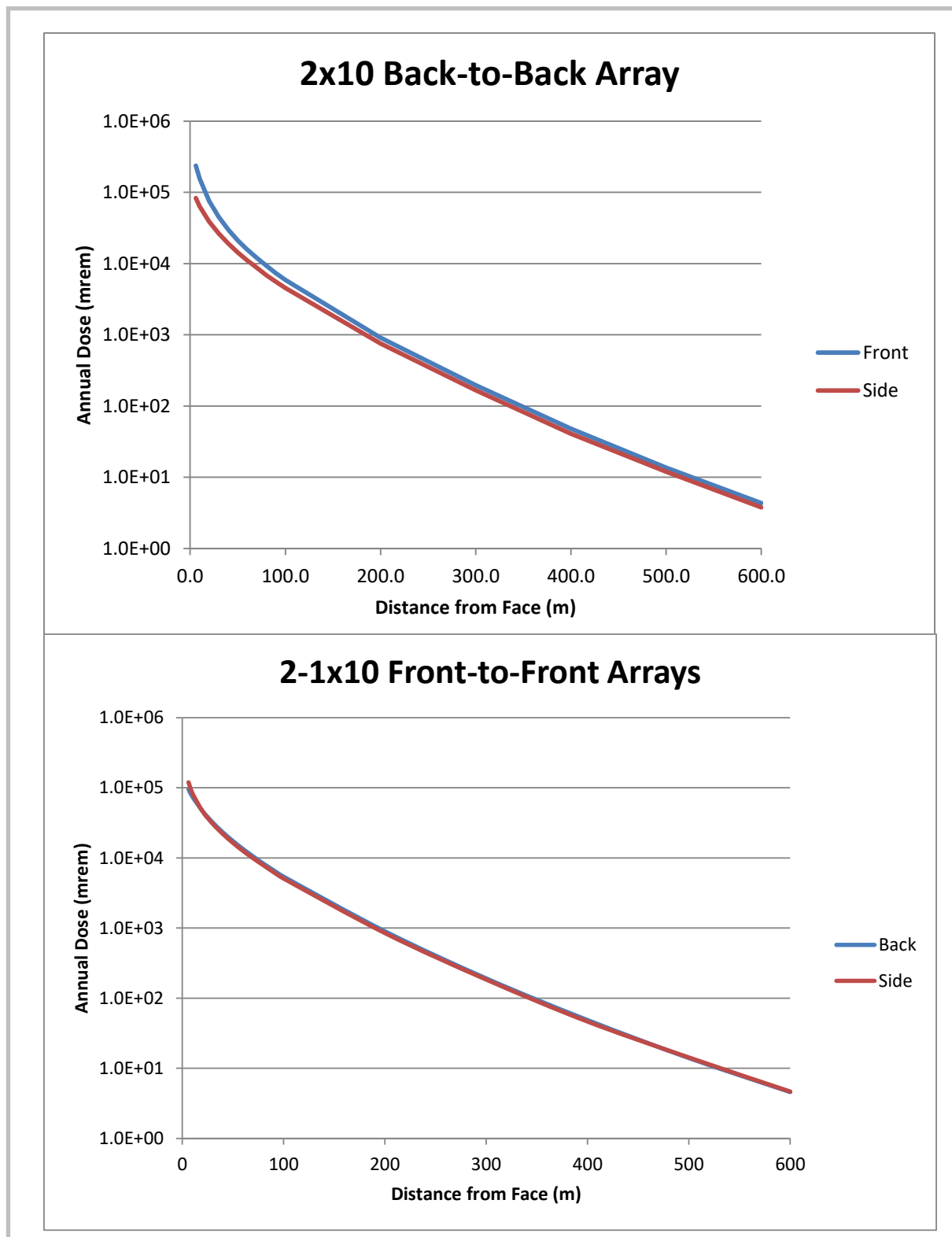


Figure 11-2
Total Annual Exposure from the ISFSI

Components	UFSAR Sections
EOS-TC loaded with EOS-37PTH DSC (Side and corner drop)	Appendices 3.9.1 - 3.9.3 and 3.9.5
EOS-TC loaded with EOS-89BTH DSC (Side and corner drop)	Appendices 3.9.1 - 3.9.3 and 3.9.5
EOS-37PTH DSC, PWR Fuel Cladding (Side and corner drop)	Appendix 3.9.6
EOS-89BTH DSC, BWR Fuel Cladding (Side and corner drop)	Appendix 3.9.6

All stresses are within allowable limits in both drop scenarios for the TC108, EOS-37PTH DSC and EOS-89BTH DSC. The largest strain in the basket is 0.9 % and 0.6 % for the EOS-TC loaded with EOS-37PTH DSC and EOS-89BTH DSC, respectively. The maximum stresses and strains in the fuel cladding for the side and corner drops remain below the applicable yield strength, therefore there is no fuel deformations.

72.48

The strain is limited in effect given the mode of deformation as the basket plates maintain their general shape. This deformation is limited and the position of the fuel assemblies is maintained from their initial positions relative to each other. The deformations of the basket plates are approximately uniform in the direction of impact and the fuel does not change configuration. Therefore, these deformations do not have an effect on criticality control.

Accident Dose Calculation

Based on analysis results presented in Appendix 3.9.3, Sections 3.9.3.3 and 3.9.3.4, the accidental EOS-TC drop scenarios do not breach the EOS-37PTH or the EOS-89BTH DSC confinement boundaries. The function of EOS-TC lead shielding is not compromised by these drops. The EOS-TC neutron shield, however, may be damaged in an accidental drop.

Dose rates are computed at 100 m from the EOS-TC with the neutron shield removed, which is the minimum allowed distance to the site boundary. As presented in Chapter 6, Table 6-54, the maximum dose rate at 100 m from an EOS-TC during a loss of neutron shield and lead slump in an accidental drop accident is 3.74 mrem/hr. Based on the discussion in Section 6.2.8, the maximum accident dose rate is doubled to 7.5 mrem/hr. If an 8-hour recovery time is assumed, the dose to an individual at the site boundary is $7.5 \times 8 = 60$ mrem, which is significantly below the 10 CFR 72.106 dose limit of 5 rem.

Corrective Actions

Recovery actions for an accident condition where the neutron shield and air circulation are lost would include the following actions immediately after an accident:

The evaluation for the impact on public exposure, a 2 x 10 back to back array of EOS-HSMs and a distance to the site boundary of 450 m is used. As documented in Chapter 11, Section 11.3.2, for a 2x10 ISFSI configuration, the accident dose rate is approximately 2.6 mrem/hour and 0.1 mrem/hr at a distance of 200 m and 450 m respectively from the ISFSI. It is assumed that the recovery time for this accident is five days (120 hours). Therefore, the total exposure to an individual at a distance of 200 m and 450 m is 312 mrem and 12 mrem respectively. Both values are significantly less than the 10 CFR 72.106 limit of 5 rem.

Corrective Action

After the accident, the HSM is inspected for damage. Any debris is removed. Any damage resulting from impact with a missile is evaluated to verify that the system is still within the licensed design basis.

The need for temporary shielding is evaluated and HSM repairs are performed to return the HSM to pre-accident design conditions.

12.3.4 Tornado Wind and Tornado Missiles Effect on EOS-TC

Cause of Accident

The EOS-TC is evaluated for the tornado wind speed and missile whose design parameters are specified in Chapter 2, Section 2.3.2. The maximum design basis tornado (DBT) tornado wind speed of 230 mph in accordance with Reg. Guide 1.76, Revision 1 [12-10] was considered. The 4000 pound automobile, as well as a 287-pound schedule 40 pipe, and a 1-inch solid steel missiles are considered. The other types of missiles are enveloped by the schedule 40 pipe missile.

This analysis is performed for the EOS-TC, secured in the horizontal position on the support skid. The following criteria are used to evaluate the adequacy of the EOS-TC for the loads described above.

- Stability analysis
- Penetration resistance
- Impact stress analysis

Accident Analysis

The EOS-TC is evaluated for tornado wind and missile effects in Appendix 3.9.5 and 3.9.7.

Thermal analysis is based on fuel assemblies with decay heat up to 50.0 kW per DSC for the EOS-37PTH and up to 48.2 kW per DSC for the EOS-89BTH. Zoning is used to accommodate high per assembly heat loads. The heat load zoning configurations for the DSCs are shown in Figure 1A through Figure 1K of the Technical Specifications [A.2-18] for the EOS-37PTH and Figures 2a through 2f of Chapter 2 for the EOS-89BTH DSC, respectively. Among the various HLZCs presented in Figure 1 for EOS-37PTH DSC, only HLZC # 7 through 9 and 11 presented in Figure 1G through Figure 1I and Figure 1K are applicable for storage in the HSM-MX. Similarly for the EOS-89BTH, among the various HLZCs presented in Figures 2a through 2f of Chapter 2, only HLZCs # 3-6 are permitted for storage in the HSM-MX.

72.48

The thermal analyses for storage are performed for the environmental conditions listed in Table A.2-2. The remainder of the environment conditions are provided in Table 2-9.

Peak clad temperature of the fuel at the beginning of the long-term storage does not exceed 400 °C for normal conditions of storage, and for short-term operations, including DSC drying and backfilling. Fuel cladding temperature shall be maintained below 570 °C (1058 °F) for accident conditions involving fire or off-normal storage conditions.

For onsite transfer in the EOS-TC, air circulation may be used, as a recovery action, to facilitate transfer operations as described in the Technical Specifications [A.2-18].

A.2.4.4 Shielding/Confinement/Radiation Protection

The HSM-MX provides the bulk of the radiation shielding for the DSCs. The HSM-MX designs can be arranged in either a single-row or a back-to-back arrangement. The nominal thickness of the HSM-MX roof is 50 inches for biological shielding. Additionally, the front wall has a minimum thickness of 39 inches. Sufficient shielding is provided by thick concrete side walls between HSM-MXs in an array to minimize doses in adjacent HSM-MXs during loading and retrieval operations. Section A.11.3 provides a summary of the offsite dose calculations for representative arrays of design basis HSM-MXs providing assurance that the limits in 10 CFR 72.104 and 10 CFR 72.106(b) are not exceeded.

There are no radioactive releases of effluents during normal and off-normal storage operations. Also, there are no credible accidents that cause significant releases of radioactive effluents from the DSC. Therefore, there are no off-gas or monitoring systems required for the HSM-MX.

A.2.4.5 Criticality

No change to Section 2.4.5.

A.2.4.6 Material Selection

No change to Section 2.4.6.

A.2-18 CoC 1042 Appendix A, NUHOMS® EOS System Generic Technical Specifications, Amendment 3.

A.2-19 NOT USED

A.2-20 ANSI 57.9-1984, Design Criteria for an Independent Spent Fuel Storage Installation (Dry Type).

A.4 THERMAL EVALUATION

The thermal evaluation described in this chapter is applicable to the NUHOMS® EOS System that includes EOS-37PTH or EOS-89BTH dry shielded canisters (DSCs) loaded inside the NUHOMS® MATRIX (HSM-MX).

A summary of the EOS-37PTH and EOS-89BTH DSC configurations analyzed in this chapter for storage operations in HSM-MX is shown below:

DSC Type	Basket Assembly Type	HLZC	Max. Heat Load (kW)	Transfer Cask	Storage Module
EOS-37PTH	4H	7	50.00	EOS-TC125/ EOS-TC135 and EOS-TC108 ⁽³⁾	HSM-MX
	4H/4L/5	8 ⁽¹⁾	46.40 ⁽²⁾		
	4H/4L/5	9	37.80		
	4H	11	44.50	EOS-TC125/EOS-TC135	
EOS-89BTH	3	3	34.44	EOS-TC125/ EOS-TC108	
	I	4	48.2	EOS-TC125	
		5	48.2		
		6	48.2		

Note:

- (1) Basket Type 5 can only accommodate Intact FAs. Therefore, damaged or Failed FAs allowed per HLZC 8 shall only be loaded in Basket Type 4L.
- (2) The maximum decay heat per DSC is limited to 41.8 kW when a damaged or failed FA is loaded
- (3) *Transfer operations in EOS-TC108 are permitted for HLZCs 4 through 9 in EOS-37PTH DSC only with Basket Type 4H.*

The various basket types within the EOS-37PTH DSC and EOS-89BTH DSC are described in Chapter 1, Section 1.1 and Appendix 4.9.6, Section 4.9.6.1.1.

Descriptions of the detailed analyses performed for normal, off-normal, and hypothetical accident conditions are provided in Section A.4.4 for storage operations. Transfer operations for the EOS-37PTH DSC with HLZCs 7 through 9 are presented in Section 4.9.6.2. Transfer operations for the EOS-89BTH DSC with HLZC 3 are presented in Section 4.5.6. *Transfer operations for the EOS-89BTH DSC with HLZCs 4 through 6 are presented in Appendix 4.9.8.3.*

In order to accommodate lessons learned from the mockup development, the original HSM-MX design has been slightly revised for improved fabricability. Section A.4.5 evaluates the thermal performance of the updated HSM-MX with the EOS-37PTH and EOS-89BTH DSCs under the bounding normal, off-normal, and accident storage conditions.

Storage Evaluation for EOS-37PTH DSC with Basket Type 4H for HLZC 11 in HSM-MX is presented in Section A.4.6.

A.4.2 Material and Design Limits

To establish the heat removal capability, several thermal design criteria are established for the NUHOMS® EOS System.

- Design criteria for the EOS-37PTH and EOS-89BTH DSCs are identical to those described in Chapter 4, Section 4.2.
- For normal and off-normal conditions, the maximum concrete temperature limit is 300 °F, as noted in Section 3.5.1.2 of [A.4-1]. For the accident conditions, if the concrete temperature exceeds the short-term limit of 350 °F noted in Appendix E.4 of ACI 349-06 [A.4-4], concrete testing will be performed, as described in Chapter A.8, Section A.8.2.1.3.

A.4.2.1 Summary of Thermal Properties of Materials

The thermal properties of the materials used in the thermal evaluation for *EOS-37PTH DSC with* Type 4H baskets *and EOS-89BTH DSC* are the same as those specified in Chapter 4, Section 4.2.1. The basket material properties for *EOS-37PTH DSC with* Type 4L/5 baskets are discussed in Appendix 4.9.6, Section 4.9.6.1.1.

Proprietary Information on This Page
Withheld Pursuant to 10 CFR 2.390

Proprietary Information on This Page
Withheld Pursuant to 10 CFR 2.390

A.4.5.4 EOS-37PTH DSC with Basket Type 4H – Storage in Updated HSM-MX

A.4.5.4.1 Convergence of the CFD Model

A.4.5.4.2 Temperature Calculations

The maximum temperatures of fuel cladding and concrete of the updated HSM-MX loaded with the EOS-37PTH DSC for the bounding normal, off-normal, and accident storage conditions are summarized in Table A.4-16.

The maximum temperatures of various components of the HSM-MX loaded with the EOS-37PTH DSC for the bounding normal, off-normal, and accident storage conditions are summarized in Table A.4-17. The average temperatures of key components of the HSM-MX loaded with the EOS-37PTH DSC for the bounding normal, off-normal, and accident storage conditions are summarized in Table A.4-18.

Figure A.4-25 presents the average temperatures of fuel cladding and key components of the EOS-37PTH DSC with Basket Type 4L/5 loaded in the updated HSM-MX based on HLZCs 8 and 9 during storage operations.

Figure A.4-25 and Figure A.4-26 present the temperature profiles of key components in the HSM-MX loaded with the EOS-37PTH DSC for HLZCs 8 and 9, respectively.

Comparison with HLZC 7

Table A.4-26 presents a comparison of the maximum temperatures for HLZCs 8 and 9 with the bounding design basis values from HLZC 7. As shown in the comparison, the majority of the maximum component temperatures determined for HLZC 7 with 50 kW remain bounding for HLZCs 8 and 9. The maximum temperature of the heat shield in the upper compartment for HLZC 8 is slightly higher (2 °F) than that for HLZC 7.

Similar to the normal condition, the maximum temperatures during off-normal and accident storage conditions for HLZCs 8 or 9 will also remain bounded by HLZC 7. Therefore, no further evaluation is required for off-normal and accident storage condition with HLZCs 8 and 9.

Based on this discussion, all design criteria are satisfied for storage of the EOS-37PTH DSC with HLZCs 8 or 9 in the updated HSM-MX.

A.4.5.6 EOS-89BTH DSC - Storage in Updated HSM-MX

This section evaluates the thermal performance of the EOS-89BTH DSC during storage in the updated HSM-MX.

A.4.5.6.1 Description of Load Cases for Storage of EOS-89BTH DSC in Updated HSM-MX

To determine the thermal performance of the updated HSM-MX loaded with the EOS-89BTH DSC, the load cases (LCs) listed in Table A.4-43 are evaluated for normal, off-normal, and accident conditions using the CFD model described in Section A.4.5.6.2.

HLZC 3 considered in this evaluation is described in Figure 2-2c in Chapter 2 for the EOS-89BTH DSC. HLZCs 4, 5, and 6 are described in Figure 2-2d, Figure 2-2e, and Figure 2-2f in Chapter 2, respectively. As shown in Figure 2-2c in Chapter 2, HLZC 3 has the same maximum heat load of 34.44 kW for both of the upper and lower compartments of the HSM-MX. As shown in Figure 2-2d through Figure 2-2f, HLZCs 4 through 6 have identical zoning between the upper and lower compartments of the HSM-MX but the allowable heat loads are different.

The heat loads considered in this evaluation for HLZCs 3 through 6 are summarized below:

Proprietary Information on This Page
Withheld Pursuant to 10 CFR 2.390

Among the various LCs shown in Table A.4-43, LCs 1a, 2a, 3a, and 4a evaluate the bounding normal hot storage conditions for the EOS-89BTH DSC with HLZCs 3 through 6, respectively.

LCs 1b, 2b, 3b, and 4b evaluate the off-normal hot storage condition with 117 °F ambient temperature.

LCs 1c, 2c, 3c, and 4c perform a transient analysis assuming complete blockage of the inlet vents with 117 °F ambient temperature. Initial temperatures are taken from steady-state results of off-normal hot storage condition (LCs 1b, 2b, 3b, and 4b). Blocked vents accident transient conditions are considered for up to 32 hours. The test requirements for concrete at elevated temperatures are described in Chapter A.8, Section A.8.2.1.3.

Proprietary Information on Pages A.4-36 and A.4-37
Withheld Pursuant to 10 CFR 2.390

A.4.5.6.4 EOS-89BTH DSC with HLZCs 4, 5, and 6 - Storage Evaluation

Based on this discussion, the thermal calculations are computationally convergent.

A.4.5.6.4.2 Temperature Calculations

The maximum temperatures of fuel cladding and concrete of the updated HSM-MX loaded with the EOS-89BTH DSC for the bounding normal, off-normal, and accident storage conditions are summarized in Table A.4-45. As shown in Table A.4-45, the maximum fuel cladding and concrete temperatures under the normal storage condition determined for HLZC 4 (Load Case 2a) bound the maximum temperatures for HLZCs 5 and 6 (Load Cases 3a and 4a). Therefore, for off-normal and accident storage conditions, it is expected that the maximum fuel cladding and concrete temperatures for HLZC 4 also bound those for HLZCs 5 and 6.

The maximum temperatures of various components of the updated HSM-MX loaded with the EOS-89BTH DSC for the bounding normal, off-normal, and accident storage conditions are summarized in Table A.4-46. The average temperatures of key components of the updated HSM-MX loaded with the EOS-89BTH DSC for the bounding normal, off-normal, and accident storage conditions are summarized in Table A.4-47. As shown in Table A.4-46 and Table A.4-47, most of the maximum and average component temperatures under the normal storage condition determined for HLZC 4 (Load Case 2a) bound those for HLZCs 5 and 6 (Load Cases 3a and 4a). Therefore, for off-normal and accident storage conditions, it is expected that the maximum and average component temperatures for HLZC 4 also bound those for HLZCs 5 and 6, with the adjustments on certain components as noted in Table A.4-46 and Table A.4-47.

Typical temperature plots for the key components in the updated HSM-MX loaded with the EOS-89BTH DSC with HLZC 4 are shown in Figure A.4-32, Figure A.4-33, and Figure A.4-34, respectively, for the bounding normal hot, off-normal hot, and accident conditions.

A.4.5.6.4.3 Airflow Calculations

The streamlines for the airflow inside the updated HSM-MX loaded with the EOS-89BTH DSC under normal hot storage condition are shown in Figure A.4-35. Cool air enters into the HSM-MX from the inlet, absorbs the heat from the EOS-89BTH DSC, and leaves the HSM-MX through the outlet with higher temperatures. Table A.4-48 summarizes the air temperatures and mass flow rates at the inlet and outlet for the bounding normal and off-normal storage conditions of the EOS-89BTH DSC with HLZC 4. [

]

A.4.7 References

- A.4-1 NUREG-1536, “Standard Review Plan for Spent Fuel Dry Cask Storage Systems at a General License Facility,” Revision 1, U.S. Nuclear Regulatory Commission, July 2010.
- A.4-2 NUREG-2174, “Impact of Variation in Environmental Conditions on the Thermal Performance of Dry Storage Casks - Final Report,” U.S. Nuclear Regulatory Commission, March 2016.
- A.4-3 J.M. Cuta, U.P. Jenquin, and M.A. McKinnon, “Evaluation of Effect of Fuel Assembly Loading Patterns on Thermal and Shielding Performance of a Spent Fuel Storage/Transportation Cask,” , PNNL-13583, Pacific Northwest National Laboratory, November 2001.
- A.4-4 ACI 349-06, “Code Requirements for Nuclear Safety Related Concrete Structures” American Concrete Institute.
- A.4-5 ANSYS FLUENT, ANSYS FLUENT Users Guide, Version 17.1, ANSYS, Inc.
- A.4-6 ANSYS ICEM CFD, Version 17.1, ANSYS, Inc.
- A.4-7 NUREG-2152, “Computational Fluid Dynamics Best Practice Guidelines for Dry Cask Applications,” U.S. Nuclear Regulatory Commission, March 2013.
- A.4-8 American Society of Mechanical Engineers, “Standard for Verification and Validation in Computational Fluid Dynamics and Heat Transfer,” ASME V&V 20-2009, November 30th, 2009.
- A.4-9 I. E. Idelchik, “Handbook of Hydraulic Resistance,” 3rd Edition, Begell House, Inc., 1996.
- A.4-10 A Zigh, J Solis, “Computational Fluid Dynamics Best Practice Guidelines in Analysis of Dry Storage Cask,” WM2008 Conference, Phoenix, AZ, February 24-28, 2008.
- A.4-11 ASHRAE Handbook, Fundamentals, SI Edition, American Society of Heating, Refrigerating and Air-Conditioning Engineers, Inc., 1997.
- A.4-12 P. J. Roache, “Quantification of Uncertainty in Computational Fluid Dynamics,” Annual Review of Fluid Mechanics, Vol. 29, 123-160, 1997.
- A.4-13 CoC 1042 Appendix A, NUHOMS® EOS System Generic Technical Specifications, Amendment 3.
- A.4-14 ANSYS Mechanical APDL, Version 17.1, ANSYS, Inc.*

Table A.4-43
EOS-89BTH DSC in Updated HSM-MX, Design Load Cases for Storage Conditions

Load Case	Operating Condition	HLZC	Description	Ambient Temperature (°F) ⁽¹⁾
<i>1a</i>	<i>Normal</i>	<i>3</i>		<i>100</i>
<i>1b</i>	<i>Off-Normal</i>			<i>117</i>
<i>1c</i>	<i>Accident</i>			<i>117</i>
<i>2a</i>	<i>Normal</i>	<i>4</i>		<i>100</i>
<i>2b</i>	<i>Off-Normal</i>			<i>117</i>
<i>2c</i>	<i>Accident</i>			<i>117</i>
<i>3a</i>	<i>Normal</i>	<i>5</i>		<i>100</i>
<i>3b ⁽²⁾</i>	<i>Off-Normal</i>			<i>117</i>
<i>3c ⁽³⁾</i>	<i>Accident</i>			<i>117</i>
<i>4a</i>	<i>Normal</i>	<i>6</i>		<i>100</i>
<i>4b ⁽²⁾</i>	<i>Off-Normal</i>			<i>117</i>
<i>4c ⁽³⁾</i>	<i>Accident</i>			<i>117</i>

Notes:

- (1) Daily average temperatures are used as noted in Section A.4.3.
- (2) The off-normal Load Cases 3b and 4b for EOS-89BTH DSC with HLZCs 5 and 6 are bounded by Load Case 2b for EOS-89BTH DSC with HLZC 4.
- (3) The accident Load Cases 3c and 4c for EOS-89BTH DSC with HLZCs 5 and 6 are bounded by Load Case 2c for EOS-89BTH DSC with HLZC 4.

Proprietary Information on This Page
Withheld Pursuant to 10 CFR 2.390

Table A.4-45
Maximum Fuel Cladding and Concrete Temperatures for Storage Conditions of
EOS-89BTH DSC in Updated HSM-MX with HLZCs 3 through 6

Load Case ⁽¹⁾	Description	Max Fuel Cladding Temperature (°F)			Concrete Temperature (°F)	
		Upper Compartment	Lower Compartment	Limit ⁽²⁾	Maximum ⁽⁴⁾	Limit ⁽²⁾
1a ⁽³⁾		<731	<711	752	<281	300
1b ⁽³⁾		<678	<718	752	<240	300
1c ⁽³⁾		<750	<790	1058	<354	500 ⁽⁶⁾
2a		731	711	752	281	300
2b		678	718	752	240	300
2c		750	790	1058	354	500 ⁽⁶⁾
3a		677	677	752	281	300
3b ⁽⁴⁾		<678	<718	752	<240	300
3c ⁽⁵⁾		<750	<790	1058	<354	500 ⁽⁶⁾
4a		686	685	752	278	300
4b ⁽⁴⁾		<678	<718	752	<240	300
4c ⁽⁵⁾		<750	<790	1058	<354	500 ⁽⁶⁾

Notes:

- (1) See Table A.4-43 for the description of the LCs.
- (2) The temperature limits are from NUREG-1536 [A.4-1].
- (3) Load Cases 1a, 1b and 1c are bounded by Load Cases 2a, 2b and 2c, respectively, due to lower heat load.
- (4) Load Cases 3b and 4b are bounded by Load Case 2b.
- (5) Load Cases 3c and 4c are bounded by Load Case 2c.
- (6) The temperature limit for concrete at accident condition is 500 °F. The maximum concrete temperature for accident conditions is above the 350 °F limit given in ACI 349-06 [A.4-4]. Testing will be performed, as described in Chapter A.8, Section A.8.2.1.3.

Proprietary Information on Pages A.4-96 through A.4-98
Withheld Pursuant to 10 CFR 2.390

Table A.4-49
Comparison of Average Gas Temperature in EOS-89BTH DSC Cavity

Load Case ⁽¹⁾	Average Temperature of Helium in DSC (K)		Temperature Difference (K)
	Bounding Design Basis [See Table 4-46]	Updated HSM-MX	
<i>1a</i> ⁽²⁾	572	<564	< -8
<i>1b</i> ⁽²⁾	572	<555	< -17
<i>1c</i> ⁽²⁾	671	<597	< -74
<i>2a</i>	572	564	-8
<i>2b</i>	572	555	-17
<i>2c</i>	671	597	-74
<i>3a</i>	572	552	-20
<i>3b</i> ⁽³⁾	572	<555	< -17
<i>3c</i> ⁽⁴⁾	671	<597	< -74
<i>4a</i>	572	556	-16
<i>4b</i> ⁽³⁾	572	<555	< -17
<i>4c</i> ⁽⁴⁾	671	<597	< -74

Notes:

- (1) See Table A.4-43 for the description of the LCs.
- (2) Load Cases 1a, 1b and 1c are bounded by Load Cases 2a, 2b and 2c, respectively, due to lower heat load.
- (3) Load Cases 3b and 4b are bounded by Load Case 2b.
- (4) Load Cases 3c and 4c are bounded by Load Case 2c.

Proprietary Information on Pages A.4-155 through A.4-166
Withheld Pursuant to 10 CFR 2.390

A.6.1 Discussions and Results

The following is a summary of the methodology and results of the shielding analysis of HSM-MX. More detailed information is presented in the body of the chapter.

Source Terms

For the HSM-MX, the DSC in the lower compartment is limited to 50.0 kW, while the DSC in the upper compartment is limited to 41.8 kW. PWR heat load zone configurations (HLZC) 7, 8, 9, and 11 are used with the HSM-MX, as well as boiling water reactor (BWR) HLZC 3, 4, 5, and 6. The PWR HLZCs are defined in the Technical Specifications [A.6-2], and the BWR HLZCs are defined in Chapter 2.

Dose rate evaluations are performed for the HSM-MX filled with either the EOS-89BTH or EOS-37PTH DSC. EOS-89BTH DSC source terms are developed for the EOS-HSM analysis in Section 6.2. These source terms are used without modification in the HSM-MX analysis in both the lower and upper compartments. The source terms are developed for a shielding HLZC that bounds HLZC 1 through 6. This approach adds significant conservatism because the shielding HLZC features 1.3 kW/FA and 1.7 kW/FA on the basket periphery, with a total peripheral as-modeled loading of 42.8 kW. The total as-modeled loading within the basket is 82.8 kW/DSC. The maximum allowed heat load per EOS-89BTH DSC is 48.2 kW. Furthermore, each fuel assembly includes five irradiated stainless steel rods consistent with a reconstituted fuel assembly source.

EOS-37PTH DSC HLZC 4 and 10 source terms are developed for the EOS-HSM analysis in Section 6.2, and it is demonstrated that HLZC 10 bounds HLZC 4. Therefore, HLZC 10 sources are used in HSM-MX analysis in both the upper and lower compartments. HLZC 10 is not authorized for use in the HSM-MX but results in bounding source terms and dose rates compared to HLZC 11. In addition, the same control component (CC) source is used in each basket location, as defined in Table 6-37.

Dose Rates

The EOS-37PTH and EOS-89BTH DSCs are transferred to the HSM-MX using the EOS-TC. The EOS-TC dose rates provided in Chapter 6 are applicable to transfer to the HSM-MX. Therefore, the dose rates reported in this appendix are limited to the HSM-MX.

The Monte Carlo transport code, MCNP5 [A.6-1], is used to compute dose fields around the HSM-MX using detailed 3D models. [

] *Summaries of the limiting HSM-MX dose rates are provided in Table A.6-2 and Table A.6-2a for the EOS-89BTH and EOS-37PTH DSC, respectively. Dose rates are higher for the EOS-89BTH DSC. The dose rate excluding the contribution from the inlet and outlet vents is small, as the dose rates are due primarily to streaming from the vents. The maximum dose rates at the inlet and outlet vents are 4,330 mrem/hr and 3,390 mrem/hr, respectively. The average dose rate on the front face of the module is 144 mrem/hr, and the average dose rate on the roof above the vent covers is 535 mrem/hr. The dose rate at the door centerline is 3.69 mrem/hr. The fluxes and dose rates on the surface of the HSM-MX are used as input to a generic site dose evaluation documented in Chapter A.11.*

The shielding effectiveness of the HSM-MX is not affected by any off-normal events. The following geometry changes may occur in an accident:

- Loss of outlet vent covers
- Loss of dose reduction hardware
- Damage to interior walls due to missile impact when the HSM-MX is in the construction joint expansion configuration with the removable end shield wall absent

10 CFR 72.106 limits the dose to an individual at the site boundary to be less than 5 rem due to an accident. Monte Carlo N-Particle (MCNP) cases are developed for the HSM-MX, in which all vent covers and dose reduction hardware are absent, which is not credible. An MCNP case is also developed for a missile impact when the HSM-MX is in the construction joint expansion configuration with the removable end shield wall absent. In this configuration, it is conservatively assumed that two interior walls are penetrated. The HSM-MX accident for the EOS-89BTH DSC increases the average dose rate on the front, roof, and end of the module to 278 mrem/hr, 14,800 mrem/hr, and 9,240 mrem/hr, respectively, which are higher than the HSM-MX accident dose rates for the EOS-37PTH DSC. The fluxes and dose rates on the surface of the HSM-MX in an accident condition are used as input to an accident site dose evaluation documented in Chapter A.11.

A.6.2 Source Specification

Source term information in Section 6.2 is applicable to the HSM-MX evaluation.

A.6.2.1 Computer Programs

No change to Section 6.2.1.

A.6.2.2 PWR and BWR Source Terms

Dose rate evaluations are performed for the HSM-MX filled with either the EOS-89BTH or EOS-37PTH DSC. EOS-89BTH DSC source terms are developed for the EOS-HSM analysis in Section 6.2 for HLZC 1. These source terms are provided in Table 6-27 through Table 6-29a and maximize the dose rates at the vents. These source terms are used without modification in the HSM-MX analysis in both the lower and upper compartments. The source terms are developed for a shielding HLZC that bounds HLZC 1 through 6. This approach adds significant conservatism because the shielding HLZC features 1.3 kW/FA and 1.7 kW/FA on the basket periphery, with a total peripheral as-modeled loading of 42.8 kW. The total as-modeled loading within the basket is 82.8 kW/DSC. The maximum allowed heat load per EOS-89BTH DSC is 48.2 kW. Furthermore, each fuel assembly includes five irradiated stainless steel rods consistent with a reconstituted fuel assembly source.

EOS-37PTH DSC HLZC 4 and 10 source terms are developed for the EOS-HSM analysis in Section 6.2, and it is demonstrated that HLZC 10 bounds HLZC 4. Therefore, HLZC 10 sources are used in HSM-MX analysis in both the upper and lower compartments. HLZC 10 sources are defined in Table 6-19a through Table 6-19c. HLZC 10 is not authorized for use in the HSM-MX but results in bounding source terms and dose rates compared to HLZC 11. HLZC 10 allows eight 3.5 kW FAs, while HLZC 11 allows only four 3.5 kW FAs and four 3.2 kW FAs in the lower compartment and allows only eight 3.0 kW FAs in the upper compartment. In addition, the same control component (CC) source is used in each basket location, as defined in Table 6-37.

A.6.2.3 Axial Source Distributions and Subcritical Neutron Multiplication

No change to Section 6.2.3.

A.6.2.4 Control Components

No change to Section 6.2.4.

A.6.4 Shielding Analysis

A.6.4.1 Computer Codes

MCNP5 v1.40 is used in the shielding analysis [A.6-1]. MCNP5 is a Monte Carlo transport program that allows full 3D modeling of the HSM-MX. Therefore, no geometrical approximations are necessary when developing the shielding models.

A.6.4.2 Flux-to-Dose Rate Conversion

No change to Section 6.4.2.

A.6.4.3 EOS-TC Dose Rates

No change to Section 6.4.3.

A.6.4.4 HSM-MX Dose Rates

[

]

The maximum dose rate at the roof outlet vent is 3,390 mrem/hr. The maximum dose rate at the lower compartment inlet vent is 4,330 mrem/hr, while the maximum dose rate at the upper compartment inlet vent is 4,020 mrem/hr.

The total dose rate is dominated by primary gammas, while the dose rate from neutrons and secondary gammas is negligible. The bulk shielding of the HSM-MX is very effective in the absence of streaming. The average dose rate on the rear and end (side) shield walls is 1.63 mrem/hr and 3.0 mrem/hr, respectively. The dose rate at the door centerline is 3.69 mrem/hr. These surfaces do not contain streaming paths, although the average rear and end dose rates are computed to the top of the vent covers and include contribution from the roof vents. The average dose rate on the front face of the module is 144 mrem/hr, and the average dose rate on the roof above the vent covers is 535 mrem/hr.

Input for Site Dose Evaluation

The average dose rate and flux on the surface of the HSM-MX is of interest for use in the generic site dose evaluations. The site dose evaluations are documented in Chapter A.11, although the inputs to the site dose evaluation are obtained from the HSM-MX evaluations described in the current chapter.

[

]

A.6.5 Supplemental Information

A.6.5.1 Fuel Qualification

No change to Section 6.5.1.

A.6.5.2 References

- A.6-1 Oak Ridge National Laboratory, “MCNP/MCNPX – Monte Carlo N-Particle Transport Code System Including MCNP5 1.40 and MCNPX 2.5.0 and Data Libraries,” CCC-730, RSICC Computer Code Collection, January 2006.
- A.6-2 CoC 1042 Appendix A, NUHOMS® EOS System Generic Technical Specifications, Amendment 3.
- A.6-3 ADVANTG – An Automated Variance Reduction Parameter Generator, Oak Ridge National Laboratory, August 2015.

Proprietary Information on This Page
Withheld Pursuant to 10 CFR 2.390

Proprietary Information on Pages A.6-15 through A.6-24
Withheld Pursuant to 10 CFR 2.390

Proprietary Information on This Page
Withheld Pursuant to 10 CFR 2.390

A.11.2 Occupational Dose Assessment

This section provides estimates of occupational dose for typical EOS transfer cask (EOS-TC) and ISFSI loading operations. Assumed annual occupancy times, including the anticipated maximum total hours per year for any individual, and total person-hours per year for all personnel for each radiation area during normal operation and anticipated operational occurrences, will be evaluated by the licensee in a 10 CFR 72.212 evaluation to address the site-specific ISFSI layout, inspection, and maintenance requirements. In addition, the estimated annual collective doses associated with loading operations will be addressed by the licensee in a 10 CFR 72.212 evaluation.

A.11.2.1 EOS-DSC Loading, Transfer, and Storage Operations

The dose rates used in the occupational dose assessment are summarized in Table A.11-1. The EOS-TC loading and transfer dose rates are unchanged from the values presented in Chapter 11. The HSM-MX dose rate reported in Table A.11-1 is the average dose rate on the front surface of an HSM-MX and is obtained from Chapter A.6.

The estimated occupational exposures to ISFSI personnel during loading, transfer, and storage operations using the EOS-TC108 (time and number of workers may vary depending on individual ISFSI practices) are provided in *Table A.11-1a* and Table A.11-2 for the *EOS-37PTH DSC* and *EOS-89BTH DSC*, respectively. Similar operations for the EOS-TC125/135 are provided in Table A.11-3 and Table A.11-4. The task times, number of personnel required, and total doses are listed in these tables. The total exposure results are as follows:

- EOS-TC108 with EOS-37PTH DSC: 8,690 person-mrem (~8.7 person-rem)
- EOS-TC108 with EOS-89BTH DSC: 4,535 person-mrem (~4.5 person-rem)
- EOS-TC125/135 with EOS-37PTH DSC: 4,231 person-mrem (~4.2 person-rem)
- EOS-TC125 with EOS-89BTH DSC: 10,038 person-mrem (~10.0 person-rem)

The exposures provided above are bounding estimates. Measured exposures from typical NUHOMS® System loading campaigns have been 600 mrem or lower per canister for normal operations, and exposures for the HSM-MX are expected to be similar.

Regulatory Guide 8.34 [A.11-4] is to be used to define the onsite occupational dose and monitoring requirements.

A.11.2.2 EOS-DSC Retrieval Operations

Occupational exposures to ISFSI personnel during EOS-DSC retrieval are similar to those exposures calculated for EOS-DSC insertion. Dose rates for retrieval operations will be lower than those for insertion operations due to radioactive decay of the spent fuel inside the HSM-MX. Therefore, the dose rates for EOS-DSC retrieval are bounded by the dose rates calculated for insertion.

A.11.2.3 Fuel Unloading Operations

No change to Section 11.2.3.

A.11.2.4 Maintenance Operations

The dose rates for surveillance activities are shown in Table A.11-7 and Table A.11-8 for doses rates 6.1 m from the front of an HSM-MX. The 6.1-meter dose rate is a conservative estimate for surveillance activities. The HSM-MX surface dose rates provided in Chapter A.6 can be used for temperature sensor maintenance activities, including calibration and repair.

The general licensee will evaluate the additional dose to personnel from ISFSI operations, based on the particular storage configuration and site personnel requirements.

A.11.2.5 Doses during ISFSI Expansion

During the ISFSI expansion using the construction joint option, the removable end shield wall is absent, and the two complete compartments (one upper and one lower) at the end of the module are empty. The maximum dose rate at the end of the module for the array expansion configuration is 17.7 mrem/hr, which is low (see Section A.6.4.4). If the array terminates at an expansion joint, two empty compartments (one upper and one lower) are also required at the end of the array, and dose rates are bounded by the construction joint option. The maximum dose rate on the surface of the integral shield wall is 22.8 mrem/hr (see Table A.6-2). Therefore, the end dose rate during array expansion activities is approximately the same as the end dose rate with an integral end shield wall, and elevated dose rates during array expansion activities are not anticipated.

A.11.3 Offsite Dose Calculations

Calculated dose rates in the immediate vicinity of the HSM-MX are presented in Chapter A.6, which provides a detailed description of source term configuration, analysis models, and bounding dose rates. The *bounding* HSM-MX dose rates reported in Chapter A.6 are conservatively based on the EOS-89BTH DSC. Offsite dose rates and annual exposures are presented in this section. Neutron and gamma-ray offsite dose rates are computed, including skyshine, in the vicinity of the two generic ISFSI layouts containing design-basis contents.

A.11.3.1 Normal Conditions (10 CFR 72.104)

Offsite dose rates are a result of direct radiation from the ISFSI. The operation of loading an HSM-MX occurs over a very short time period and contributes negligibly to the offsite dose rates. Therefore, normal condition offsite dose rate calculations are computed only for a loaded ISFSI. No off-normal conditions have been identified that affect offsite dose rates.

Two generic ISFSI configurations are considered that each store 22 EOS-DSCs. In the first configuration, the 22 DSCs are stored in a single HSM-MX with the DSCs in a 2x11 back-to-back configuration. In the 2x11 back-to-back configuration, the front of the modules face outward and the rows are separated by a wall of concrete. In the second configuration, the 22 DSCs are stored in two HSM-MX systems that each contain 11 DSCs in a 1x11 configuration. In the two 1x11 front-to-front configuration, the modules are aligned with the rear shield walls facing outward and the front of the modules facing inward, separated by 32 ft. This configuration has the advantage of minimizing the dose rate near the ISFSI because the inlet vents are directed inward in an area that would not normally be occupied.

It is noted in Chapter A.6 that HSM-MX *vent* dose rates are larger for the EOS-89BTH DSC compared to the EOS-37PTH DSC. Therefore, offsite dose rates are computed only for the bounding EOS-DSC. This evaluation provides results for distances ranging from 6.1 to 600 m from each face for the two configurations.

The Monte Carlo computer code Monte Carlo N-Particle Version 5 (MCNP5) [A.11-5] is used to calculate the dose rates at the specified locations around the HSM-MX. The results of this evaluation provide an example of how to demonstrate compliance with the relevant radiological requirements of 10 CFR 20, 10 CFR 72, and 40 CFR 190 for a specific site. Each user must perform site-specific calculations to account for the actual layout of the HSM-MXs and fuel source.

The total annual exposure for each ISFSI layout as a function of distance from each face is given in Table A.11-5 and plotted in Figure A.11-1. The total annual exposure estimates are based on 100% occupancy for 365 days. At large distances, the annual exposure from the 2x11 back-to-back configuration is similar to the two 1x11 front-to-front configuration. Per 10 CFR 72.104, the annual whole-body dose to an individual at the site boundary is limited to 25 mrem. Based on the data shown in Table A.11-5, the offsite dose rate drops below 25 mrem at a distance of approximately 450 m from the ISFSI. Therefore, 450 m is the minimum distance with design basis fuel to the site boundary for the HSM-MX system with 22-DSCs; however, a shorter distance can be demonstrated in a site-specific calculation.

The methodology, inputs, and assumptions for the MCNP analyses are summarized in the following paragraphs.

- The 2x11 back-to-back configuration is modeled as a box enveloping the HSM-MX, including the 44 inch thick shield walls on the two ends. Source particles are started on the surfaces of the box. A sketch of this geometry is shown in Figure A.11-2. The interiors of the HSM-MX and shield walls are modeled as air. Most particles that enter the interiors of the HSM-MX and shield walls will, therefore, pass through unhindered.
- The HSM-MXs in the two 1x11 front-to-front configuration are modeled as two boxes that envelop each 1x11 row, including the 44-inch thick shield walls on the two ends and 44 inch thick rear shield wall in each row. Source particles are started on the surfaces of one of the modules, which is modeled as air. The opposite module is modeled as solid concrete. A sketch of this geometry is shown in Figure A.11-3. The dose field is then created for a source in both modules by accounting for model symmetry, as indicated in Figure A.11-3.
- The ISFSI approach slab is modeled as concrete. Because the ground composition has, at best, only a secondary impact on the dose rates at the detectors, any differences between this assumed layout and the actual layout would not have a significant effect on the site dose rates.
- The “universe” is a sphere surrounding the ISFSI. To account for skyshine, the radius of this sphere ($r=500,000$ cm) is more than 10 mean free paths for neutrons and 50 mean free paths for gammas in air, thus ensuring that the model is of a sufficient size to include all interactions, including skyshine, affecting the dose rate at the detectors.
- The 2x11 and two 1x11 surface sources are input to reproduce the average dose rate and spectrum on the surface of the HSM-MX, as computed in Chapter A.6. The surface average fluxes on the front, roof, side, and rear of the HSM-MXs with the EOS-37PTH DSC are explicitly computed and are provided in Table A.6-9 through Table A.6-11. *The EOS-37PTH DSC surface average fluxes are not used in the bounding EOS-89BTH DSC offsite dose rate analysis but could be used for an EOS-37PTH DSC offsite dose rate analysis. The surface average fluxes used for the EOS-89BTH DSC are provided in Table A.6-3 through Table A.6-5.* The primary and secondary gamma fluxes are simply summed in the gamma input file. These surface spectra are directly input to MCNP for each face.

- Source particles on the ISFSI surface are specified with a cosine distribution. For a cosine distribution, the outward particle current is equal to half of the flux. The MCNP source description requires the number of source particles per second emitted on each face (particle current). Because the current is half of the flux for a cosine distribution, and the flux at each face is known, the input current for each face (particles/s) is computed as $A \cdot F/2$, where A is the area of the face (cm^2) and F is the total flux on each face ($\text{particles}/\text{cm}^2\text{-s}$). The surface source evaluations are summarized in Table A.11-6.
- ANSI/ANS 6.1.1-1977 flux-to-dose rate factors are utilized [A.11-6]. These factors are provided in Table 6-51.
- For the 2x11 back-to-back configuration with end shield walls, the “box” dimensions are 1260 cm wide, 2096 cm long, and 903 cm high. For the two 1x11 front-to-front configuration with end and back shield walls, the “box” dimensions are 704 cm wide, 2096 cm long, and 903 cm high. The two 1x11 rows are 975 cm (32 ft) apart.
- Dose rates are calculated for distances of 6.1 m (20 ft) to 600 m from the edges of the two ISFSI configurations. Point detectors are placed at the following locations, as measured from each face of the “box”: 6.095 m (20 ft), 10 m, 20 m, 30 m, 40 m, 50 m, 60 m, 70 m, 80 m, 90 m, 100 m, 200 m, 300 m, 400 m, 500 m, and 600 m. Each point detector is placed 91 cm (~3 ft) above the ground.

The MCNP results for the 2x11 back-to-back and two 1x11 front-to-front configurations are summarized in Table A.11-7 and Table A.11-8, respectively. At near distances, the 2x11 configuration results in larger front dose rates than the outward rear of the two 1x11 configuration. For example, the 6.1 m front dose rate is 50.8 mrem/hr for the 2x11 configuration compared to 3.67 mrem/hr for the two 1x11 configuration. However, at near distances, the two 1x11 configuration results in nominally larger side dose rates than the 2x11 configuration.

At large distances, the dose rates are approximately the same, regardless of configuration or direction from the ISFSI, as the dose rate at large distances is dominated by skyshine from the radiation streaming from the roof outlet vents. Also, note that the neutron dose rate is negligible compared to the gamma dose rate at all dose rate locations.

The total Monte Carlo uncertainty is < 5% for all dose rate locations. The annual exposures reported in Table A.11-5 are simply the computed dose rates multiplied by 8760 hours (1 year).

The preceding analyses and results are intended to provide high estimates of dose rates for generic ISFSI layouts. The written evaluations performed by a general licensee for the actual ISFSI must consider the type and number of storage units, layout, characteristics of the irradiated fuel to be stored, site characteristics (e.g., berms, distance to the controlled area boundary, etc.), and reactor operations at the site in order to demonstrate compliance with 10 CFR 72.104.

A.11.3.2 Accident Conditions (10 CFR 72.106)

Per 10 CFR 72.106, the exposure to an individual at the site boundary due to an accident is limited to 5 rem. In an accident, the HSM-MX outlet vent covers and all dose reduction hardware may be lost. In addition, it is assumed that the HSM-MX is in an expansion configuration with the removable end shield wall absent and that a missile strike has damaged two interior walls. This accident scenario results in elevated dose rates on the front, roof, and side of the ISFSI. The average HSM-MX roof, front, and side dose rates and fluxes for the EOS-37PTH DSC in an accident are provided in Chapter A.6, Table A.6-12 through Table A.6-14. *The EOS-37PTH DSC surface average accident fluxes are not used in the bounding EOS-89BTH DSC offsite accident dose rate analysis but could be used for an EOS-37PTH DSC offsite accident dose rate analysis. The surface average accident fluxes used for the EOS-89BTH DSC are provided in Tables A.6-6 through Table A.6-8.*

Table A.11-9 shows the bounding dose rate as a function of distance from a 2x11 back-to-back configuration of HSM-MXs for the accident configuration described above. These dose rates are calculated assuming damage to every module in the array. This is a highly conservative scenario that is not credible, as an accident is not expected to damage every module.

MCNP inputs for a 2x11 ISFSI accident configuration are prepared using the same method as described for the normal condition models. At a distance of 200 m from the ISFSI, *which is significantly closer than the minimum estimated site boundary distance of 450 m*, the accident dose rate is approximately *1.34 mrem/hr, rounded up to 1.5 mrem/hr*. It is assumed that the recovery time for this accident is five days (120 hours). Therefore, the total exposure to an individual at a distance of 200 m is approximately *180 mrem*. This is significantly less than the 10 CFR 72.106 limit of 5 rem.

The EOS-TC may also be damaged in an accident during transfer operations, which would result in an offsite dose, see the discussion in Section 11.3.2.

Table A.11-1
Occupational Dose Rates

			Dose Rate (mrem/hr)			
			EOS-TC108		EOS-TC125/135	
Dose Rate Location	Averaged Segments	Config.	<i>EOS-37PTH DSC</i>	EOS-89BTH DSC	EOS-37PTH DSC	EOS-89BTH DSC
DRL1 through DRL10	(1)	(1)	(1)	(1)	(1)	(1)
HSM-MX (HMX)	Front face surface average	-	60	50	60	160

Note 1: Information pertaining to dose rate locations DRL1 through DRL10 is provided in Table 11-1.

Table A.11-4
Occupational Exposure, EOS-TC125 with EOS-89BTH DSC
 (2 Pages)

No. ⁽¹⁾	Operation	Configuration	Dose Rate Location	No. of People	Duration (hr)	Dose Rate (mrem/hr)	Dose (person-mrem)	% of Total Dose
1	Drain neutron shield if necessary. Place an empty EOS-DSC into an EOS-TC and prepare the EOS-TC for placement into the spent fuel pool.	N/A	N/A	6	4.00	0	0	0%
2	Move the EOS-TC containing an EOS-DSC without fuel into the spent fuel pool.	N/A	N/A	6	1.50	0	0	0%
3	Remove a loaded EOS-TC from the fuel pool and place in the decontamination area. Refill neutron shield tank if necessary.	Decon.	DRL1	2	0.25	389	195	2%
4	Decontaminate the EOS-TC and prepare welds.	Decon.	DRL2	2	1.75	1139	3987	40%
		Decon.	DRL3	2	0.50	161	161	2%
5	Weld inner top cover plate.	Welding	DRL3	2	0.75	209	314	3%
6	Vacuum dry and backfill with helium.	Welding	DRL3	2	0.50	209	209	2%
7	Weld outer top cover plate and port covers, perform non-destructive examination.	Welding	DRL3	2	0.50	209	209	2%
8	Drain annulus. Install EOS-TC top cover. Ready the support skid and transfer trailer.	Transfer	DRL5	1	0.50	931	466	5%
9	Place the EOS-TC onto the skid and trailer. Secure the EOS-TC to the skid.	Transfer	DRL2	2	0.33	1221	806	8%
10	Install RRT.	Transfer	HMX	2	2.00	160	640	6%
11	Transfer the EOS-TC to ISFSI.	N/A	N/A	6	1.83	0	0	0%

Table A.11-4
Occupational Exposure, EOS-TC125 with EOS-89BTH DSC
 (2 Pages)

No. ⁽¹⁾	Operation	Configuration	Dose Rate Location	No. of People	Duration (hr)	Dose Rate (mrem/hr)	Dose (person-mrem)	% of Total Dose
12	Position the EOS-TC inside the loading crane (MX-LC).	Transfer	HMX+DRL2	2	0.50	1381	1381	14%
13	Remove forced cooling system (if used) and install the ram cylinder assembly.	Transfer	DRL9	2	0.50	164	164	2%
14	Remove HSM-MX door.	Transfer	HMX	2	0.50	160	160	2%
15	Remove the EOS-TC top cover.	Transfer	HMX+DRL6	2	0.67	244	327	3%
16	Align and dock the EOS-TC with the HSM-MX. Secure the EOS-TC to the HSM-MX.	Transfer	HMX+DRL7	2	0.25	351	176	2%
17	Transfer the EOS-DSC from the EOS-TC to the HSM-MX using the ram cylinder.	N/A	N/A	3	0.50	0	0	0%
18	Disengage the ram and un-dock the EOS-TC from the HSM-MX.	Transfer	HMX+DRL10	2	0.08	286	46	0.5%
19	Install HSM-MX access door. Move EOS-TC to the transfer skid for removal.	Transfer	HMX	2	0.50	160	160	2%
20	Uninstall RRT.	Transfer	HMX	2	2.00	160	640	6%
						Total ⁽²⁾	10,038	

Note:

(1) Occupational exposures for steps 1 through 9 are consistent with Chapter 11, Table 11-5.

(2) Use of an aluminum cask lid increases the total occupational exposure by approximately 130 person-mrem.

(3) A crane hang-up off-normal event adds 1556 person-mrem (DRL1/decon * 4 workers * 1 hour).

Table A.11-5
Total Annual Exposure from ISFSI

Distance (m)	2x11		Two 1x11	
	Front Total Dose (mrem)	Side Total Dose (mrem)	Back Total Dose (mrem)	Side Total Dose (mrem)
6.1	4.45E+05	4.04E+04	3.21E+04	1.80E+05
10	2.71E+05	3.11E+04	2.60E+04	9.60E+04
20	1.01E+05	1.90E+04	1.72E+04	3.47E+04
30	4.97E+04	1.31E+04	1.22E+04	1.90E+04
40	2.91E+04	9.49E+03	9.13E+03	1.23E+04
50	1.88E+04	7.17E+03	7.00E+03	8.70E+03
60	1.30E+04	5.61E+03	5.51E+03	6.51E+03
70	9.42E+03	4.39E+03	4.38E+03	5.02E+03
80	7.06E+03	3.52E+03	3.53E+03	3.94E+03
90	5.44E+03	2.86E+03	2.89E+03	3.19E+03
100	4.26E+03	2.35E+03	2.39E+03	2.59E+03
200	6.46E+02	4.37E+02	4.54E+02	4.68E+02
300	1.49E+02	1.09E+02	1.16E+02	1.17E+02
400	4.31E+01	3.21E+01	3.46E+01	3.43E+01
500	1.38E+01	1.07E+01	1.17E+01	1.18E+01
600	4.83E+00	3.80E+00	4.08E+00	4.22E+00

Table A.11-6
ISFSI Surface Sources

2x11 Back-to-Back Configuration			
Source	Area (cm²)	Neutron Source (n/s)	Gamma Source (γ/s)
Roof	2.640E+06	4.034E+08	8.237E+11
Front 1	1.892E+06	2.075E+08	2.772E+11
Front 2	1.892E+06	2.075E+08	2.772E+11
Side 1	1.137E+06	1.540E+06	1.658E+09
Side 2	1.137E+06	1.540E+06	1.658E+09
Total	8.697E+06	8.215E+08	1.381E+12
Two 1x11 Front-to-Front Arrays (source for one of the two rows)			
Source	Area (cm²)	Neutron Source (n/s)	Gamma Source (γ/s)
Roof	1.474E+06	2.253E+08	4.600E+11
Front	1.892E+06	2.075E+08	2.772E+11
Back	1.892E+06	2.279E+06	2.929E+09
Side 1	6.351E+05	8.601E+05	9.262E+08
Side 2	6.351E+05	8.601E+05	9.262E+08
Total	6.528E+06	4.368E+08	7.420E+11

Table A.11-7
2x11 Back-to-Back Dose Rates
 (2 Pages)

In Front of ISFSI				
Distance (m)	Gamma Dose Rate (mrem/hr)	Neutron Dose Rate (mrem/hr)	Total Dose Rate (mrem/hr)	σ
6.1	5.01E+01	6.90E-01	5.08E+01	0.03%
10	3.05E+01	4.31E-01	3.10E+01	0.03%
20	1.13E+01	1.61E-01	1.15E+01	0.1%
30	5.59E+00	7.94E-02	5.67E+00	0.1%
40	3.27E+00	4.59E-02	3.32E+00	0.1%
50	2.12E+00	2.89E-02	2.15E+00	0.1%
60	1.47E+00	1.96E-02	1.49E+00	0.1%
70	1.06E+00	1.38E-02	1.08E+00	0.1%
80	7.96E-01	1.01E-02	8.06E-01	0.2%
90	6.13E-01	7.62E-03	6.20E-01	0.2%
100	4.80E-01	5.87E-03	4.86E-01	0.2%
200	7.28E-02	9.60E-04	7.37E-02	0.6%
300	1.68E-02	2.71E-04	1.71E-02	0.6%
400	4.82E-03	9.76E-05	4.92E-03	1.5%
500	1.54E-03	3.63E-05	1.57E-03	1.7%
600	5.36E-04	1.53E-05	5.51E-04	1.8%

Table A.11-7
2x11 Back-to-Back Dose Rates
 (2 Pages)

At Side of ISFSI				
Distance (m)	Gamma Dose Rate (mrem/hr)	Neutron Dose Rate (mrem/hr)	Total Dose Rate (mrem/hr)	σ
6.1	4.48E+00	1.26E-01	4.61E+00	0.2%
10	3.45E+00	9.82E-02	3.55E+00	0.1%
20	2.12E+00	5.58E-02	2.17E+00	0.2%
30	1.46E+00	3.50E-02	1.49E+00	0.2%
40	1.06E+00	2.31E-02	1.08E+00	0.1%
50	8.02E-01	1.62E-02	8.18E-01	0.2%
60	6.29E-01	1.16E-02	6.41E-01	0.8%
70	4.92E-01	8.62E-03	5.01E-01	0.2%
80	3.96E-01	6.54E-03	4.02E-01	0.2%
90	3.21E-01	5.04E-03	3.26E-01	0.2%
100	2.64E-01	4.03E-03	2.68E-01	0.3%
200	4.91E-02	7.24E-04	4.98E-02	0.4%
300	1.22E-02	2.31E-04	1.24E-02	0.7%
400	3.58E-03	9.03E-05	3.67E-03	1.0%
500	1.19E-03	3.19E-05	1.22E-03	1.7%
600	4.21E-04	1.27E-05	4.34E-04	1.6%

Table A.11-8
Two 1x11 Front-to-Front Dose Rates
 (2 Pages)

In Back of ISFSI				
Distance (m)	Gamma Dose Rate (mrem/hr)	Neutron Dose Rate (mrem/hr)	Total Dose Rate (mrem/hr)	σ
6.1	3.56E+00	1.06E-01	3.67E+00	0.1%
10	2.88E+00	8.50E-02	2.97E+00	0.1%
20	1.91E+00	5.08E-02	1.96E+00	0.3%
30	1.36E+00	3.24E-02	1.40E+00	0.1%
40	1.02E+00	2.18E-02	1.04E+00	0.1%
50	7.84E-01	1.51E-02	7.99E-01	0.1%
60	6.18E-01	1.10E-02	6.29E-01	0.2%
70	4.92E-01	8.21E-03	5.00E-01	0.2%
80	3.97E-01	6.22E-03	4.03E-01	0.2%
90	3.25E-01	4.88E-03	3.29E-01	0.2%
100	2.68E-01	3.89E-03	2.72E-01	0.3%
200	5.11E-02	7.08E-04	5.18E-02	0.4%
300	1.30E-02	2.21E-04	1.32E-02	0.6%
400	3.87E-03	8.40E-05	3.95E-03	0.9%
500	1.30E-03	3.32E-05	1.34E-03	1.6%
600	4.53E-04	1.34E-05	4.66E-04	1.3%

Table A.11-8
Two 1x11 Front-to-Front Dose Rates
 (2 Pages)

At Side of ISFSI				
Distance (m)	Gamma Dose Rate (mrem/hr)	Neutron Dose Rate (mrem/hr)	Total Dose Rate (mrem/hr)	σ
6.1	2.02E+01	3.29E-01	2.05E+01	0.1%
10	1.08E+01	1.91E-01	1.10E+01	0.1%
20	3.89E+00	7.62E-02	3.97E+00	0.1%
30	2.12E+00	4.19E-02	2.16E+00	0.1%
40	1.38E+00	2.64E-02	1.40E+00	0.1%
50	9.76E-01	1.74E-02	9.94E-01	0.2%
60	7.31E-01	1.23E-02	7.43E-01	0.2%
70	5.64E-01	9.04E-03	5.73E-01	0.2%
80	4.43E-01	6.74E-03	4.49E-01	0.2%
90	3.58E-01	5.38E-03	3.64E-01	0.3%
100	2.92E-01	4.09E-03	2.96E-01	0.4%
200	5.27E-02	7.10E-04	5.35E-02	0.5%
300	1.31E-02	2.03E-04	1.33E-02	0.8%
400	3.84E-03	7.92E-05	3.92E-03	0.9%
500	1.32E-03	2.91E-05	1.35E-03	2.2%
600	4.70E-04	1.22E-05	4.82E-04	2.9%

Table A.11-9
2x11 Back-to-Back Accident Dose Rates
 (2 Pages)

In Front of ISFSI				
Distance (m)	Gamma Dose Rate (mrem/hr)	Neutron Dose Rate (mrem/hr)	Total Dose Rate (mrem/hr)	σ
6.1	1.72E+02	1.37E+00	1.74E+02	0.05%
10	1.21E+02	9.59E-01	1.22E+02	0.1%
20	6.42E+01	4.61E-01	6.47E+01	0.1%
30	4.11E+01	2.70E-01	4.14E+01	0.1%
40	2.88E+01	1.75E-01	2.90E+01	0.1%
50	2.14E+01	1.20E-01	2.15E+01	0.1%
60	1.64E+01	8.70E-02	1.65E+01	0.1%
70	1.29E+01	6.50E-02	1.29E+01	0.2%
80	1.03E+01	5.00E-02	1.03E+01	0.2%
90	8.31E+00	3.89E-02	8.35E+00	0.2%
100	6.80E+00	3.15E-02	6.83E+00	0.2%
200	1.28E+00	6.15E-03	1.28E+00	0.5%
300	3.21E-01	1.86E-03	3.23E-01	0.8%
400	9.33E-02	6.86E-04	9.40E-02	0.9%
500	2.87E-02	2.70E-04	2.90E-02	1.0%
600	1.03E-02	1.07E-04	1.04E-02	2.7%

Table A.11-9
2x11 Back-to-Back Accident Dose Rates
 (2 Pages)

At Side of ISFSI				
Distance (m)	Gamma Dose Rate (mrem/hr)	Neutron Dose Rate (mrem/hr)	Total Dose Rate (mrem/hr)	σ
6.1	4.20E+02	1.41E+00	4.21E+02	0.05%
10	2.48E+02	9.29E-01	2.48E+02	0.1%
20	9.86E+01	4.21E-01	9.90E+01	0.1%
30	5.48E+01	2.43E-01	5.51E+01	0.1%
40	3.57E+01	1.59E-01	3.59E+01	0.1%
50	2.52E+01	1.12E-01	2.53E+01	0.1%
60	1.87E+01	8.02E-02	1.88E+01	0.1%
70	1.44E+01	6.05E-02	1.44E+01	0.2%
80	1.13E+01	4.61E-02	1.14E+01	0.2%
90	9.04E+00	3.62E-02	9.07E+00	0.2%
100	7.39E+00	2.93E-02	7.42E+00	0.4%
200	1.33E+00	5.78E-03	1.34E+00	0.4%
300	3.31E-01	1.88E-03	3.32E-01	0.7%
400	9.76E-02	6.71E-04	9.83E-02	1.0%
500	3.12E-02	2.58E-04	3.15E-02	1.2%
600	1.07E-02	1.29E-04	1.09E-02	1.6%

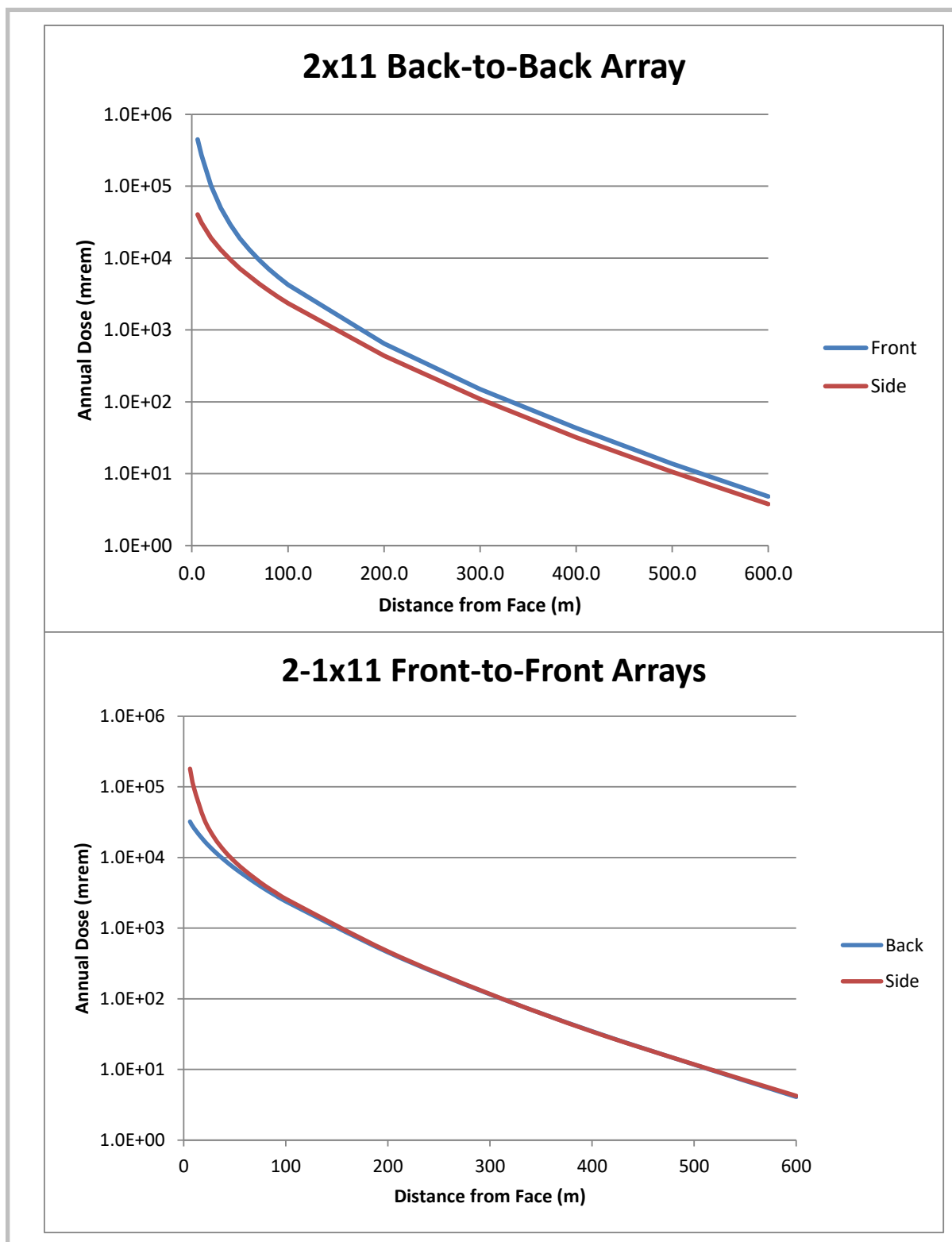


Figure A.11-1
Total Annual Exposure from the ISFSI

Accident Analysis

Stability and stress analyses are performed to determine the response of the HSM-MX to flood, massive missile impact and tornado wind pressure loads.

The stress analyses are performed using the ANSYS [A.12-7]. HSM-MX storage modules arranged in a back-to-back row array provides a conservative estimate of the response of the HSM-MX under postulated static and dynamic loads for any HSM-MX array configurations. These analyses are described in Appendix A.3.9.4.

The sliding and overturning stability analyses due to wind, flood and massive impact loads are performed using closed-form calculation methods to determine the sliding and overturning response of the HSM-MX. A non-linear seismic stability analysis is performed using LS-DYNA [A.12-8]. These analyses are described in Appendix A.3.9.7, Section A.3.9.7.1.

Thus, the requirements of 10 CFR 72.122 are met.

Accident Dose Calculation

As discussed in the evaluations, the tornado wind and tornado missiles do not breach the HSM-MX to the extent that the DSC confinement boundary is compromised. Localized scabbing of the end shield wall of a HSM-MX array may be possible. When the array is in the expansion configuration with the removable end shield wall absent, two inner walls may be damaged as a result of a missile impact.

The HSM-MX outlet vent covers and all dose reduction hardware (DRH) may be lost due to a tornado or tornado missile event. The assumed accident damage increases the dose rates on the front, roof, and end (side) of the HSM-MX. The effect on the average rear dose rate is negligible because the rear surface does not contain vents and sustains little damage in an accident. The HSM-MX accident increases the average dose rate on the front, roof, and end of the module to 278 mrem/hr, 14,800 mrem/hr, and 1,350 mrem/hr, respectively (see Section A.6.1).

In the evaluation for the impact on public exposure, a 2x11 ISFSI configuration and a distance to the site boundary of 450 m is used. As documented in Chapter A.11, Section A.11.3.2, for a 2x11 ISFSI configuration, the accident dose rate is approximately 1.34 mrem/hr, rounded up to 1.5 mrem/hour at a distance of 200 m from the ISFSI, which is significantly closer than the minimum estimated site boundary distance of 450 m. It is assumed that the recovery time for this accident is five days (120 hours). Therefore, the total exposure to an individual at a distance of 200 m is 180 mrem. This is significantly less than the 10 CFR 72.106 limit of 5 rem. Note that the dose is bounded by the EOS-HSM accident dose documented in Section 12.3.3.

Corrective Action

No change to corrective actions described in Section 12.3.3.

B.6 SHIELDING EVALUATION

The following radiation shielding evaluation addresses the storage of a 61BTH Type 2 DSC (61BTH DSC) in a NUHOMS® MATRIX (HSM-MX). It is demonstrated that the vent dose rates for storage of the 61BTH DSC are bounded by the vent dose rates for storage of either the EOS-37PTH or EOS-89BTH DSC documented in Chapter A.6 *of the EOS UFSAR Revision TBD*. Therefore, the site dose evaluation documented in Chapter A.11 *of the EOS UFSAR Revision TBD* for an EOS-DSC bounds the 61BTH DSC. *EOS-89BTH DSC and EOS-37PTH DSC dose rates are frozen at their Amendment 2 values per EOS UFSAR Revision TBD so that subsequent revisions of the EOS-89BTH DSC and EOS-37PTH DSC analyses will not necessitate a revision of this chapter.*

It is also demonstrated that dose rates for transfer of the 61BTH DSC within the OS197 transfer cask (TC) are similar to dose rates for transfer of the EOS-89BTH DSC within the EOS-TC125 documented in Chapter 6 *of the EOS UFSAR Revision TBD*. Therefore, the exposure estimate for transfer of the 61BTH DSC to the HSM-MX documented in Chapter B.11 is similar to the exposure estimate for transfer of the EOS-89BTH DSC to the HSM-MX documented in Chapter A.11 *of the EOS UFSAR Revision TBD*.

The 61BTH DSC may store up to 120 irradiated stainless steel rods contained within reconstituted fuel assemblies.

The 61BTH DSC may store up to 4 failed fuel canisters (FFCs) containing failed fuel, up to 61 damaged fuel assemblies, or up to 61 intact fuel assemblies. Failed and damaged fuel shall not be present within the same DSC.

The methodology, source terms, and dose rates presented in this chapter are developed to be reasonably bounding for general licensee implementation of the EOS System. The term “reasonably bounding” is quantified in Section 6.2.8. These results may be used in lieu of near-field evaluations by the general licensee, although the inputs utilized in this chapter should be evaluated for applicability by each site. Site-specific HSM-MX near-field evaluations may be performed by the general licensee to modify key input parameters.

Site dose evaluations for the HSM-MX under normal, off-normal, and accident conditions are documented in Chapter B.11. Because the arrangement and the distance to the site boundary is site-specific, compliance with 10 CFR 72.104 and 10 CFR 72.106 for the HSM-MX can only be demonstrated using a site-specific evaluation.

The *maximum* OS197 TC and EOS-TC125(89BTH) dose rates are *from the EOS UFSAR Revision TBD* compared in Table B.6-14. The dose rates computed for the OS197 TC (61BTH) are bounded by the EOS-TC125(89BTH) dose rates on the side, where the majority of operations occur. *Dose rates are similar at the top of both TCs, where their magnitudes are considerably lower.* Dose rates are larger for the OS197 TC on the bottom of the cask, although the cask bottom is inaccessible during decontamination and welding operations.

Occupational exposure for transfer of the EOS-89BTH DSC to the HSM-MX is provided in Table A.11-4 *of the EOS UFSAR Revision TBD.* *In the OS197 TC occupational dose assessment provided in Section B.11.2.1, EOS-TC125(89BTH) dose rates from the EOS UFSAR Revision TBD are conservatively applied for decontamination and welding operations, and OS197 TC dose rates are applied for transfer operations.*

Accident Conditions

The 100 m dose rate under accident conditions *with only standard fuel* is provided in Table B.6-15 and is 1.28 mrem/hr. *When 24 reconstituted FAs are loaded into the peripheral storage locations containing 5 irradiated stainless steel rods each, the dose rate decreases slightly to 1.27 mrem/hr. These values are bounded by the maximum EOS-TC dose rate from Table 6-54 of the EOS UFSAR Revision TBD.*

Proprietary Information on This Page
Withheld Pursuant to 10 CFR 2.390

B.6.5.2 References

- B.6-1 Oak Ridge National Laboratory, “MCNP/MCNPX – Monte Carlo N-Particle Transport Code System Including MCNP5 1.40 and MCNPX 2.5.0 and Data Libraries,” CCC-730, RSICC Computer Code Collection, January 2006.
- B.6-2 ADVANTG – An Automated Variance Reduction Parameter Generator, Oak Ridge National Laboratory, August 2015.
- B.6-3 NUREG/CR-7194, “Technical Basis for Peak Reactivity Burnup Credit for BWR Spent Nuclear Fuel in Storage and Transportation Systems,” US Nuclear Regulatory Commission.
- B.6-4 TN Americas LLC, “Updated Final Safety Analysis Report for the Standardized NUHOMS® Horizontal Modular Storage System for Irradiated Nuclear Fuel,” Revision 18, USNRC Docket Number 72-1004, January 2019.
- B.6-5 Oak Ridge National Laboratory, “A Modular Code System for Performing Standardized Computer Analyses for Licensing Evaluation,” ORNL/TM-2005/39, Version 6, SCALE, January 2009.
- B.6-6 CoC 1042 Appendix A, NUHOMS® EOS System Generic Technical Specifications, Amendment 3.
- B.6-7 NUREG/CR-6176, “*Recommendations on Fuel Parameters for Standard Technical Specifications for Spent Fuel Storage Casks*,” US Nuclear Regulatory Commission.

Proprietary Information on This Page
Withheld Pursuant to 10 CFR 2.390

Proprietary Information on This Page
Withheld Pursuant to 10 CFR 2.390

B.11.2 Occupational Dose Assessment

This section provides estimates of occupational dose for the OS197 TC and ISFSI loading operations. Assumed annual occupancy times, including the anticipated maximum total hours per year for any individual, and total person-hours per year for all personnel for each radiation area during normal operation and anticipated operational occurrences, will be evaluated by the licensee in a 10 CFR 72.212 evaluation to address the site-specific ISFSI layout, inspection, and maintenance requirements. In addition, the estimated annual collective doses associated with loading operations will be addressed by the licensee in a 10 CFR 72.212 evaluation.

B.11.2.1 61BTH DSC Loading, Transfer, and Storage Operations

The dose rates for the 61BTH DSC within the OS197 TC are similar to the dose rates for the EOS-89BTH DSC within the EOS-TC125 *on the top and side*, see the discussion in Section B.6.4.3. *Therefore, the decontamination and welding dose rates for the EOS-89BTH DSC within the EOS-TC125 from Table 11-1 of the EOS UFSAR Revision TBD are conservatively applied for the OS197 TC occupational dose assessment. Transfer dose rates for the OS197 TC and HSM-MX front average dose rates are obtained from the analysis documented in Chapter B.6. Dose rates used as input for the occupational dose assessment are provided in Table B.11-1 and include reconstituted FAs containing a total of 120 irradiated stainless steel rods on the periphery. Dose rate locations around the cask are analogous to the EOS-TC125 dose rate locations illustrated in Figure 11-1.*

The estimated occupational exposures to ISFSI personnel during loading, transfer, and storage operations (time and number of workers may vary depending on individual ISFSI practices) are provided in Table B.11-2. The total exposure is 2.5 person-rem.

The exposure provided is a bounding estimate. Measured exposures from typical NUHOMS® System loading campaigns have been 600 mrem or lower per canister for normal operations, and exposures for the HSM-MX are expected to be similar.

Regulatory Guide 8.34 [B.11-4] is to be used to define the onsite occupational dose and monitoring requirements.

B.11.2.2 61BTH DSC Retrieval Operations

Occupational exposures to ISFSI personnel during 61BTH DSC retrieval are similar to those exposures calculated for 61BTH DSC insertion. Dose rates for retrieval operations will be lower than those for insertion operations due to radioactive decay of the spent fuel inside the HSM-MX. Therefore, the dose rates for 61BTH DSC retrieval are bounded by the dose rates calculated for insertion.

B.11.2.3 Fuel Unloading Operations

No change to Section 11.2.3.

At the ISFSI site, the transfer skid/trailer is used in conjunction with the MATRIX loading crane (MX-LC). The MX-LC is used to assist in loading the DSC into the HSM. The MX-LC is designed, fabricated, installed, tested, inspected, and qualified in accordance with ASME NOG-1, as a Type I gantry type of crane, per the guidance provided in NUREG-0612 [B.12-5]. The transfer skid/trailer is backed up to, and aligned with, the HSM-MX using transfer equipment. The OS197-TC/MX-LC is docked with, and secured to, the HSM-MX access opening. The MX-RRT rollers are extended into HSM-MX through front wall slots for the MX-RRT and secured. The loaded DSC is transferred to or from the HSM-MX using transfer equipment. The MX-RRT is then lowered to place the DSC on the front and rear DSC supports in the HSM-MX. As a result, for a loaded OS197-TC drop accident to occur during these operations is considered non credible.

Lifts of the OS197-TC loaded with the dry storage canister are made within the existing heavy load requirements and procedures of the licensed nuclear power plant. The OS197-TC design meets requirements of NUREG-0612 [B.12-5] and American National Standards Institute (ANSI) N14.6 [B.12-6].

The OS197-TC is transferred to the ISFSI in a horizontal configuration. Therefore, the only drop accident evaluated during storage or transfer operations is a side drop or a corner drop.

The OS197-TC and DSC are evaluated for postulated side and corner drops to demonstrate structural integrity during transfer and plant handling.

Accident Analysis

No change to accident analysis as described in Sections T.11.2.5.2 of [B.12-3].

Accident Dose Calculation

The accident dose of 46 mrem at 100 m from the EOS-TC documented in Section 12.3.1 *of the EOS UFSAR Revision TBD* bounds the accident dose for the 61BTH DSC within the OS197-TC. This dose is significantly below the 10 CFR 72.106 limit of 5 rem. Accident dose rates for the OS197-TC are provided in Section B.6.4.3.

Corrective Actions

No change to corrective actions as described in Sections T.11.2.5.4 of [B.12-3].

B.12.3.2 Earthquake

Cause of Accident

No change to cause of accident as described in Section A.12.3.2.